JAERI-M
91-052

ITER NEUTRAL BEAM INJECTION SYSTEM

— JAPANESE DESIGN PROPOSAL —

March 1991

Yoshihiro OHARA, Shigeru TANAKA, Masato AKIBA
Masanori ARAKI, Noboru FUJISAWA, Masaya HANADA
Takashi INOUE, Koichi MAKI*, Makoto MIZUNO
Yoshikazu OKUMURA, Masahiro SEKI, Kazuhiro WATANABE
Taisei UEDE*, Yasuo YAMASHITA*, Akira OZAKI**
and Yasushi SAITOH**

日本原子力研究所
Japan Atomic Energy Research Institute

JAERI-Mレポートは，日本原子力研究所が不定期に公刊している研究報告書です。
入手の問合わせは，日本原子力研究所技術情報部情報資料課（〒319-11茨城県那珂郡東海村）あて，お申しこしください。なお，このほかに財団法人原子力弘済会資料センター（〒319-11 茨城県那珂郡東海村日本原子力研究所内）で複写による実費頒布をおこなっております。

JAERI-M reports are issued irregularly.
Inquiries about availability of the reports should be addressed to Information Division Department of Technical Information, Japan Atomic Energy Research Institute, Tokai-mura, Naka-gun, Ibaraki-ken 319-11, Japan.

編集兼発行　日本原子力研究所
印　　刷　いばらき印刷㈱

JAERI-M 91-052

ITER Neutral Beam Injection System
- Japanese Design Proposal -

Yoshihiro OHARA, Shigeru TANAKA, Masato AKIBA, Masanori ARAKI
Noboru FUJISAWA[+], Masaya HANADA, Takashi INOUE, Koichi MAKI[*]
Makoto MIZUNO[++], Yoshikazu OKUMURA, Masahiro SEKI, Kazuhiro WATANABE
Taisei UEDE[*], Yasuo YAMASHITA[*], Akira OZAKI[**] and Yasushi SAITOH[**]

Department of Thermonuclear Fusion Research
Naka Fusion Research Establshment
Japan Atomic Energy Research Institute
Naka-machi, Naka-gun, Ibaraki-ken

(Received February 25, 1991)

A Japanese design proposal of the ITER Neutral Beam Injection System (NBS) which is consistent with the ITER common design requirements is described. The injection system is required to deliver a neutral deuterium beam of 75MW at 1.3MeV to the reactor plasma and utilized not only for plasma heating but also for current drive and current profile control. The injection system is composed of 9 modules, each of which is designed so as to inject a 1.3MeV, 10MW neutral beam. The most important point in the design is that the injection system is based on the utilization of a cesium-seeded volume negative ion source which can produce an intense negative ion beam with high current density at a low source operating pressure. The design value of the source is based on the experimental values achieved at JAERI. The utilization of the cesium-seeded volume source is essential to the design of an efficient and compact neutral beam injection system which satisfies the ITER common design requirements.

+ Department of Large Tokamak Research
++ Department of JT-60 Facility
* Hitachi Ltd.
** Toshiba Corporation

The critical components to realize this design are the 1.3MeV, 17A electrostatic accelerator and the high voltage DC acceleration power supply, whose performances must be demonstrated prior to the construction of ITER NBI system

Keywords: ITER, Neutral Beam Injection System, Japanese Design Proposal, Negative Ion Source, 10MW, 1.3MeV

JAERI－M 91－052

ITER用中性粒子ビーム入射システム
― 日本設計案 ―

日本原子力研究所那珂研究所核融合研究部

小原　祥裕・田中　茂・秋場　真人・荒木　正則
藤沢　登[+]・花田磨砂也・井上多加志・真木　紘一[*]
水野　誠[++]・奥村　義和・関　昌弘・渡辺　和弘
上出　泰生[*]・山下　泰郎[*]・尾崎　章[**]・斉藤　靖[**]

（1991年2月25日受理）

ITER共通設計基準に基づいた中性粒子ビーム入射システム（NBS）の日本概念設計案について述べる。本システムは，1.3MeVで75MWの重水素中性粒子ビームを入射するものであり，プラズマ加熱の他電流駆動や電流分布制御にも用いられる。本システムは9ユニットより成り，各ユニット当たり最大1.3MeV，10MWのビームを入射する設計としている。本設計において最も重要な点は，原研での実験結果に基づいて，低運転ガス圧で高い負イオン電流密度を得ることができるセシウム導入型体積生成負イオン源を採用していることである。本イオン源の採用により，NBIシステムの効率を改善すると共に，ITER共通設計基準を満足するコンパクトなNBIを設計することができた。

本設計を実現する上で鍵を握る重要な機器は，1.3MeV，17Aの静電加速器と加速器用高電圧直流電源である。これらの機器性能を実証できれば，本NBIシステムの実現は可能である。

那珂研究所：　〒311－01　茨城県那珂郡那珂町大字向山801－1
+　臨界プラズマ研究部
++　JT－60試験部
*　㈱日立製作所
**　㈱東芝

Contents

目　　次

1. INTRODUCTION

Neutral beam injection systems based on the positive ion beam have made great contributions so far to the realization of high temperature tokamak plasmas in the sub-breakeven condition. In the next fusion machines which produce a dense plasma with large plasma crosssection, a neutral beam with a beam energy as high as several hundreds keV/nucleon is required to obtain sufficient penetration through the plasma. In order to obtain a neutral beam with such high energy, a negative ion beam must be utilized to attain high neutralization efficiency.

Several negative-ion-based NBI systems have been proposed so far. The LBL group proposed a system using a TFF(Transverse Field Focusing) accelerator and a photo neutralizer.[1,2] This concept is attractive from the neutron shield point of view but too aggressive to realize the system in the near future. On the other hand, the ORNL group proposed a 200keV system which is quite similar to the conventional positive-ion-based NBI system, and realistic from the engineering point of view.[3] However, the beam energy in the design is too low. Thus, these designs have some difficulties in applying these systems to the next fusion machines. Since then, no new design was proposed primarily because the negative ion sources were far from the one required for the next fusion machines. Thereafter, development of the negative ion sources has made rapid progress. Particularly, a volume production type negative ion source, which was firstly investigated by M. Bacal,[4] has evolved rapidly due to the intensive researches in many laboratories.[5,6,7] This leads us to propose a new concept of a beam-driven tokamak reactor using a negative-ion-based NBI system with a volume production type ion source.[8,9] In this reactor, the NBI system is used not only for plasma heating but also for current drive and current profile control. The NBI system with such multi-functions has a possibility to make the reactor system simple compared to the RF systems which requires different systems for each function. Furthermore, the NBI system proposed transports high energy and high current sheet beams at a distance of over 40 meters through a narrow and long neutralizer and utilizes poloidal magnetic fields to separate residual ion beams. This makes the beamline compact and simple, and makes it possible to isolate the ion source from the reactor room, so that the maintenance becomes easy.

This attractive design of the NBI system together with the beam-driven tokamak reactor concept was adopted for the INTOR Tokamak Concept Innovations in 1986,[10] and contributed to utilizing the NBI system for the primary current drive and heating system for ITER. On the basis of the recent progress on the negative ion sources and discussions in the ITER/NBI specialist meetings at Garching from 1988 to 1990, a Japanese conceptual design has been finally completed. This paper describes the details of the Japanese conceptual design of the negative-ion-based NBI system for ITER.

References

[1] O.A. Anderson, et al.: Nucl. Tech./Fusion, 4, 1418 (1983).
[2] W.S. Cooper : Nucl. Tech./Fusion, 4, 632 (1983).
[3] W.K. Dagenhart, et al.: Nucl. Tech./Fusion, 4, 1430 (1983).
[4] M. Bacal and G.W. Hamilton : Phys. Rev. Lett. 42, 1538 (1979).
[5] R.L. York, R.R. Stevens, Jr., K.N. Leung, and K.W. Ehlers : Rev. Sci. Instrum. 55 (1984).
[6] T.S. Green : Proc. 11th Symp. on Fusion Engineering, Austin, Texas (1985) 103.
[7] Y. Okumura, et al.: Proc. 11th Symp. on Fusion Engineering, Austin, Texas (1985) 113.
[8] S. Yamamoto et al.: Proc. 11th Int. Conf. on Plasma Physics and Controlled Nuclear Fusion Research, Kyoto, IAEA-CN-47/H-I-3, (1986).
[9] T. Shibata, H. Horiike, S. Matsuda, Y. Ohara, Y. Okumura and S. Tanaka : Kakuyugo Kenkyu 56, 124 (1986) [in Japanese].
[10] Y. Ohara, S. Matsuda and R. Saito : IAEA-TECDOC-373, 305 (1986).

2. OUTLINE OF THE SYSTEM DESIGN

2.1 Requirements from ITER

The physics and system requirements for the neutral beam injection system for ITER are reviewed from the viewpoints of physics and engineering.[1,2] The requirements are listed in Table 2.1-1

Table 2.1-1 Requirements for ITER NBI

Injected Power (Hydrogen or Deuterium)	: 75 MW
Energy (maximum)	: 1.3 MeV
Beam Species	: D^0 and H^0
Pulse Length (maximum)	: 350 hours
Overall System Efficiency	: > 40 %
Power Profile Shapes at Plasma	: Hollow, Flat & Peaked
Power Steps	: 10 %
Power Change Rate	: 10 MW/s
Energy Steps	: 50 %, 75 %, 100 %
Energy Step Change Rate	: 10 s
Aiming Tangency Radius	: 6.2 m
Port Dimensions	: 0.8m W x 3.4m H
Tritium Accumulation (total)	: < 10 grams
Impurity Flux into Torus (total)	: < 3.5×10^{16} atoms/s
Power Density at Far Wall	: < 0.6 MW/m^2, steady state

The ITER Current Drive and Heating (CD&H) systems are required for ionization and current initiation, non-inductive current ramp-up assist, heating of plasma to ignition, long burn with more than one thousand seconds or steady-state operation, as an ultimate goal, with full non-inductive current drive , current profile control, and burn control by modulation of an auxiliary power. Among them, the steady-state current drive is the most demanding requirement, and this has driven the choice of the ITER CD&H systems. The reference systems are as follows;

75 MW, 1.3 MeV Neutral Beam System (NBS),
50 MW, 5.0 GHz Lower Hybrid System (LHS),
20 MW, 120 GHz Electron Cyclotron System (ECS).

Combination of NB and LH waves was chosen as a reference current drive scenario because the combination provides the highest current drive efficiency and sufficient flexibility in controlling current profile. The current in the central region is supplied by the NBS, while the LH waves are used to drive current in an outer region. The NBS therefore is required the following functions ; plasma heating to ignition, long burn or steady-state operation, current profile control, and burn control by modulation of power.

The analysis on the plasma heating to ignition shows that all heating methods such as NB, ion cyclotron waves, and EC waves, except possibly LH waves (depending on density) can efficiently heat the plasma up to ignition. The time needed for plasma heating to ignition is an order of ten seconds, and the necessary power is about 50MW. The sufficient penetration of beams into the central region of a plasma with average density up to $\langle n_e \rangle = 2 \times 10^{20} m^{-3}$ should also be kept in mind and it requires at least 1MeV beam energy.

For the long burn or steady-state operation scenarios, overall considerations are necessary on physics and engineering issues, while the higher beam energy might be better from the physics point of view. The following constraints should be taken into account:(1) requirement of a power multiplication factor $Q>5$ for steady state operation, (2) considerable flexibility in tailoring a current profile to cover a wide range of operation space, (3) additional power for current drive to alpha heating power could further embarrass power and particle handling by divertor, (4) shinethrough power density should be within the allowable level of power density at the first wall, (5) the selection of beam energy should be consistent with a realistic development plan of NBS. The analysis on the long burn and steady-state operation, taking into account the real constraints of the device, shows that the NBS with the beam energy of 1.3MeV and the beam power of 75MW is compromise in the overall consideration.

As a typical steady-state operation scenario, the lower density of $\langle n_e \rangle = 0.7 \times 10^{20} m^{-3}$ and the higher temperature $\langle T_e \rangle = 20$keV are selected to increase the current drive efficiency, which turns in reduction of power requirement and alleviation of power handling by divertor. In this condition the NBS has capability of carrying the driven current of about

9MA and the LHS could drive about 4MA in the outer region. In addition to those externally driven currents, the neoclassical driven current, bootstrap current, about 6MA, could be driven, while it depends on poloidal plasma beta and plasma current profile.

The NBS should also be able to control the burn. The power requirement for this is not demanding, but the crucial characteristics is the varying rate of power, i.e., the power is required to be changed 10 MW/s in a step of 10% of full power from zero to 100% of power.

The global profile control of plasma current is provided by a combination of variation of relative NB and LH power and change of aiming of neutral beams. The latter control requires that the neutral beam footprint should be changed quite flexibly, i.e., from a peaked profile to hollow one.

The requirements on the NBS are summarized as follows.

(Beam Power)

The most demanding power requirement is the steady-state operation. From the viewpoint of current drive capability, the power more than 100MW is desirable for covering the wide range of operation space for the steady-state and long burn operations, and the power 75MW is marginal for the steady-state operation as mentioned above.

(Beam Energy)

The beam energy affects current drive efficiency and capability of tailoring global current profile. The current drive efficiency incresaes with the beam energy, as shown in Fig.2.1-1. The higher energy is preferable, and it eases power handling at divertors and improves beam penetration. The beam driven current profile is determined by the deposition profile of the beam, which is dependent on the beam stopping cross section. In those years the atomic processes for the beam stopping have been reconsidered including the multistep cross section such as excitation and subsequent ionization. It indicates that the beam stopping cross section is enhanced by a factor of 1.4 from the old one without multistep processes. Those facts have significant impact on the selection of beam energy. From the physics point of view the higher beam energy is desirable, but the 1.3MeV beam energy is somewhat compromise based on the overall consideration,

including reasonable R&D programme of the NBS. It should be noted that the beam with 1.3MeV could penetrate to the central region of plasma with $<n_e>=1.0\times10^{20}m^{-3}$, however it is not easy for the plasma with $<n_e>=1.5\times10^{20}m^{-3}$.

(Beam Species)

The H^0 and D^0 beam should be prepared to cover the ITER operation and research programme. Especially in the physics phase, lasting about 6 years before the technology phase, the experiments will be build up step by step in terms of machine activation, i.e., zero activation phase, low activation phase, and high activation phase. Even in the zero activation phase with H and He, a lot of physics issues will be tested with full machine capability, including the current drive and heating system with H^0 beam. In the high activation phase, the overall performance of D/T plasmas will be investigated with the CD&H system with D^0 beam.

(Beam Profile Control)

The stable operation of long burn could need specific plasma current profiles to sustain high beta plasmas and to avoid effects of strong sawtooth oscillations. Especially, the steady state operation needs higher beta capability and the more specific profiles for plasma current. However, it is premature to state quantitatively the requirement on beam profile control, because the requirement on plasma current profile can not be fixed. To fullfil the functions on the NBS, i.e., plasma heating to ignition, long burn and steady-state operations, and burn control, the NB must cover a wide range of beam power profile, i.e., the beam footprint in the plasma should be changed peaked profile to hollow profiles.

(Power Step and Power Change Rate)

The performance of burn stability control is governed by constraints on heating and diagnostic system. The capability of burn control has been studied by time-dependent simulations of 0-D plasma model, on a plane of neutron flux perturbations and equilibrium heating power with a parameter of heating power ramp-rate. It shows that the 10% positive and negative perturbations of neutron fluxes can be stabilized with 25MW by the heating power ramp-up rate of 10MW/s. It should be kept in mind that the analysis on the burn control is still in a preliminary stages.

(Energy Step and Energy Step Change Rate)

The change of beam energy can be used for the global current profile control, although it is not strongly requested, if the flexibility of changing the beam power profile can be sufficiently provided. Therefore the energy step of 50%, 75%, 100% and the energy step change rate of 10s are sufficient.

(Aiming Tangency Radius)

In physics points of view, the beam aiming is related to the current drive efficiency and the beam penetration. In the engineering aspect, it is connected to the port size, shine-through power load on the first wall. The current drive efficiency is roughly proportional to the beam tangency radius, R_{tang}, as shown in Fig.2.1-2, and the beam penetration is deteriorated with R_{tang} due to increase of beam pass to the plasma center($R \leq R_{tang}$). The beam shine-through power is not severe for the ITER configuration due to mainly enhanced beam stopping cross section, as mentioned later, and on the other hand the beam penetration become critical for higher density operation. The aiming tangency radius of 6.2m is chosen to optimize the drive efficiency, taking account into feasibility of tangential injection port configuration.

(Port Dimensions)

The analysis of beam driven current, taking into account the present port dimensions of 0.8mW x 3.4mH, indicates that the driven current covers a sufficiently wide range of current profile by changing beam power profiles.

(Tritium Accumuration)

The issue of tritium accumulation was discussed with the Fueling and Exhaust group and a tentative agreement was reached that no more than 10 grams of tritium should be accumulated in all the modules and in the event of a failure in the machine no more than 5 grams would be released back into the torus. It was estimated that a 10s response time to such an incident would be satisfactory.

(Impurity Flux)

The ion source selected may use either Barium or Cesium to enhance negative ion production and some of the Ba or Cs could enter the torus.

Therfore, a requirement was necessary to establish the amount of impurities that the neutral beam system could inject into the torus without deleteriously affecting plasma performance. The tentative allowed flux level for Ba or Cs is 3.5 x 10^{16} atoms/s.

(Shine-through)

It is expected that some beam will shine through the plasma and illuminate the far wall of the torus. The established agreement with the Plasma Facing Component Group is that the steady state power density, normal to the wall, should not exceed 0.6 MW/m^2. This limit assumes that the far wall will be 20 mm thick Carbon tiles which are radiatively cooled. The expected ambient temperature of the tiles is 1000°C and during normal operation the tile temperature should not exceed 1850°C or sublimation and reduced lifetime will occur and in no event should the temperature of the tiles exceed 2000°C. Neutral beam shine-through power has been evaluated for two cases with different plasma densities for ITER plasma and beam configurations. For a rather flat beam power profile (beam footprint) of a 30MW beam going through a port, a lower density case, $n_{e0}=10^{20}m^{-3}$ corresponding to $\langle n_e \rangle$ ~ $0.65x10^{20}m^{-3}$, has a peak shinethrough power of $0.02MW/m^2$, measured at a plane perpendicular to a beamline. In a higher density case, $n_0=1.5x10^{20}m^{-3}$($\langle n_e \rangle$ ~ $1.0x10^{20}m^{-3}$), a shinethrough power is remarkably reduced and a central beam power is completely absorbed. For the present beam configuration the beam shinethrough power is small, except for extreme low density plasma less than $\langle n_e \rangle$ ~ $0.5x10^{20}m^{-3}$ which is not envisaged in ITER.

On the basis of the physics and systems requirements described above and the discussions during three NBI specialist meetings at Garching, common design parameters for ITER-NBI system have been agreed by the four parties. The common design parameters are shown in Table 2.1-2.

References

[1] D.E. Post, et al.: ITER Physics, IAEA ITER Documentation Series No.21, IAEA, Vienna(1991).

[2] V. Parail, et al.: ITER Current Drive and Heating System, IAEA ITER Documentation Series no.32, IAEA, Vienna(1991).

Table 2.1-2 Common Design Parameters for ITER-NBI System

Number of NBI Ports	: 3
Beamline Modules / Port	: 3
Injected Power / Beamline Module	: 10 MW at 1.3 MeV
Beamline Dimensions	: around 4m OD x 15m L
Distance between Accelerator Exit and Aiming Tangency Point	: 46.5 meters

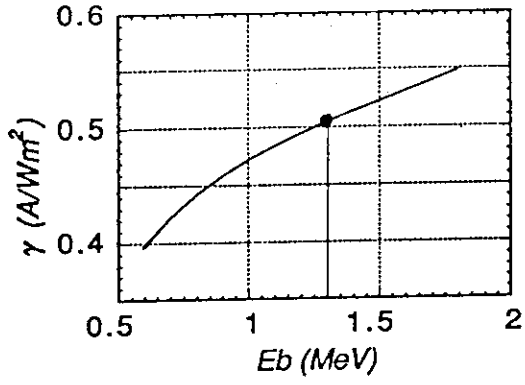

Fig. 2.1-1 Figure of merit for NB current drive efficiency, γ, is plotted as a function of beam energy, E_b, for ITER technology plasma and NB configuration, based on MS formula.

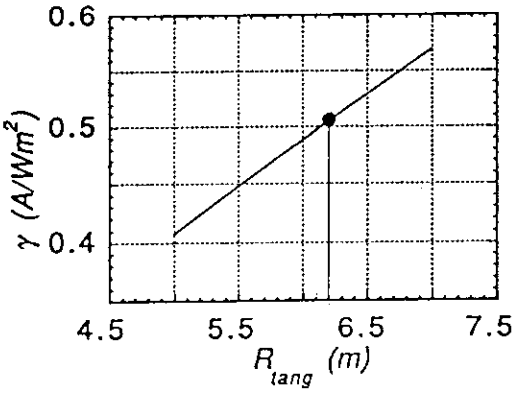

Fig. 2.1-2 Figure of merit for NB current drive efficiency, γ, is plotted as a function of beam tangency radius, R_{tang}, for ITER technology plasmas and NB configuration, based on MS formula.

2.2 Design Philosophy

The Japanese design philosophy for the ITER NBI system which satisfies the requirements mentioned above is described briefly.

The design of the NBI system will depend on the duration before its construction should be started. Since the ITER machine is expected to be completed at the head of the next century, construction of the NBI system must be started within 7 or 8 years. Therefore, what we keep in mind in designing the system is that the system whose construction can be started in 7 or 8 years must be proposed. Keeping this restriction in mind, design philosophy of each major component of the NBI system is considered.

(Ion Source)

The specifications of the negative ion generator are based on the values achieved experimentally at JAERI.[1] Since the source size is restricted, it is inevitable to apply a Cs-seeded multicusp source which can produce a high current negative ion beam at the lower operating pressure. Additionally, this source can produce a convergent negative ion beam because of a low negative ion temperature. If the Cesium has no serious influence on the reliability of the accelerator, the negative ion generator can be designed and manufactured using the present data base.

Concerning the negative ion accelerator, a mA x MeV class accelerator can be designed and manufactured using a conventional technology. However, an Ampere x MeV class accelerator has not been tried so faranywhere in the world. Though it is difficult to propose a best accelerator for the NBI system in this situation, we apply a six-stage electrostatic accelerator as the first option, since the optimization of the operation condition is easy and the required acceleration power supply system is simple. Additionally, we think it is possible to suppress the production of high energy electrons which degrade the reliability of the accelerator, by using a local transverse magnetic field in the accelerator.

(Beamline)

The beamline is designed so as to be realized without major R&D efforts. Therefore the plasma neutralizer, which is very attractive to improve the system efficiency, is not applied in the present design.

However, if an efficient plasma neutralizer will be developed, the gas neutralizer can be replaced with it easily.

The design of the beamline and also the power supply system depends considerably on the potential of the ion source plasma generator, namely, the grounded source system or high potential source system. Though it is not easy to compare merits or demerits of each system quantitatively, we think, in the grounded source system,it is quite difficult to suppress and manage in vacuum the large stored energy in the neutralizer, which affects the accelerator reliability.

(Power Supply)

In designing the acceleration power supply, it is important to protect not only the ion source but also the power supply itself against the breakdowns in the accelerator. The protection has been performed by the high speed DC switches and the surge suppression system so far. However, DC switches used in the JT-60 NBI and the 200keV Helium beam diagnostic system will not be available in the ITER 1.3MeV power supply system, because the system requires a lot of switching elements at a high potential of 1.3MV. Instead of the DC switch, an AC switch coupled with an high frequency inverter system (500Hz) is applied in the present design. The performances of this system is already verified at the JAERI Electron Beam Irradiation Stand where a 100keV, 4A electron beam is produced reliably.[2]

(Neutron Shield)

Neutron shield of the beamline modules is a critical issue to design a reactor relevant neutral beam injection system. The total neutron flux to each beamline module is of the order of 10^{14} n/s. Though it is possible to confine such a high flux neutrons with the beamline chamber wall, the weight of the beamline becomes so enormous that the remote maintenance is quite difficult. On the other hand, when we try to reduce the weight of the beamline, the room wall concrete and the air in the room will be activated, and a great amount of radio-activated materials must be handled in the decommission phase. In order to make the beamline as light as possible, the beamline chamber wall thickness is determined so that only high energy neutrons should be trapped within the beamline. Low energy scattered neutrons leaking out through the chamber wall are trapped by the neutron absorber like B_4C sticked on the room wall. Since the air in the room is replaced with innert gas like Helium, radioactivated materials are not produced.

(Remote Maintenance)

Maintenance of the beamline modules is quite difficult in the beamline room, because the activated materials and strong r-rays will be released into the room once the beamline is disassembled. Hence, the source module and/or beamline module are separated by a gate valve with double door system and are transported to a hot cell for maintenance.

References

[1] Y. Okumura, et al.: Proc. 16th Symp. on Fusion Technology, London, Sep.3-7(1990)R-07.

[2] M. Mizuno, et al.: Proc. of the 13th Symp. on Fusion Engineering, Knoxville, Oct.2-6 (1989) 574-577.

2.3 System Integration

Main components of the NBI system are shown schematically in Fig.2.3-1. The system consists of 9 beamline modules, 9 power supply units, remote maintenance system, and a NBI control system. Three civil system, namely, a cryogenic system, a fuel cycle system, and a cooling water system, are connected to the NBI system.

The top and side views of the beamline module are shown in Fig.2.3-2. The major beamline components consists of an intense negative ion source, a beam steering mechanism, a source disconnecting valve, a beam profile controller, a gas neutralizer, an ion deflection system, an ion beam dump, and cryopumps. All these components are installed in a vacuum vessel whose dimensions are approximately 4 meters in outer diameter and 17 meters in length by 10cm in thickness. The vacuum vessel is made of mild steel, and serves as an outer magnetic shield. The region of the ion source and the neutralizer is covered with an inner magnetic shield made of permalloy. The vacuum vessel has also a function to attenuate high energy neutrons leaking into the NBI room. The beamline module is connected to an injection port of the torus via a large metal seal gate valve.

The ion source produces a 1.3MeV, 17A negative deuterium ion beam. Before the ions enter the neutralizer, the beam steering angle is varied by the beam profile controller, so as to obtain various beam deposition profiles at the plasma. In the gas neutralizer, about 60% of the ion beam is converted to neutrals by the collisions with the deuterium gas molecules. The residual ions (D^-, D^+) are deflected by the magnetic field produced by a couple of coils, and guided to the ion dump. The neutral beams of about 8A are injected to the plasma through the torus injection port.

Three beamline modules are installed on each injection port. The layout of nine beamline modules and power supplies is shown in Figures 2.3-3(a) and (b). Figures 2.3-4(a) and (b) show a relative size of the NBI system in the ITER building.

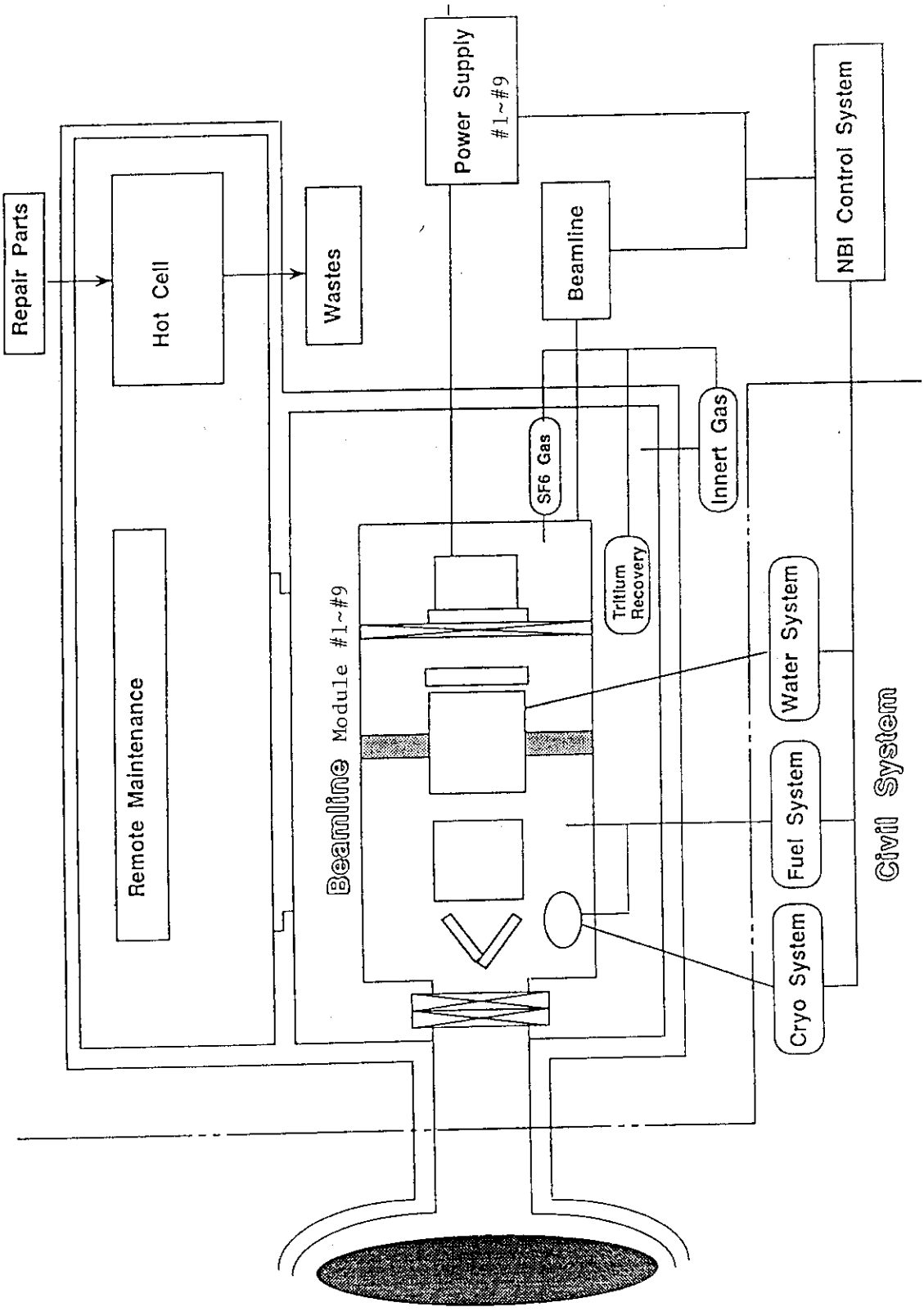

Fig. 2.3-1 Main components in the NBI system

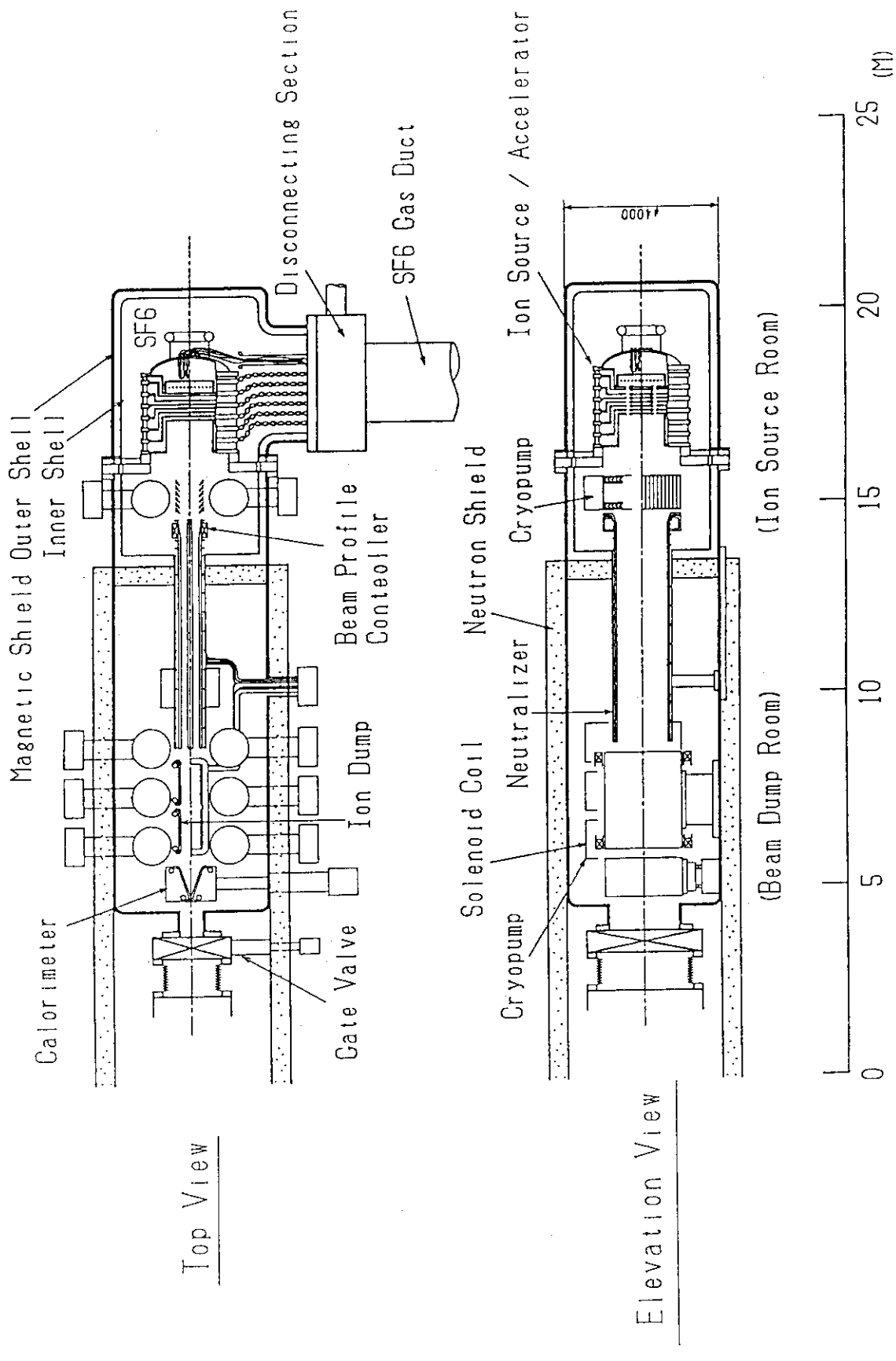

Fig. 2.3-2 Cross section view of a 1.3MeV x 10MW NBI beamline for ITER.

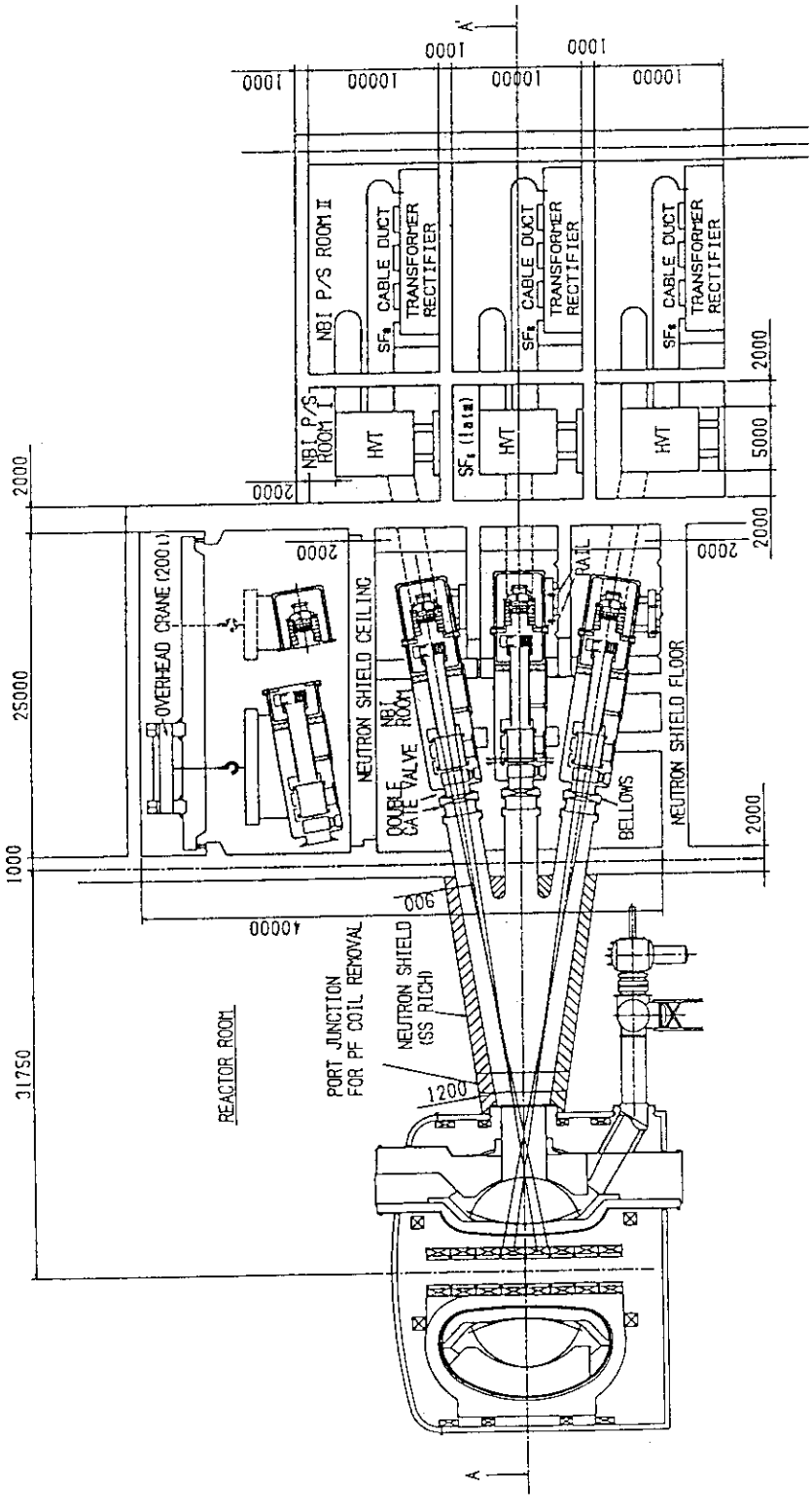

VIEW OF SECTION B-B'

Fig. 2.3-3(a) Layout of the beamline and power supply system for ITER-NBI (Elevation View)

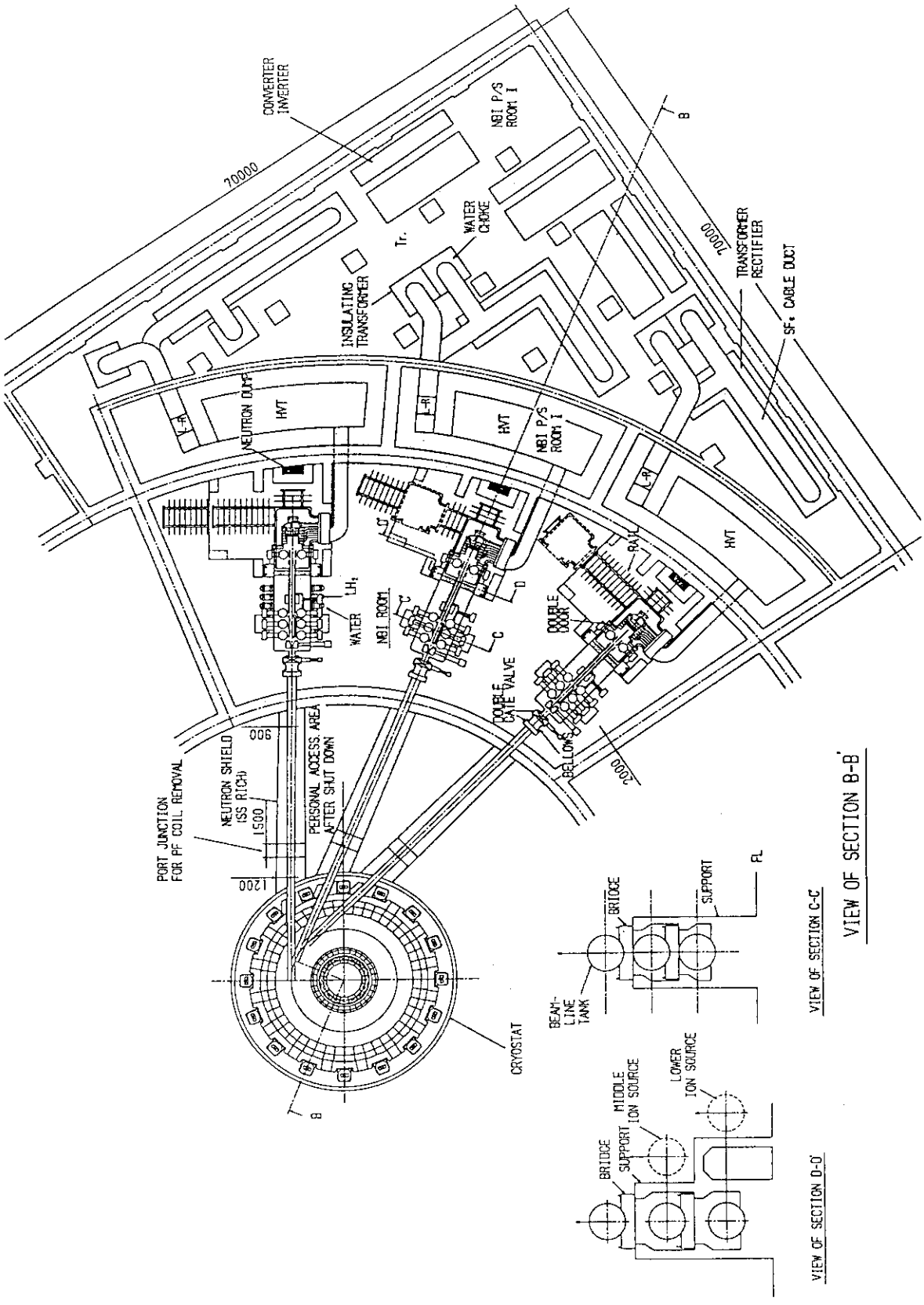

Fig. 2.3-3(b) Layout of the beamline and power supply system for ITER-NBI (Top View)

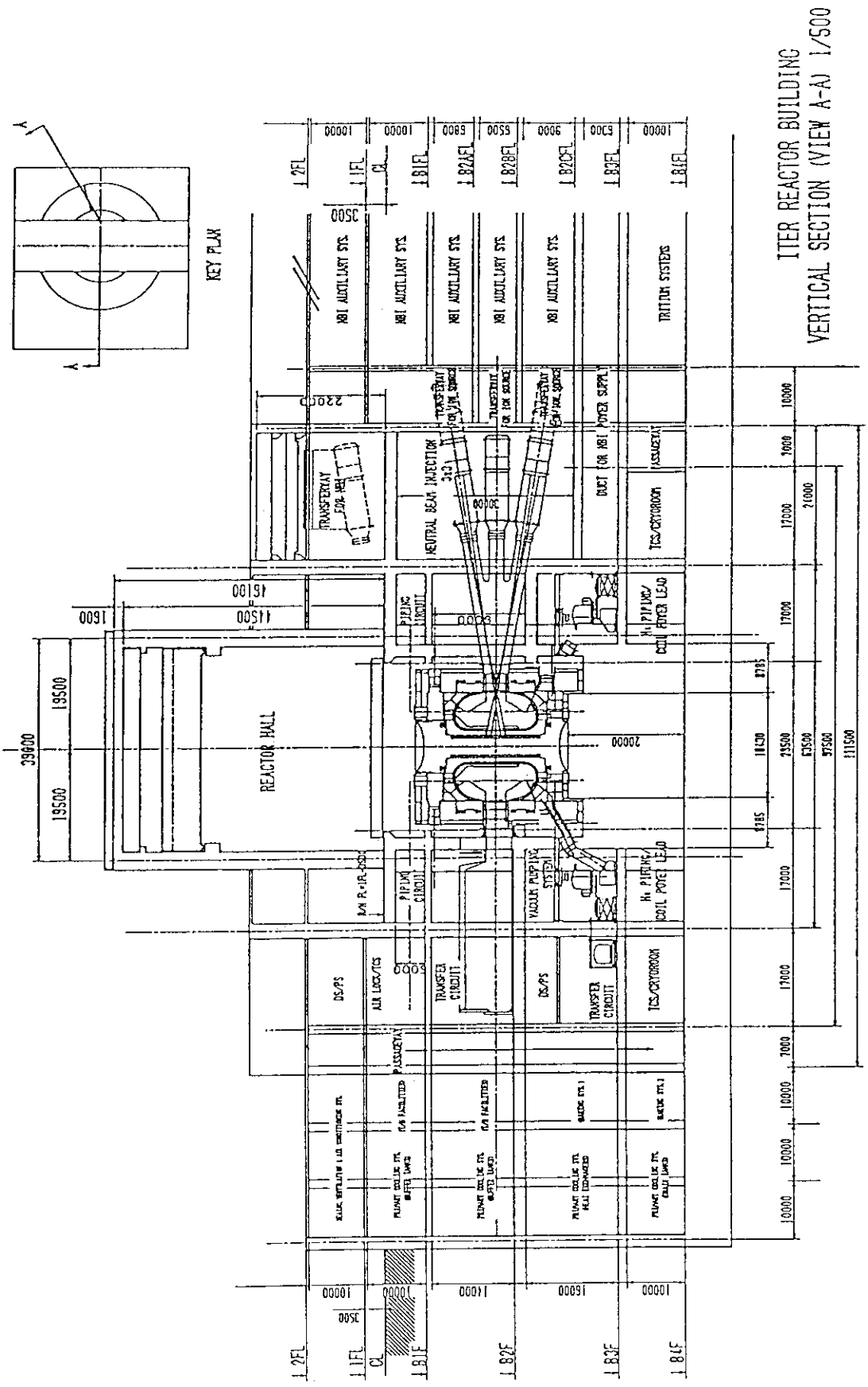

Fig. 2.3-4(a) Layout of the NBI system in the ITER building.
(Elevation View)

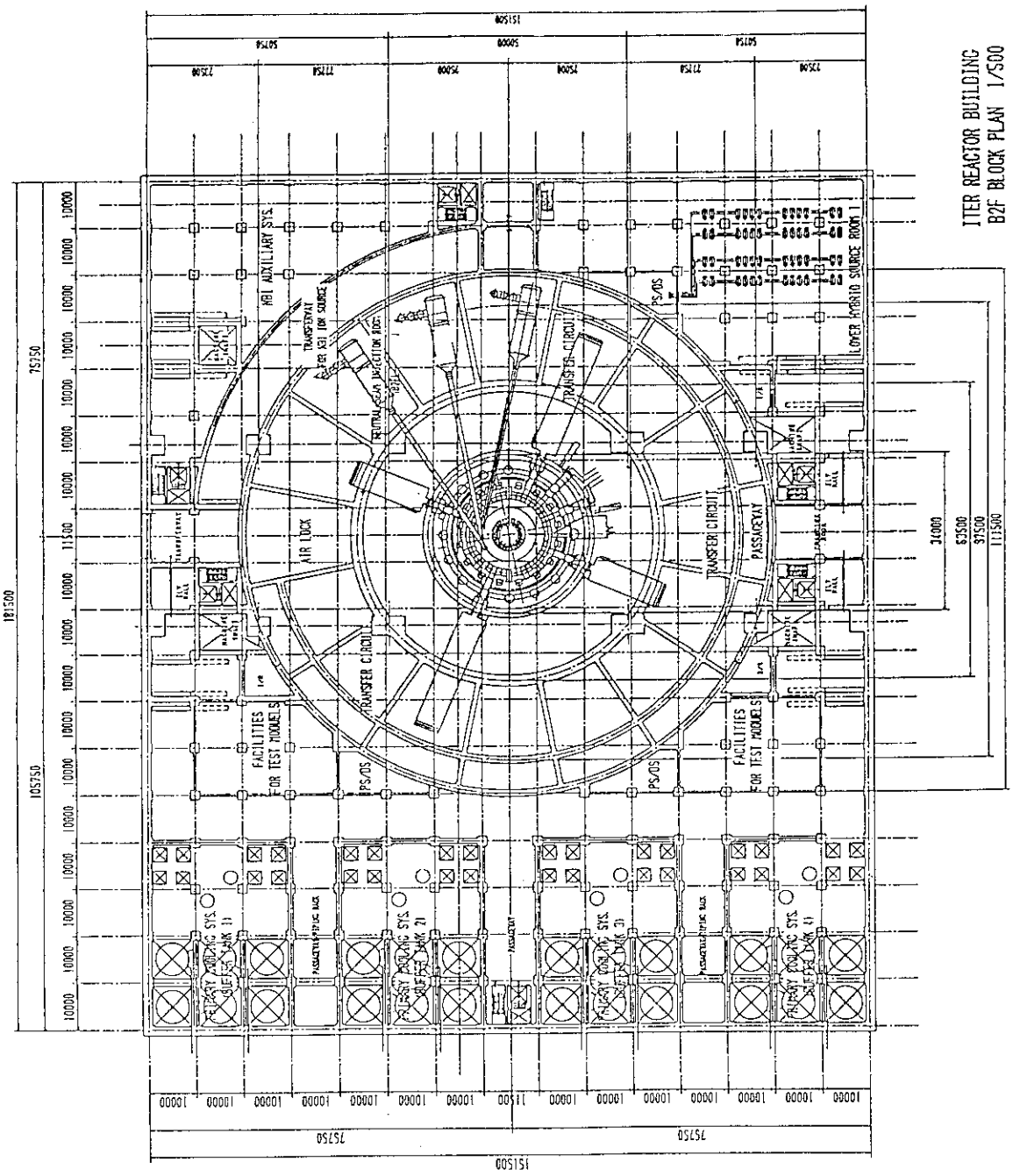

Fig. 2.3-4(b) Layout of the NBI system in the ITER building (Top View)

2.4 Gas Flow and Power Flow

Typical power and gas flows in the beamline are shown in Fig.2.4-1. Out of 26.1A of D^- ions extracted from the negative ion generator, 16.5A D^- ions are accelerated up to 1.3MeV, while 9.6A D^- ions are lost by the collisions with gas molecules in the extractor and accelerator. Namely, 37% of the extracted ions are lost in the extractor and accelerator, when the source filling pressure and the source gas temperature are 0.5 Pa and 1400 K, respectively. The 16.5A D^- ions are injected to the gas neutralizer, while 0.3A D^- ions are lost geometrically on the inner wall of the neutralizer. Since 60% of the negative ions are converted to neutrals in the neutralizer, the equivalent current of neutral beams coming out of the neutralizer is 9.8A. Unneutralized negative ions (3.2MW) and reionized positive ions (4.95MW) are deflected magnetically and handled by the beam dump. In the injection port region, 1.2A deuterium neutrals are lost geometrically, and 0.5A neutrals are lost by reionization. After all, 8.3A equivalent neutrals whose power is 10.8MW are injected into the ITER plasma. The D_2 gas is introduced both into the ion source and the neutralizer with the flow rate of 5.4 $Pa.m^3/s$ and 4.1 $Pa.m^3/s$, respectively. The gas is evacuated by cryopumps mounted in the ion source room and the beam dump room. The pumping speed of the cryopump in the ion source room is determined to keep the pressure in this room around 0.02 Pa. The lower pressure causes space-charge blown-up and the higher pressure increases the stripping loss in the accelerator. The pumping speed in the ion dump room is determined to keep the pressure in this room below 0.003 Pa, so that the reionization loss in the port region can be suppressed to 4% of the neutral beam.

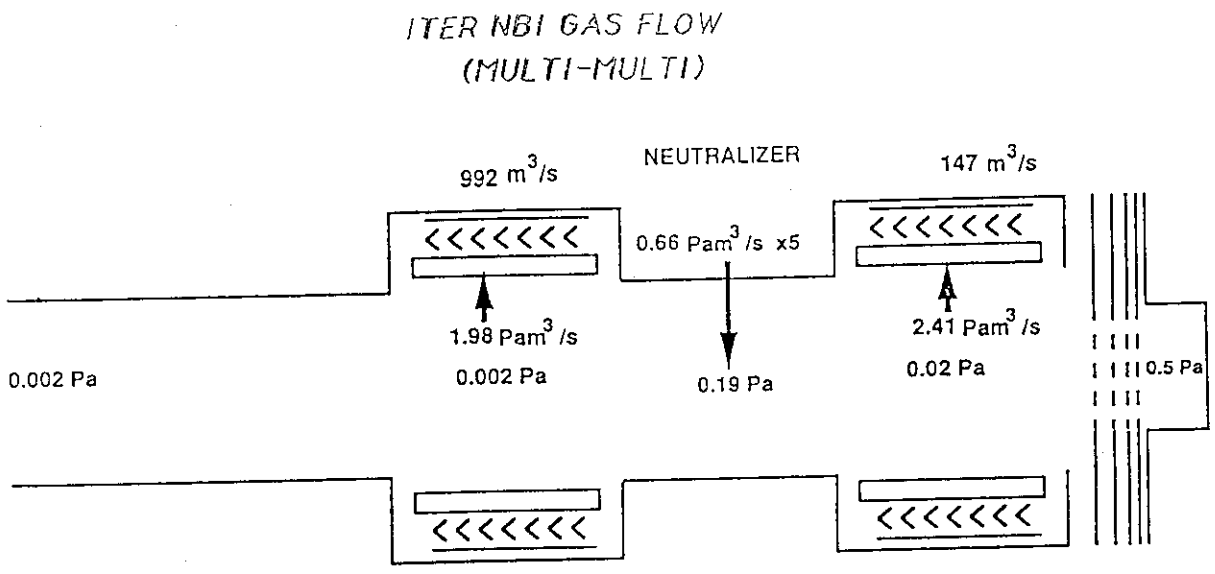

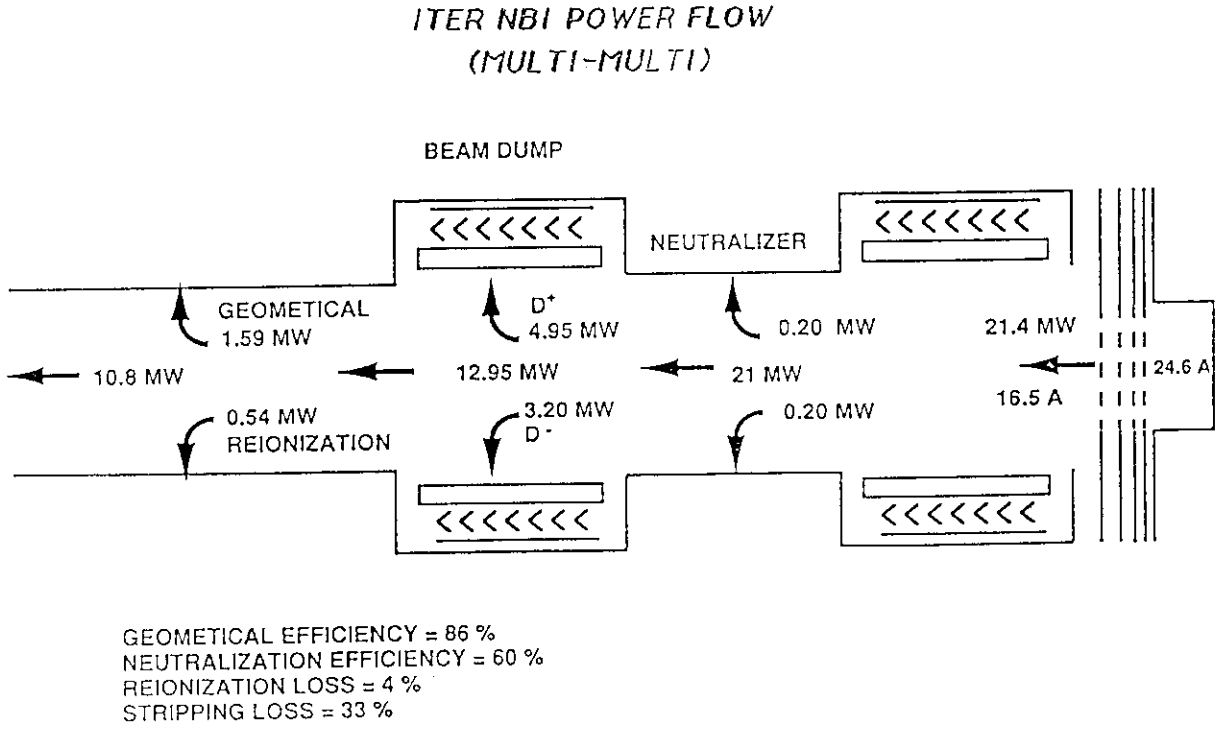

Fig. 2.4-1 Gas flow and power flow in the beamline.

2.4.1 Stripping Loss in the Ion Source

Using a 3D Monte-Carlo gas flow code developed at JAERI[1], we estimated stripping losses in two types of the accelerator. They are a multi-single type and a multi-multi type, whose configurations are shown schematically in Fig.2.4-2. The model for the calculation is as follows;

(1) The gas molecules D_2 flow downstream only through the apertures in the accelerator grids for simplicity. Therefore, we can estimate the stripping loss only by calculating the density distribution in the single channel.
(2) Mirror reflection of molecules is assumed at the boundary between the grids.
(3) The molecular reflection on the grid surface depends on the cosine law.
(4) The velocity distribution of the molecules at the starting plane in the arc chamber is Maxwellian.
(5) The energy loss which is caused by the collisions of molecules with the grids is expressed by an accommodation coefficient. The accommodation coefficient of deuterium molecules incident on copper is assumed to be 0.3.
(6) The temperature of the grids is kept to be 300K because the grids are cooled by water.
(7) The density during the arc discharge is calculated at a constant gas flow rate, i.e., the density during the discharge(n_a) is expressed by the equation of

$$n_a = n_b \sqrt{T_b/T_a}$$

Here, T_a is a temperature during the arc discharge, T_b the temperature before the arc discharge, which corresponds to 300K, and n_b the density before the arc discharge.

Figure 2.4-3 shows the temperature distribution. The temperature rapidly decreases down to the grid temperature of 300K in the extraction region, because of the frequent collisions of the molecules with the grids surface. Thus, the density distribution in the extraction region tends to become flat as shown in Fig.2.4-4.

From the density distribution, the stripping loss was calculated. Figure 2.4-5 shows the dependence of the stripping loss on the pressure

in the arc chamber before the arc discharge. At the pressure of 0.5 Pa and the source temperature of 1000K, the stripping loss is 40 % in the multi-single type, and 60 % in the multi-multi type. With increasing temperature of the molecules during the arc discharge, the stripping loss tends to decrease as shown in Fig.2.4-6. Therefor, the multi-single type accelerator is preferable compared with the multi-multi type accelerator.

References

[1] M. Hanada et.al.: To be published.

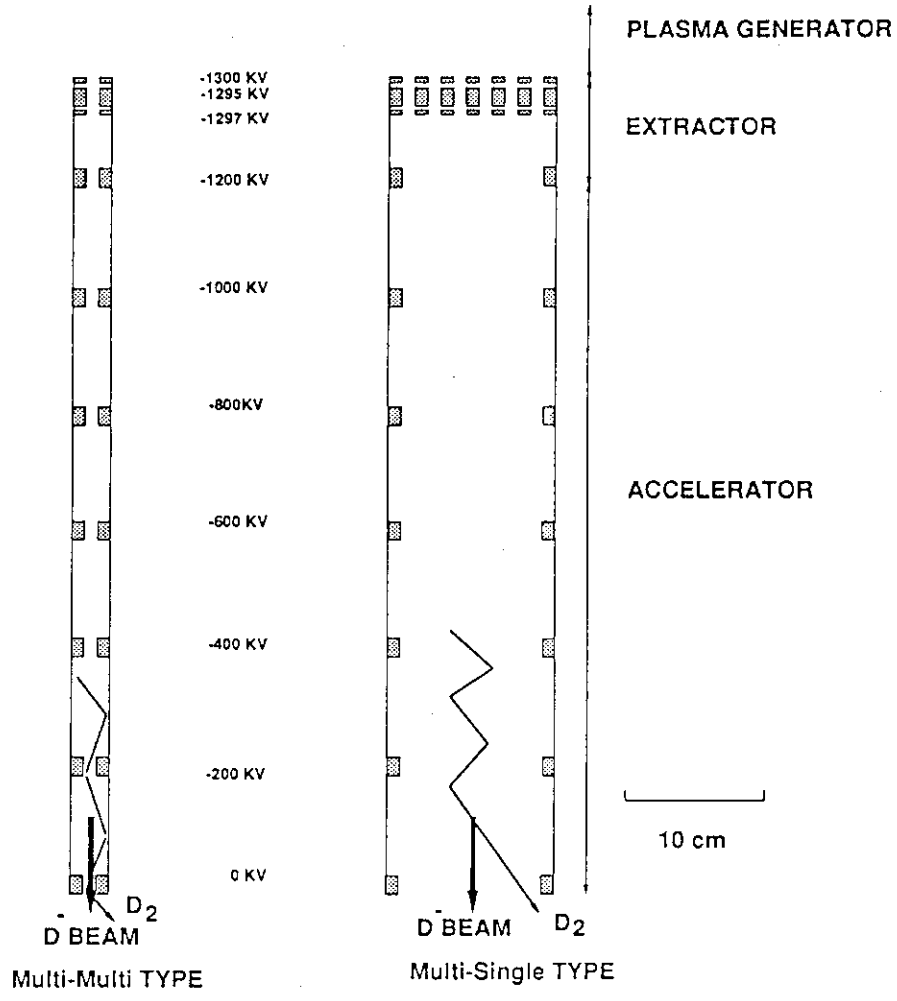

Fig.2.4-2 Geometories of the multi-single type accelerator and the multi-multi type acclerator.

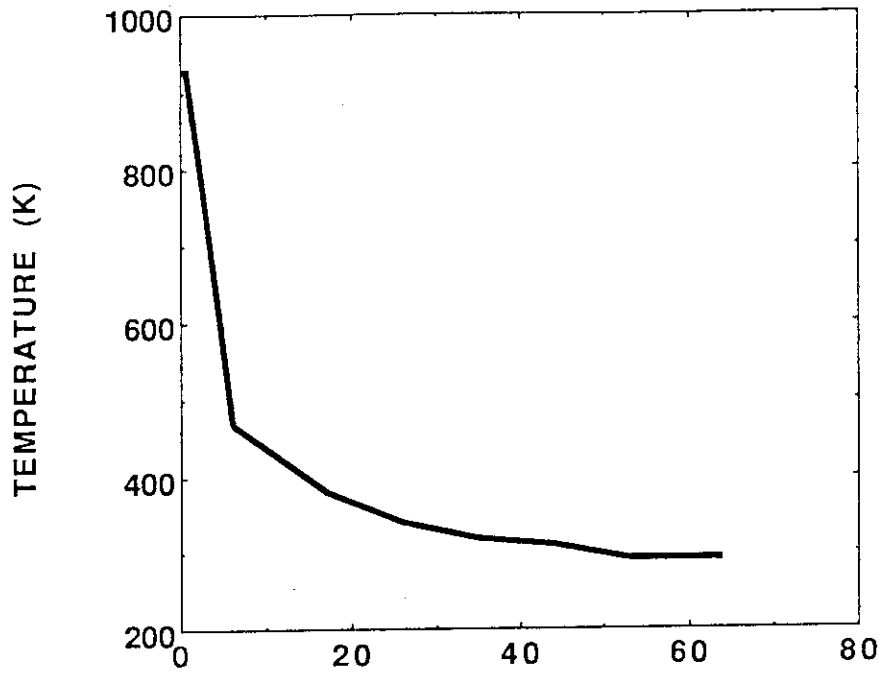

Fig. 2.4-3 Gas temperature distribution along the beam aix.

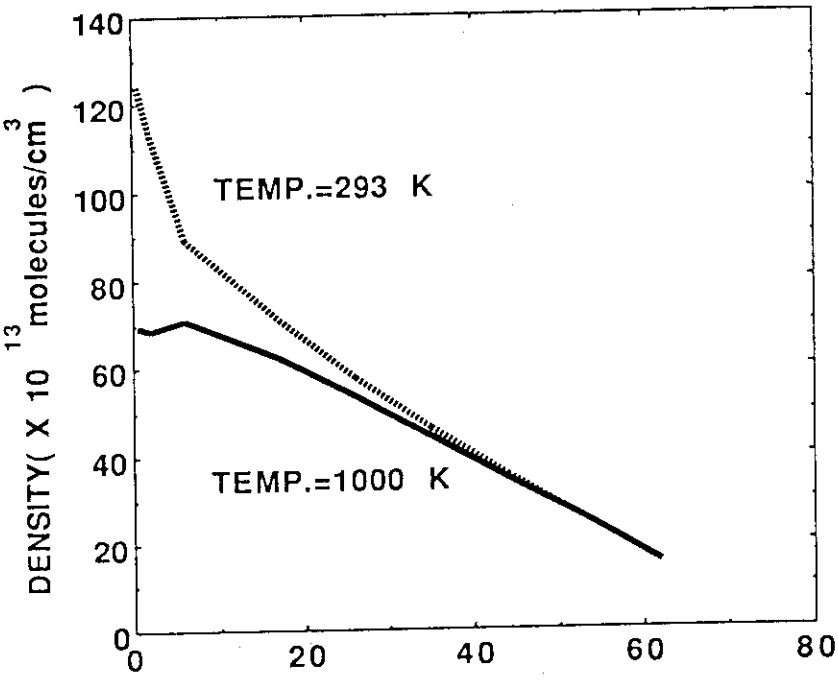

Fig 2.4-4 Gas desity distribution along the beam axis.

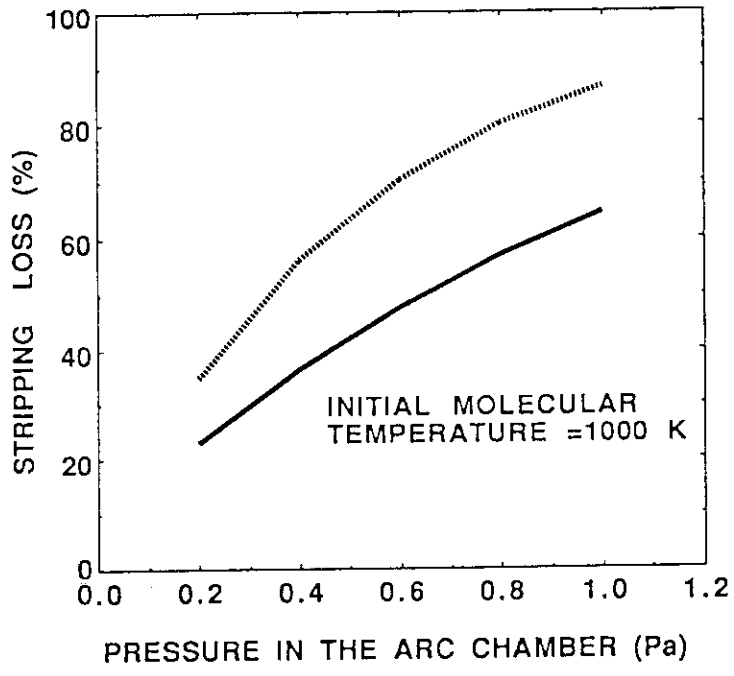

Fig. 2.4-5 Depedence of the stripping loss on the gas pressure before the discharge at the constant molecular temperature.

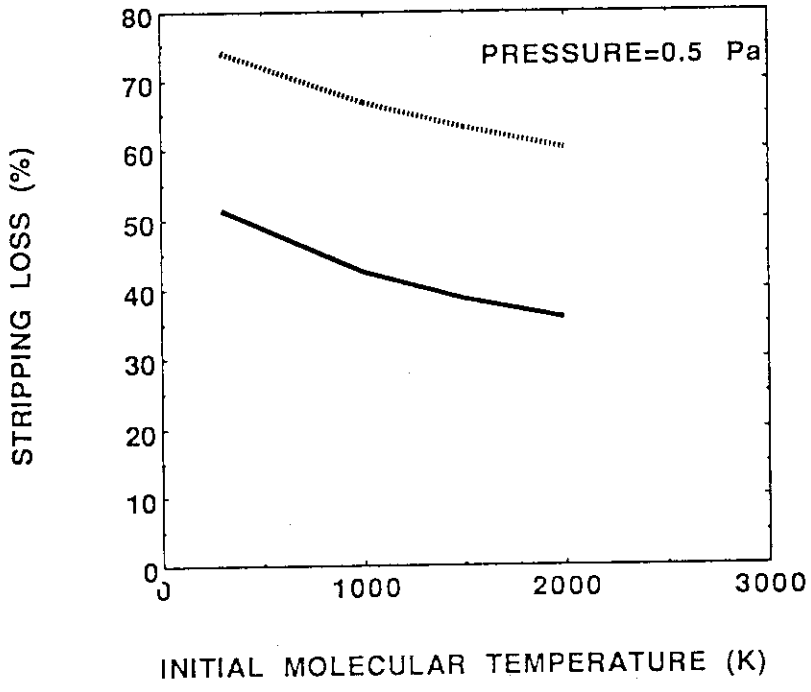

Fig. 2.4-6 Dependence of the stripping loss on the initial molecular temperature at the constant pressure of 0.5 Pa.

2.4.2 Geometric Transmission Efficiency

Geometric transmission efficiency of ITER/NBI modules were calculated, using a computer code BEAMPROF. Geometrical configuration used for the calculation is shown in Fig.2.4-7. As described in Section 3.1, the extraction grid area of 0.4 m wide x 1.0 m high of the ion source is divided by the central non-beam forming region into two, each of which has an area of 0.14 m wide x 1.0 m high. Corresponding to this splitting of the source, the cross-section of the neutralizer of 0.46 m wide x 1.3 m high is also divided by the central plate into two, each of which has an area of 0.2 m wide x 1.3 m high. The calculation of the geometrical efficiency takes into account these effects.

As can be seen from Fig.2.4-7, the geometrical configuration is symmetric with respect to the Y-Z plane for all three modules, and is symmetric with respect to the X-Z plane for the middle module. In the calculation, any focusing of beamlets in the X direction or in the Y direction is not considered,i.e. the axis of every beamlet is parallel to the axis of the whole beam. Notation in this section is as follows;

ω : divergence of beamlet,

$\Delta\theta_X$:deviation angle of the ion source in the X direction (rotation around the Y axis),

$\Delta\theta_Y$:deviation angle of the ion source in the Y direction (rotation around the X axis),

η_G:geometrical efficiency(fraction of neutral beams which originate from the ion source and reach torus plasma without interception by any walls).

We assume that beam axes of three ion sources cross with each other at a point (0,0,39.6m) when $\Delta\theta_X=0$ and $\Delta\theta_Y=0$ for all the three ion sources.

(a)Dependence on beamlet divergence

Table 2.4-1 indicates the calculated results of beam deposition fraction as a parameter of beamlet divergence when $\Delta\theta_X=0$ and $\Delta\theta_Y=0$. Fraction of beam deposition on the neutralizer and the drift duct increases with increasing beamlet divergence. On the other hand, fraction of beam deposition on the torus plasma(geometrical efficiency) decreases with the beamlet divergence.

Figure 2.4-8 shows the calculated geometical efficiency as a function of beamlet divergence for both middle and upper/lower modules.

Geometrical efficiency for the middle module is larger than that for the upper/lower module. The difference between them increases with increasing beamlet divergence. At the design point of beamlet divergence (5.24 mrad), the geometrical efficiency is 96% for the middle module, and 95% for the upper/lower module.

(b)Dependence on deviation angle in the X direction

Figure 2.4-9 indicates the calculated geometrical efficiency as a function of deviation angle in the X direction when ω =5.24 mrad and $\Delta\theta_y$=0. The efficiency decreases with increasing deviation angle $\Delta\theta_x$, because the fraction of beam deposition on the neutralizer and the drift duct increases with the deviation angle. The geometrical efficiency for the upper/lower module is always lower by about 1% than that for the middle module. If we intend to suppress the decrease in the geometrical efficiency within 1%, the absolute value of the deviation angle $\Delta\theta_x$ should be smaller than 1.5 mrad.

(c)Dependence on deviation angle in the Y direction

Figure 2.4-10 shows the geometrical efficiency as a function of deviation angle in the Y direction when ω =5.24 mrad and $\Delta\theta_x$=0. The efficiency decreases with increasing deviation angle $\Delta\theta_y$. The efficiency curve for the upper/lower module is not symmetric with respect to $\Delta\theta_y$=0. the reason for which can be understood from Fig.2.4-7. If we intend to suppress the decrease in the geometrical efficiency within 1%, the deviation angle $\Delta\theta_y$ should be smaller than 15 mrad in the absolute value for the middle module, and be within the region from $\mp$ 17.5 mrad to ±2.5 mrad for the upper/lower module. That is, range of permissible value for the deviation angle $\Delta\theta_y$ is much wider than that for $\Delta\theta_x$.

Table 2.4-1 Calculated results of beam deposition as a parameter of beamlet divergence when $\Delta\theta_x=0$ and $\Delta\theta_y=0$.
(a)middle module (b)upper/lower module

[Middle Module]

ω (mrad)	1.745	3.49	5.24	6.98	8.73
Z_{SP}(m)	39.6	39.6	39.6	39.6	39.6
$\Delta\theta_x$(mrad)	0.0	0.0	0.0	0.0	0.0
$\Delta\theta_y$(mrad)	0.0	0.0	0.0	0.0	0.0
Neutralizer	0.000087	0.009132	0.039485	0.082174	0.131028
Drift Duct	0.000313	0.000063	0.00009	0.000566	0.001012
Torus	0.9996	0.990805	0.960425	0.91726	0.86796

[Upper/Lower Module]

ω (mrad)	1.745	3.49	5.24	6.98	8.73
Z_{SP}(m)	39.6	39.6	39.6	39.6	39.6
$\Delta\theta_x$(mrad)	0.0	0.0	0.0	0.0	0.0
$\Delta\theta_y$(mrad)	0.0	0.0	0.0	0.0	0.0
Neutralizer	0.000087	0.009132	0.039485	0.082174	0.131028
Drift Duct	0.000343	0.00188	0.008562	0.017915	0.027129
Torus	0.99957	0.988988	0.951953	0.899911	0.841843

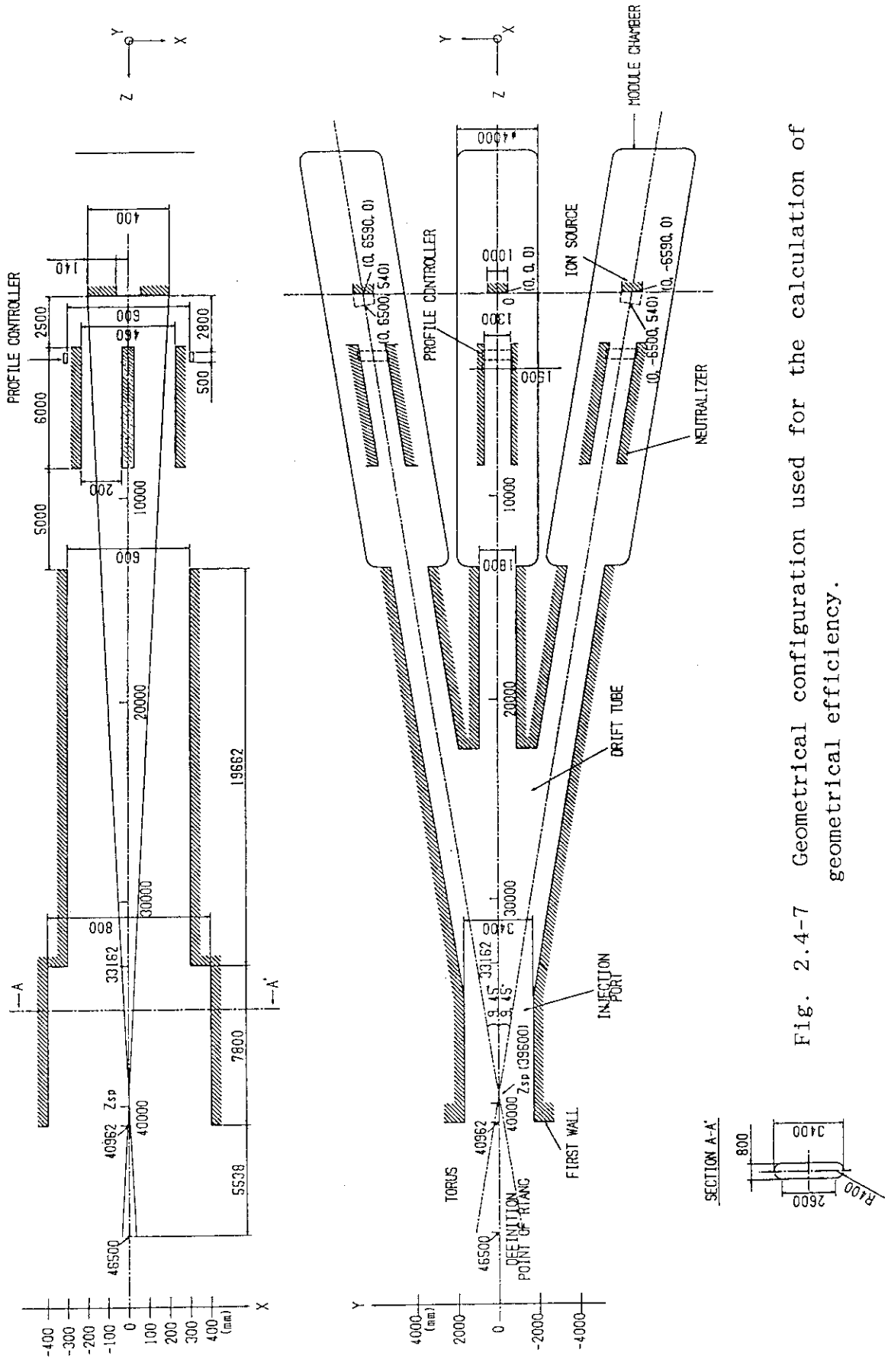

Fig. 2.4-7 Geometrical configuration used for the calculation of geometrical efficiency.

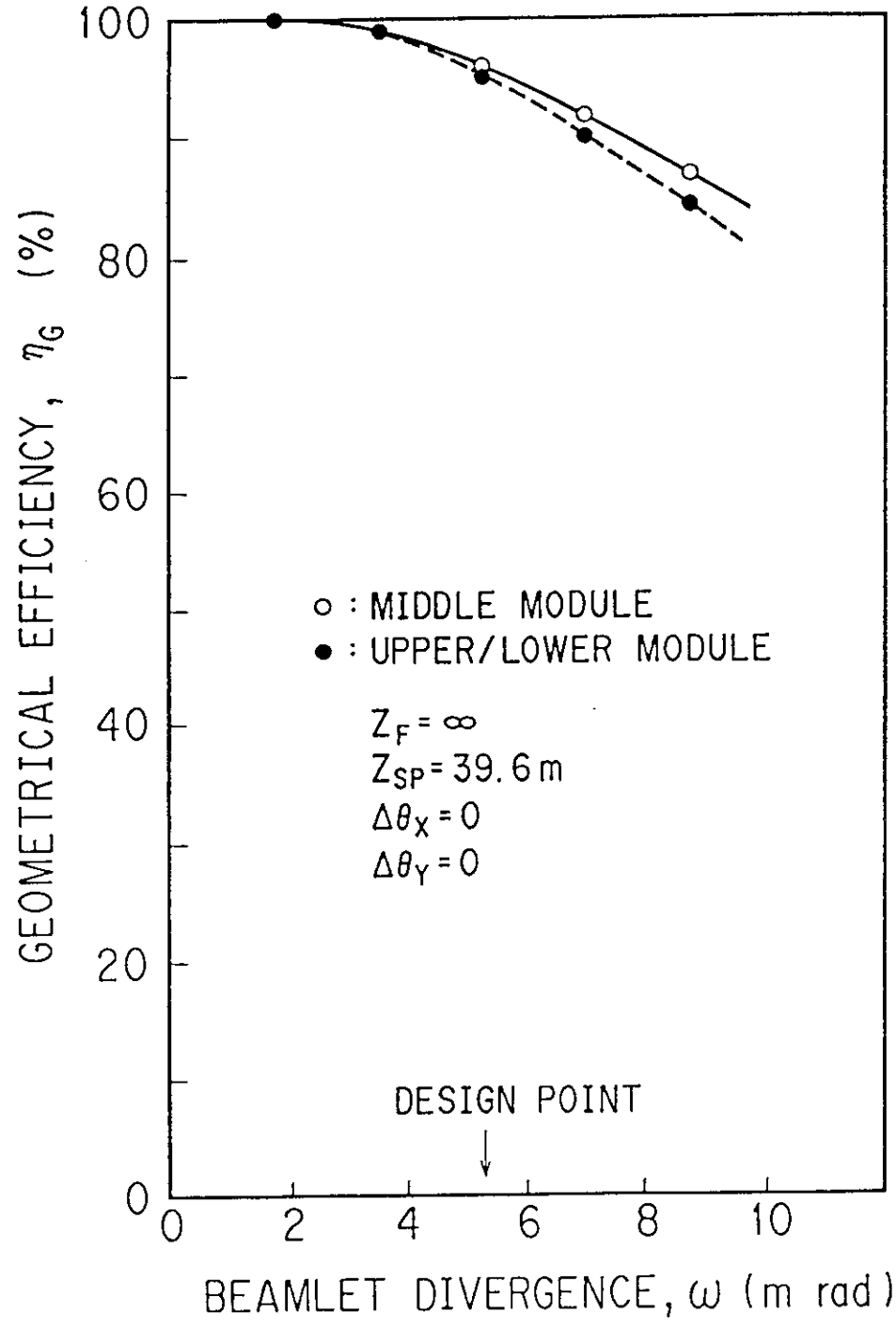

Fig. 2.4-8 Calculated geometrical efficiency as a function of beamlet divergence when $\Delta\theta_x$=0 and $\Delta\theta_y$=0 for both middle and upper/lower modules.

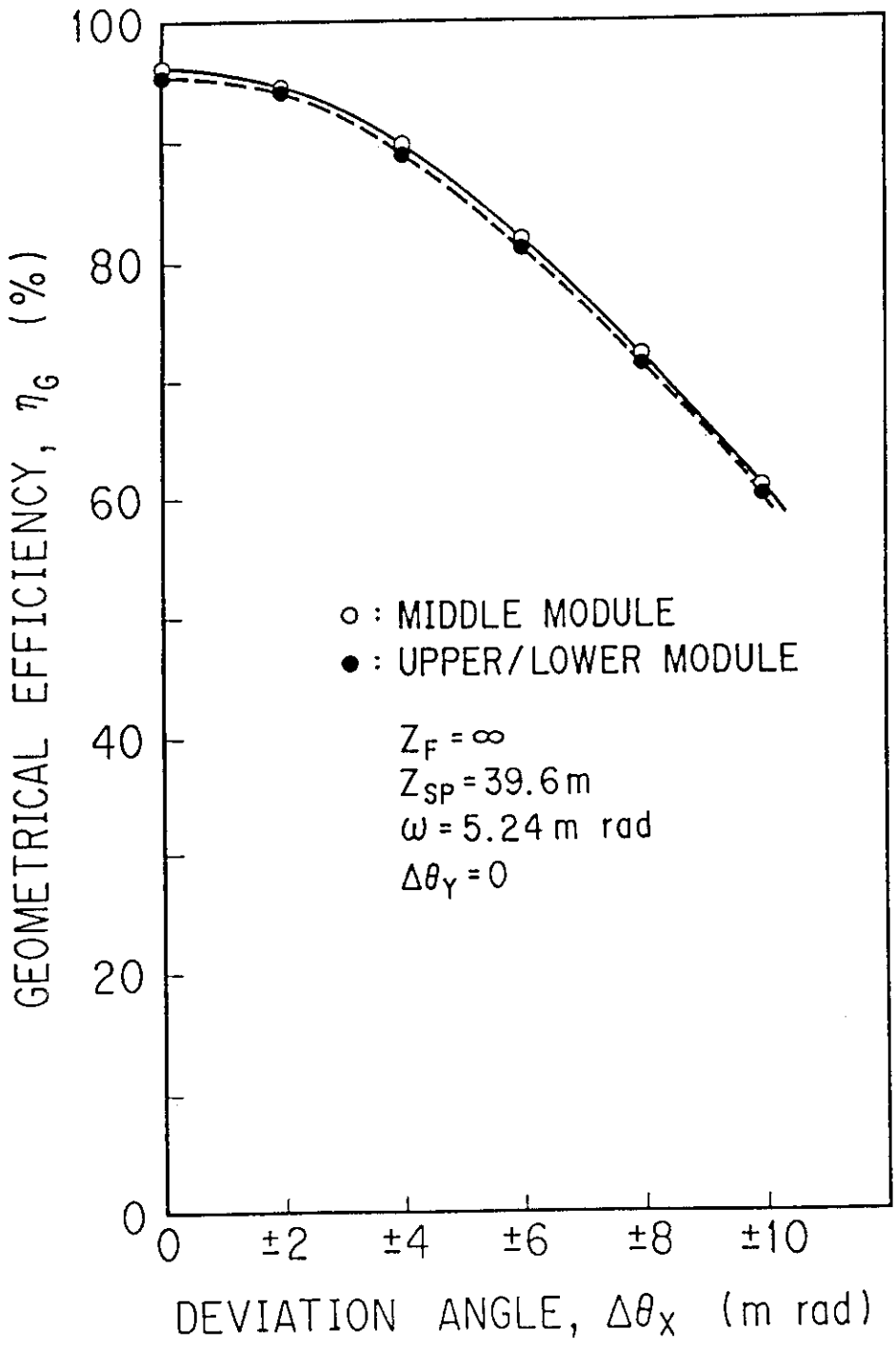

Fig.2.4-9 Calculated geometrical efficiency as a function of deviation angle in the X direction when ω =5.24 mrad and $\Delta\theta_y$=0.

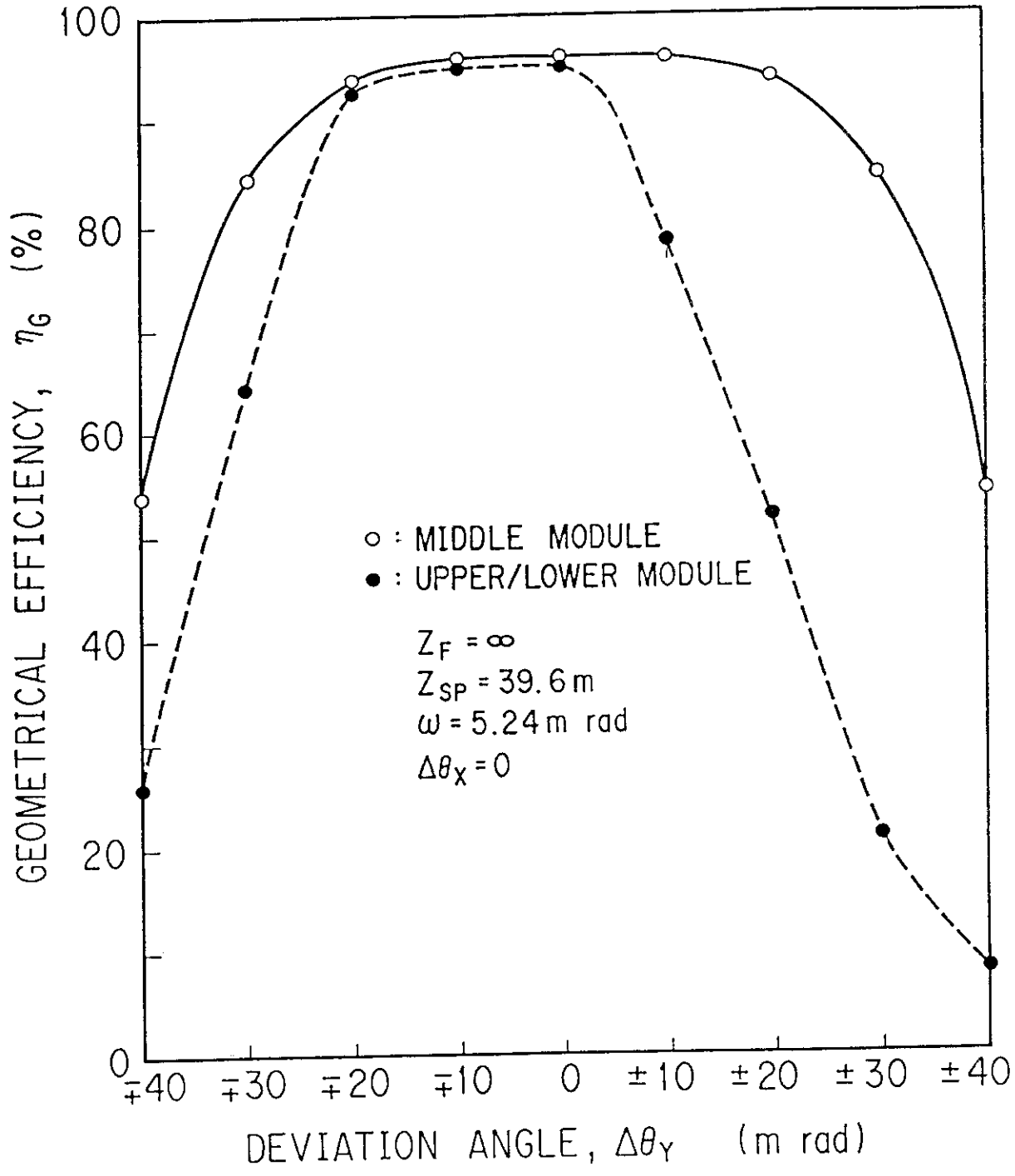

Fig.2.4-10 Calculated geometrical efficiency as a fumction of deviation angle in the Y direction when ω =5.24 mrad and $\Delta\theta_x$=0.

2.4.3 Neutralization Efficiency

The accelerated D^- ions are converted to D^0 by the collision with D_2 molecules in the neutralizer. Neutralization efficiency strongly depends on a beam energy and a line density in the neutralizer. To obtain maximum neutralization efficiency, we need to increase the line density with the beam energy. Figure 2.4-11 shows the relation between the beam energy and the optimum line density. The optimum line density which gives maximum neutralization efficiency tends to increase with the beam energy. At the beam energy of 1.3 MeV, the optimum line density is 1.7×10^{16} molecules/cm^2. The neutralization efficiency is 62 % as shown in Fig.2.4-12. The fractions of D^+ ions and D^- ions are 23 % and 15 %, respectively.

In the initial phase of the ITER experiment, hydrogen discharge is planned. The optimum line density for hydrogen is 3.0×10^{16} molecules/cm^2, which is about twice the value for deuterium as shown in Fig.2.4-13.

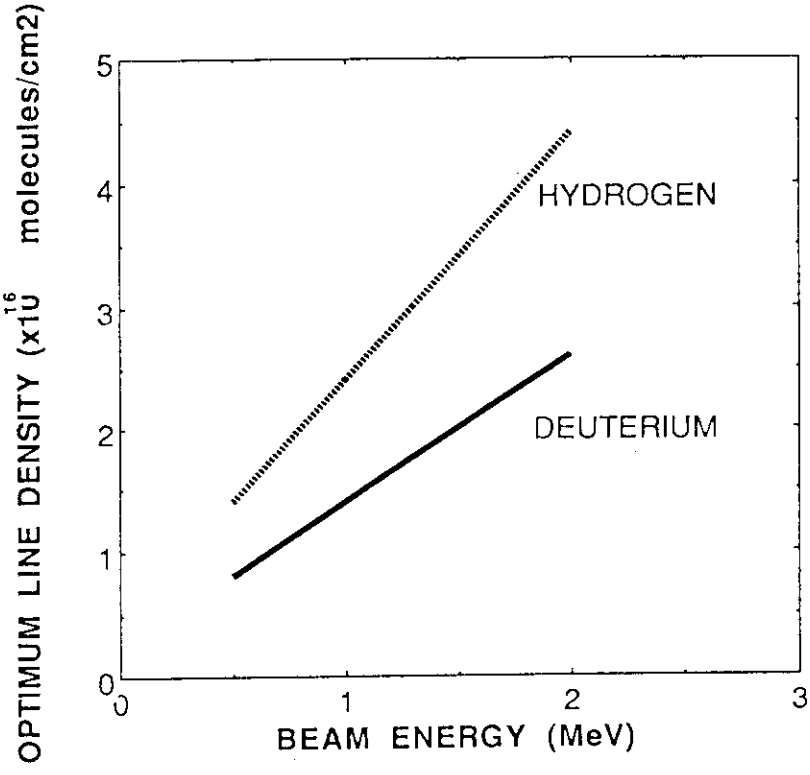

Fig.2.4-11 Dependence of the optimum line density on the beam energy.

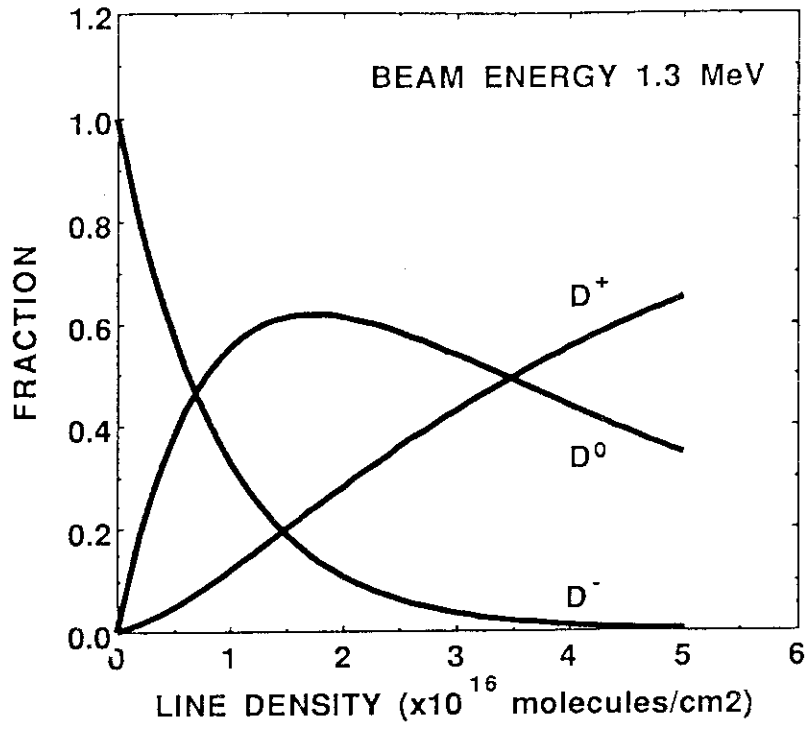

Fig.2.4-12 Dependence of the fraction of deuterium beams on the line density at a beam energy of 1.3 MeV.

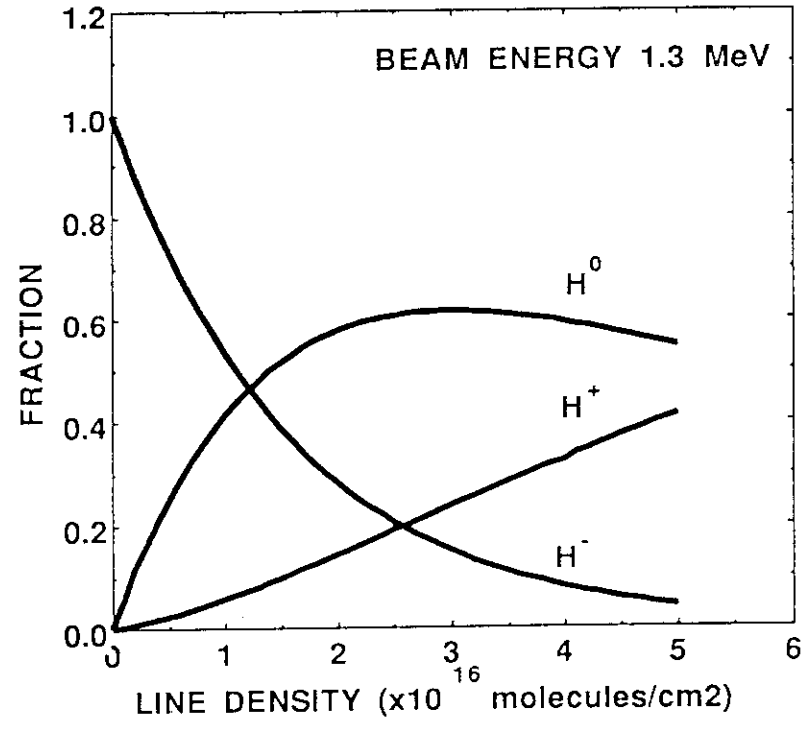

Fig.2.4-13 Dependence of the fraction of the hydrogen beams on the line density at a beam energy of 1.3 MeV.

2.4.4 Reionization Loss

The neutral beam transported through the long drift tube is lost by the reionization process. The loss is given by the following equation,

$$\eta_{RI} = 1 - \exp(-n\,\sigma\,L),$$

where σ is the cross section for the electron stripping, which depends only on the beam energy, and nL is the line density in the drift tube. The line density is calculated by the equation of

$$nL = \frac{(P_T + P_{BD})}{2} \times 2.66\times10^{14} \times L \ (\text{molecules/cm}^2)$$

where P_T is the pressure at the first wall position of the NBI port, and P_{BD} is the pressure in the beam dump room. Though the pressure P_T is estimated to be less than 1×10^{-3} Pa[1], it is not clear yet due to the inflow of scattered molecules from the first wall. Therefore, we assumed P_T be 0.002 Pa which includes some margin. The reionization loss can be reduced by decreasing the pressure P_{BD}. However, the decrease of P_{BD} is limited because the big cryo-pump is needed. From the view point that the reionization loss must be less than 5 % and the pumping speed be less than about 1000 m^3/s, the design value of P_{BD}=0.003 Pa is adopted. This value can be maintained by the cryo-pump of 1000 m^3/s. When the drift tube length L is 32 m, and then the line density is 2.2×10^{15} molecules/cm^2, the value of η_{RI} is calculated as the function of the beam energy , which is shown in Fig.2.4-14. The reionization loss is no more than 5 % at the beam energy of 1.3 MeV. This value is allowable enough to transport the neutral beam efficiently. When the hydrogen working gas is used at the beginning of the experiment, the reionization loss becomes 3 %, so long as the pressure PBD can be fixed.

Reference

[1] S.A. Cohen and H.J. Hopman : ITER Report (ITER-JL-HD-4-9-11) (1989)

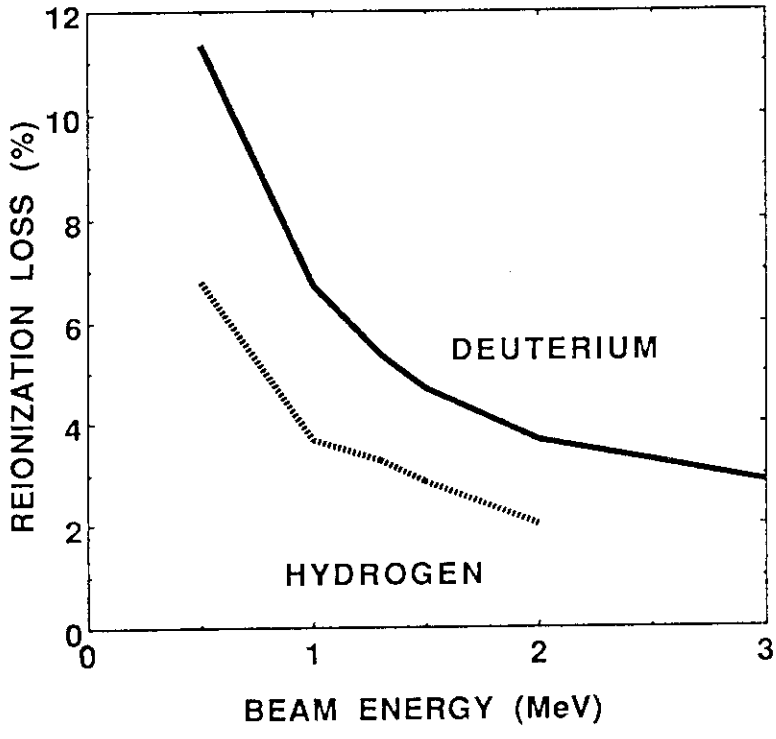

Fig.2.4-14 Dependence of the reionization loss of 1.3 MeV beams on the beam energy at the constant pressure of P_T=0.02 Pa and P_{BD}=0.03 Pa.

2.5 System Efficiency

Maximum injection power P_{INJ} of each unit is 10 MW at the beam energy of 1.3 Mev. Required acceleration current I_{ACC} is 17.5A, which was obtained using the following equation.

$$I_{ACC} = P_{INJ} / E_B \times (1-e_{RI}) \times e_G \times e_N \times e_{ACC}$$

where

P_{INJ}	: Injection power	= 10 MW
E_B	: Beam energy	= 1.3 MeV
e_{RI}	: Reionization loss	= 5 %
e_G	: Geometric efficiency	= 86 %
e_N	: Neutralization efficiency	= 61 %
e_{ACC}	: Acceleration efficiency	= 33 %

is I_{acc} = 17 A. Extracted current I_{D-} from the ion source is I_{D-} = 26.8 A. In this case outputs of power supplies are as follows:

Cathode Power Supply	:	15 V x 6000 A
Arc Power Supply	:	70 V x 3000 A
Bias Power Supply	:	2 V x 300 A
PG Filter Power Supply	:	2 V x 4 kA
Extraction Power Supply	:	8 kV x 60 A
Electron Suppression Power Supply	:	5 kV x 12 A
EG Filter Power Supply	:	2 V x 2 kA
Pre-acceleration Power Supply	:	92 kV x 23.1 A
Acceleration Power Supply	:	1200 kV x 16.5 A

Efficiency of each power supply is

Cathode, Bias, PG Filter, EG Filter	: 40 %
Arc	: 60 %
Extraction, Electron Suppression, Pre-acceleration	: 90 %
Acceleration	: 85 %

and total input power of power supply system is 26862 kW.

Auxiliary facility power for cooling water system, vaccum system etc. are 9 MW for 9 units. Required total power per unit is 27862 kW. Therefore, system efficiency e_{NBI} of NBI system is 0.359.

3. BEAMLINE MODULE

3.1 Ion Source

The ion source produces 16.5 A, 1.3 MeV D^- ion beams continuously with good beam optics. The design parameters of the ion source are principally based on the experimental results on the JAERI Multi-Ampere H^- Ion Source, which produced a 10 A, 50 keV H^- ion beam in the Cs-seeded operation[1].

Figure 3.1-1 shows the structure of the ion source. The source consists of a plasma generator, an extrator, an acclerator, and a high voltage insulator. The D^- ions are produced in the Cs-seeded plasma generator and extracted by the extractor. In the extractor, the D^- ions are pre-accelerated up to 100 keV. The electrons extracted from the plasma are deflected magnetically and removed from the beam. Only the negative ions are accelerated up to 1.3 MeV in the six-stage electrostatic accelerator. The major specifications of the source are listed in Table 3.1-1.

Reference

[1] Y. Okumura et al.: Proc. 16th Symp. on Fusion Technology, London, UK, Sept. 1990.

Table 3.1-1 Basic Specifications of the Ion Source

Ion Species	: D^- and H^-
Energy (Maximum)	: 1.3 MeV
Current	: 16.5 A
Pulse Length (Maximum)	: 350 hours
Beam Divergence	: 5 mrad
Gas Input	: 5.4 $Pa.m^3/s$
Power Input	: 250 kW (Plasma Genertor) 2.8 MW (Extractor) 23 MW (Accelerator)
Dimensions	: 2.5 m in outer diameter about 2.6 m in height
Weight	: 25 ton

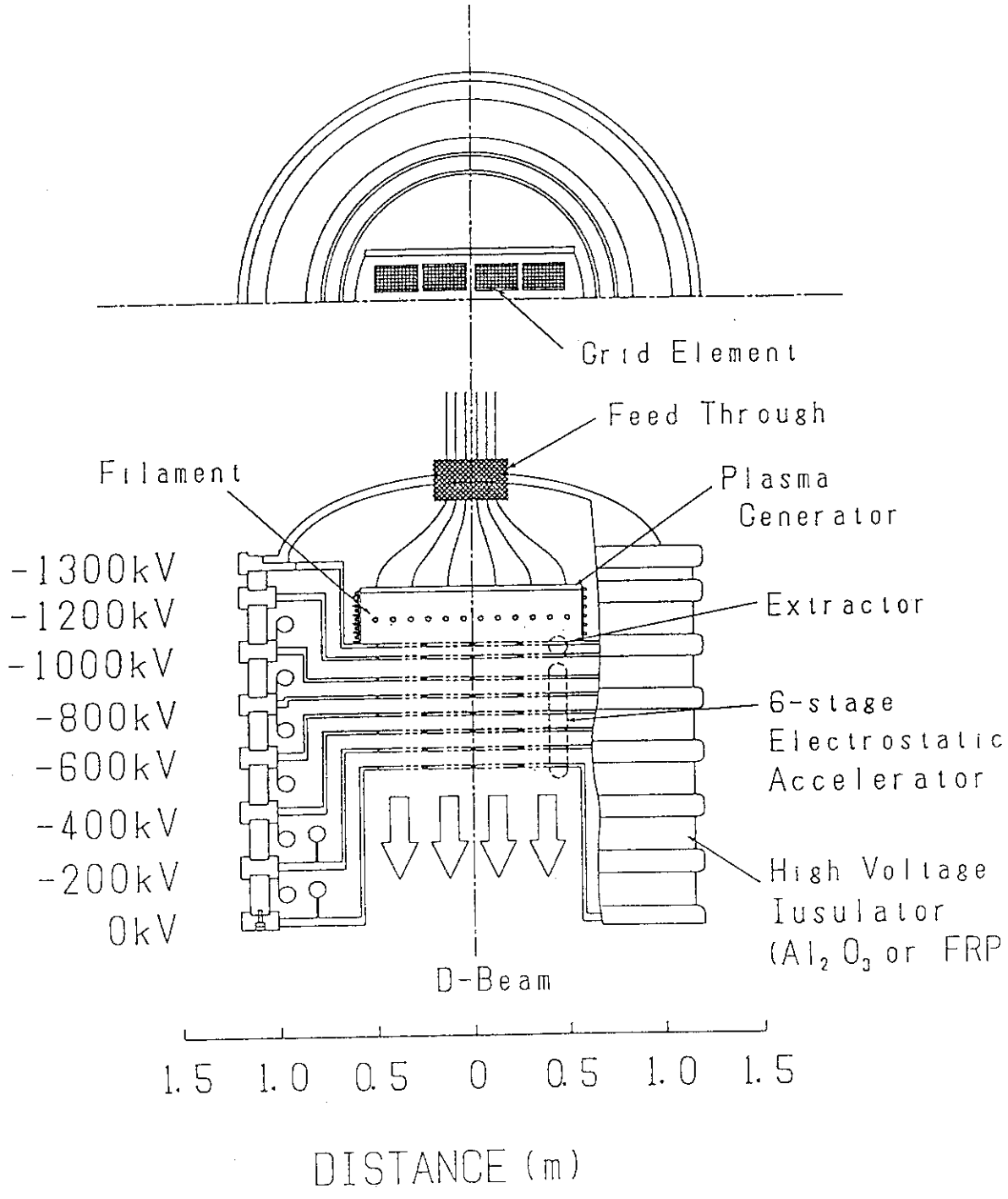

Fig. 3.1-1 A Cross-sectional view of the 1.3 MeV, 16.5 A negative deuterium ion source

3.1.1 Plasma generator

The plasma generator should produce enough density of D^- ions over the large extraction area of 40 cm x 104 cm with a good gas and an electrical efficiencies. The major specifications are as follows;

1.	Type	: Magnetically Filtered Cs-seeded Multicusp Source
2.	Size	: 116 cm x 52 cm
3.	Magnetic Filter	: PG Filter (Electro-Magnetic Filter)
4.	Current Density	: 22 mA/cm^2 for D^-
5.	Gas Pressure	: 0.5 Pa
6.	Gas Flow Rate	: 5.4 $Pa.m^3/s$
7.	Arc Current	: 3 kA
8.	Arc Voltage	: 70 V
9.	Cathode	: Impregnated Cathode
10.	Cs Consumption Rate	: < 5.8 g/two weeks

Source Type

Out of three major methods to generate negative ions; i.e. double-charge exchange, surface production and volume production, the volume production is the most attractive one for use in neutral beam injector. Because this method has big advantages over the other two methods;

(1) The structure of the source is simple, and scale-up is easy.
(2) Produced negative ions have low thermal energies. Hence, low beam divergence is expected.
(3) Operation of the source is easy and reliable.

However, it has been turned out that the current density obtained in the 'pure' volume source is limited to be a moderate value (< 10 mA/cm^2). Although higher current density is achievable by increasing the operating pressure, the source has to be operated at a pressure lower than 0.5 Pa. Otherwise the stripping loss of the negative ions becomes very big, resulting in a low acceleration efficiency and a severe heat dissipation in the accelerator electrodes. In addition, a large amount of electrons tend to be extracted with the negative ions, causing severe heat loadings to the extractor.

These defects of the 'pure' volume source can be overcomed by seeding a small amount of cesium into the source [1][2]. In the Cs-seeded source, not only the negative ion yield is enhanced but also the operating pressure can be decreased drastically. Besides, the extracted electron current can be reduced almost zero.

Hence, we chose the Cs-seeded volume source. The magnetically filtered multicusp plasma generator is considered to be the most promissing one in scaling up the source.

Current Density

Although the highest current denisty achieved in the JAERI Multi-Ampere Source was 37 mA/cm^2 at the exit of the source (more than 50 mA/cm^2 at the plasma emitter), the design value was chosen to be 22 mA/cm^2 at the plasma emitter. Besides the isotope effect on H^- and D^- ions, there are several reasons why we chose the moderate current density;

a) Reducing the operating pressure is necessary to reduce the stripping loss of negative ions in the acclerator column at the expense of the current density.

b) Lower current dinsity is preferable for reliable operation because the required electric field becomes lower.

c) In practice, increasing the current density is not effective very much to reduce the size of the ion source, because the size is mainly determined by the distance required for high voltage insulation.

Figure 3.1-2 shows the H^- ion beam current achieved in the JAERI Multi-Ampere Source as a function of the pressure in the plasma generator. The source produced a 7.4 A H^- ion beam at 0.5 Pa. As the total extraction hole area is 276 cm^2, the current density is 27 mA/cm^2. Since about 16 % of the extracted H^- ions are stripped in the extractor, the current density at the plasma emitter is estimated to be 32 mA/cm^2. Assuming the isotope effect being $J_{H^-} : J_{D^-} = 1 : 1/\sqrt{2}$, the D^- current of 22 mA/cm^2 is achievable.

The isotope effect was studied by US-Japan Collaborative Experiment on D^- production in 1989 and found that the current density of D^- ions was 80 % of that of H^- in the 'pure' volume source [3]. We have not the data base for the isotope effect on the Cs-seeded volume source.

Magnetic Filter

In order to enhance the negative ion production and to reduce the destruction of the negative ions, the plasma generator is divided into two regions by a transverse magnetic field, which is called magnetic filter. In the ITER ion source, the magnetic filter is formed by flowing a big current into the plasma grid itself. This filter called "PG Filter" [4] has several advantages over other filters such as "Virtual Filter" and "Rod Filter";

(a) A uniform filter field can be produced over a wide extraction area.

(b) The field strength is tunable by adjusting the flowing current.

(c) There are no obstacles such as the rods in the source plasma.

The current of 8 kA is enough to produce 500 Gauss-cm filter field over the area of 0.4 m x 1.1 m extractor.

Size

The largest negative ion source developed at JAERI has 34 cm x 104 cm semi-cylindrical plasma generator. Scaling up of the multicusp source to 52 cm x 116 cm will be easy.

Plasma Production

The source plasma is generated by arc discharge between the anode and the cathode. Tungstein filament, which is now being used as the cathode, will not be utilized because the life time is too short for the long pulse duration of 350 hours. Long life cathode such as the impregnated cathode should be utilized.

Plasma production by RF is preferable. Although we are trying to produce a dense plasma by both microwave (2.45 GHz) [5] and RF (2-10 MHz), we have not enough data base to design the source.

Cs Consumption Rate

The cesium effect is considered to be due to the surface processes on the cesiated plasma grid surface. Hence, the cesium consumption rate is principally zero once the surface is coated by cesium.

Experimentally, the JAERI Multi-Ampere Source could be operated for 10 days without additional cesium, once 200 mg cesium was injected before operation.

Provided that the consumption rate in the JAERI Multi-Ampere Source is determined by the evaporation rate of cesium from the inner surface of the plasma genertor, the rate in the ITER ion source is estimated to be;

R =(40cmx104cm)/(15cmx40cm) x (2weeks/80 hrs) x 0.2g= 5.8 g/2weeks

This estimation is based on the data shown in Table 3.1-2. However, during the arc discharge, almost all the evapolated cesium is considered to be ionized positively by the collision with electrons (see below estimate), and those ionized cesium will be confined electrostatically in the plasma generator. Hence, the consumption rate will be lower than this estimate.

Table 3.1-2 Comparison of the Cesium Consumption Rate

	Multi-Ampere Source	ITER Ion Source
Extractor Dimension	15 cm x 40 cm	40 cm x 104 cm
Current	10 A (H^-)	16.5 A (D^-)
Consumption Rate	0.2 g/ 80hrs*	5.8 g/ 2weeks

*) Total operation time at high temperature

Consumption Ratio of Cesium

Rate equation of cesium ions is given by;

$$V_p n_o n_e \langle \sigma v \rangle_{ion} = n^+ C_s S_L$$

V_p : Plasma volume
n_o : Density of cesium neutral particles
n_e : Density of electrons which has enough energy to ionize
$\langle \sigma v \rangle_{ion}$: Rate coefficient for ionization
n^+ : Density of cesium ions
C_s : Ion acoustic speed
S_L : Total loss area for cesium ions

Therefore,

$$n^+/n_o = n_e \langle \sigma v \rangle_{ion} V_p / C_s S_L$$

Substituting following parameters;

$n_e = 10^{11}$ cm^{-3}
$\langle \sigma v \rangle_{ion} = 10^{-8}$ cm^3/s
$C_s = 10^3$ cm/s
$V_p/S_L = 40$ cm

The ratio of ions to neutrals is given by;

$$n^+/n_o = 40$$

Therefore, the evapolated cesium is considered to be almost fully ionized and confined electrostatically in the plasma generator.

Impurities

The impurity content in the negative ion beam was measured in the JAERI Multi-Ampere Source [6]. The beam contained O^-, OH^-, and O_2^- ions, whose contents were less than 1 %. No metal impurity was found. Assuming the beam contains 1 % impurities and those injection efficiency is same as the D^- ions, the number of the energetic impurity particles injected into the torus is estimated to be 5.2×10^{-17} atoms/s.

References

[1] Y. Okumura et al.; Proc. 5th International Symp. on Production and Neutralization of Negative Ions and Beams, BNL, American Institute of Physics Conference Proc. No.210, 1990, p.169
[2] Y. Okumura et al.; Proc. 13th Symp. on Ion Source and Ion-Assisted Technology, Tokyo, June 1990, p.149
[3] T. Inoue et al.; Rev. Sci. Instrum. 61, 1990, p.496
[4] M. Hanada et al.; Rev. Sci. Instrum. 61, 1990, p.499
[5] Y. Matsuda et al.; Proc. 12th Symp. on Ion Source and Ion-Assisted Technology, Tokyo, June 1989, p.107
[6] Y. Okumura et al.; JAERI-M 89-090 (1989)

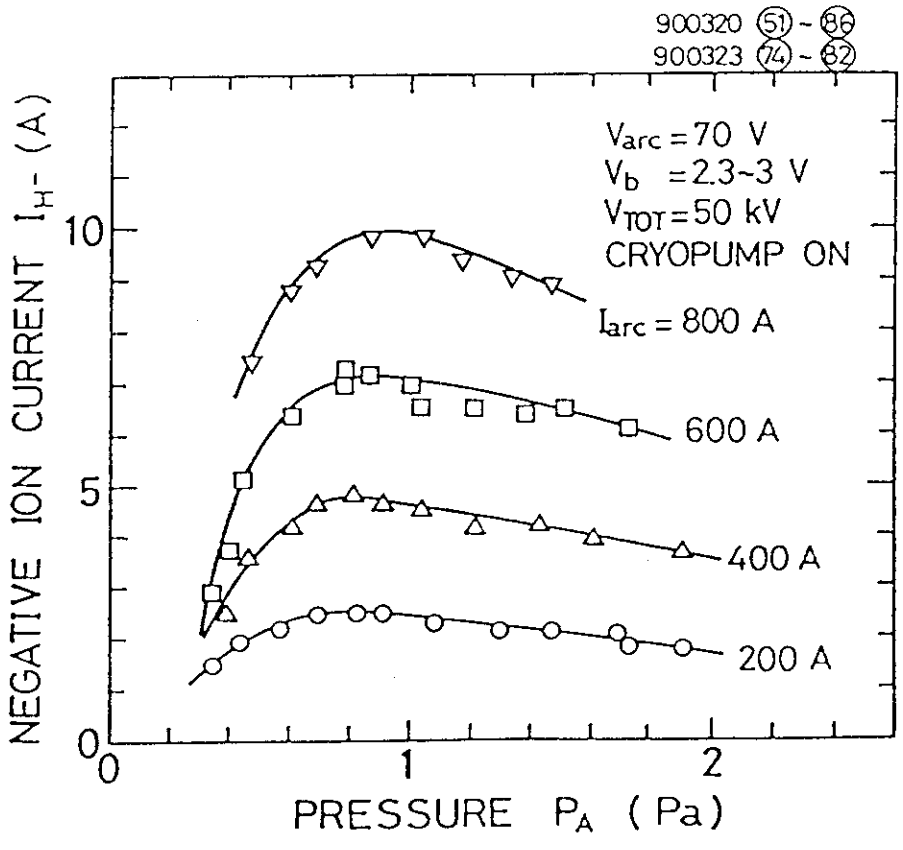

Fig. 3.1-2 The H^- ion current obtained in the JAERI Multi-Ampere Source as a function of the operating pressure. The equivalent current of the design value of the ITER ion source is shown by a black circle.

3.1.2 Extractor

The negative ions are extracted and pre-accelerated up to 100 keV by the extractor with good beam optics. Although some amount of electrons are extracted with the negative ions, those electrons are deflected and eliminated from the beam in the extractor.

The major specifications of the extractor are as follows;

1.	Type	: Two-Stage Extraction, Multi-Aperture, 4 Grids
2.	Extraction Area	: 40 cm x 104 cm, 8 segments
3.	Size of the Segment	: 16 cm x 24 cm
4.	Apertures	: 14 mm ID x 96 apertures x 8 segments (1182 cm^2)
5.	Transparency	: 38 %
6.	D^- Current	: 26 A (at the plasma emitter)
7.	Extraction Voltage	: 10 kV
8.	Pre-Accel. Voltage	: 100 kV
9.	Stripping Loss	: 24 % (0-100kV)
10.	Electron Suppression	: Magnetic Field produced by PG/EG Filter

Structure

The extractor consists of four grids called plasma, extraction, electron suppression and pre-acceleration grids. Each grid is divided into 8 segments, and each segment has 96 apertures. The diameter of the apertures is 14 mm in the plasma grid. These segments are installed on grid supports and adjusted individually so as to offer geometrical focusing of the beam.

Figure 3.1-3 shows the aperture pattern of the segment. An example of the beam trajectory in the extractor is shown in Fig.3.1-4.

Electron Suppression

In order to prevent the electrons from being extracted and accelerated, the electrons are suppressed in the following three stages;

1. By biasing the plasma grid positively with respect to the anode, the electrons are swept away to the plasma grid.

2. Extracted electrons are deflected by the transverse magnetic field in the extraction grid.

3. The secondary and/or the reflected electrons at the extraction grid are suppressed by applying a negative bias voltage to the electron suppression grid.

EG Filter

By flowing a reverse current in the extraction grid with respect to the PG filter current, a strong magnetic field can be produced between the plasma and the extraction grids. This field called EG filter can be used for the electron suppression.

In addition, the beamlet axis can be adjusted by controlling the PG/EG filter current.

The currents of 9 kA to the PG filter and 4 kA to the EG filter are enough to produce 500 Gauss-cm filter field in the plasma generator and 240 Gauss-cm magnetic field for the electron deflection.

Extracted Electron Current

The electron current extracted in the Cs-seeded source is very small. For example, only 5 A electron current was flowing into the extraction grid when 10 A H^- ion beam was produced in the JAERI Multi-Ampere Source. The electron current is estimated to be an order of 15 A. The heat load of the extraction grid is therefore around 75 W/cm^2 in average, which is a permissible value for the long pulse operation.

Stripping

Although 26 A D^- ions are extracted from the source plasma, about 24 % of the ions are neutralized in the extractor as estimated in 2.4.1.

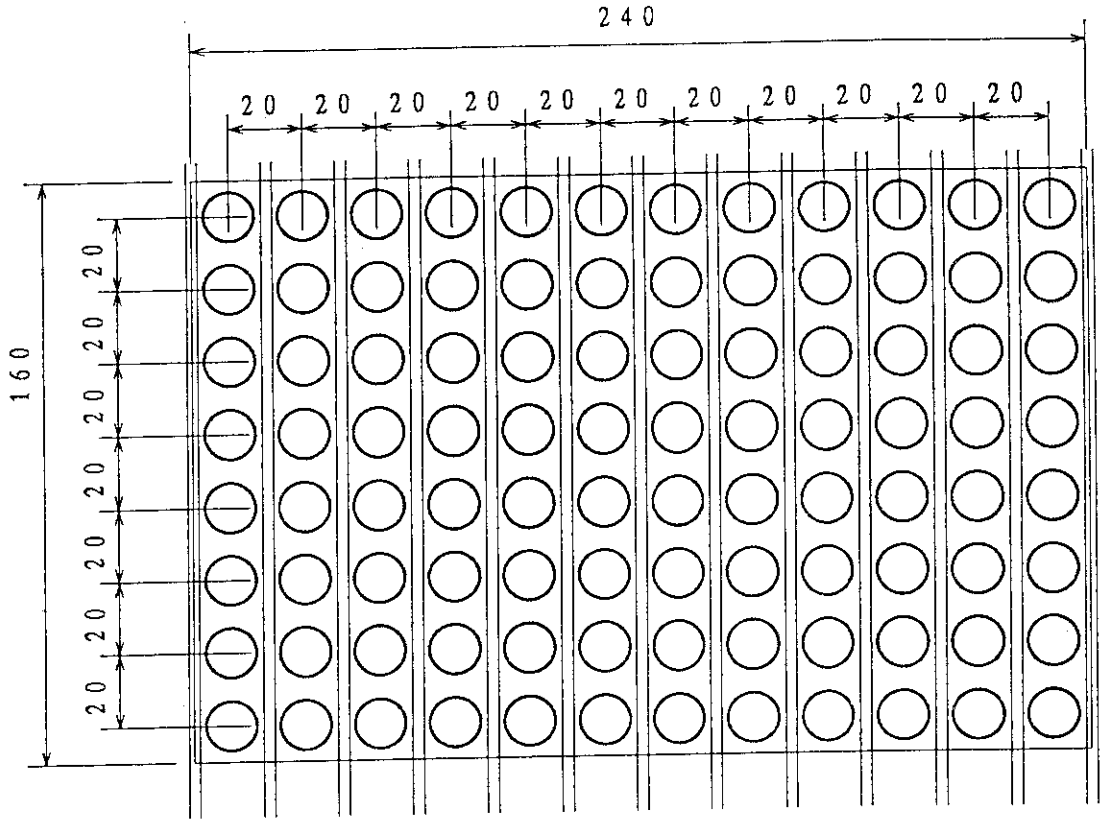

Fig. 3.1-3 The extraction aperture pattern in the plasma grid segment. Each grid has 8 segment of the size of 16 cm x 24 cm.

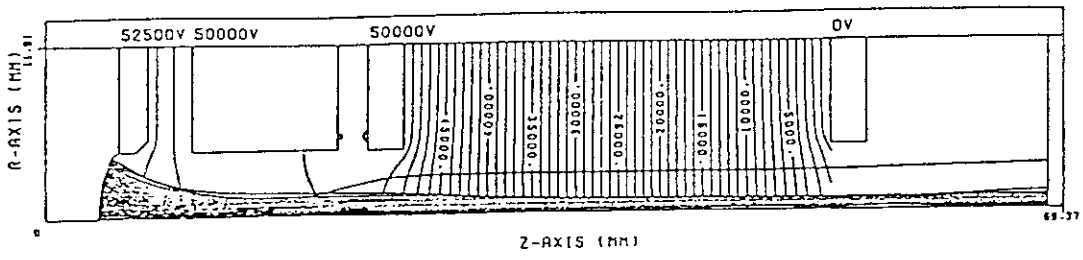

Fig. 3.1-4 An example of the beam trajectory in the extractor.

3.1.3 Accelerator

The D^- ion beams formed in the extractor are acclererated up to 1.3 MeV by the accelerator with keeping good beam optics.

The major specifications are as follows;

1. Type	:	Electro-Static Acceleration, 6 Stages, Multi-Single Acceleration
2. Acceleration Area	:	40 cm x 104 cm, 8 Segments
3. Size of the Segment	:	16 cm x 24 cm
4. Accel. Voltage	:	200 kV/stage
5. Accel. Current	:	16.5 A
6. Stripping Loss	:	12 % (0.1-1.3 MeV)
7. Electron Suppression	:	Magnetic Field across the Aperture
8. Ion Suppression Grid	:	None
9. Beam Divergence	:	< 5 mrad

Structure

The accelerator consists of 6 grids or 6 stages, in each stage the negative ion beam is accelerated by 200 keV. Figure 3.1-5 shows a schematic of the acclerator. Multiple beamlets from the extractor are merged and accelerated through a large aperture or slot in the accelerator. This 'multi-single' type accelerator is adopted to reduce the stripping loss in the accelerator.

In the conventional 'multi-multi' accelerator, where each beamlet from the extractor is accelerated through an individual channel of the accelerator, the conductance of the accelerator is poor so that the residual gas pressure becomes high.

The stripping loss in the multi-single type is estimated to be approximately half of that in the multi-multi type.

Electron Suppression

Free electrons are produced by the stripping, ionization and secondary electron emission in the acceleration gaps. Preventing those electrons from being accelerated at a high energy is very important to

improve the voltage holding and to reduce the acceleration drain current.

To suppress those electrons, small permanent magnet is installed in the accelerator apertures. The electrons with energy of 200 keV can well be reflected by the transverse magnetic flux of 1500 Gauss-cm.

CCVV(Constant Current Variable Voltage) Operation

The CCVV operation can be realized with this acceleration system. As the acceleration power supply is composed of 200 keV power supply modules, the beam energy can be varied from 100 keV to 1.3 MeV, by switching on or off the modules. This concept is shown in Fig. 3.1-5.

Ion Suppression Grid

Backstreaming positive ions from the neutralizer plasma is estimated to be 0.07 % of the accelerated negative ion beams at 1.3 MeV. Hence, the ion suppression grid was eliminated.

3.1.4 High Voltage Insulator

The insulator should have enough voltage holding power and enough strength to support the total weight of the ion source. Besides, the insulator should endure the baking to avoid the cesium condensation. The major specifications are as follows;

1. Size	: 2.4 m OD, 30 cm height
2. Material	: Almina Ceramic
3. Voltage Holding in Vacuum	: > 10 kV/cm
4. Outgas	: $< 10^{-4}$ Pa.m^3/s
5. Carbonization	: Small
6. Baking Temperature	: 150-200°C
7. Neutron Damage	: $> 10^{16}$ n/cm^2

A large insulator (2.4 m OD, 24 cm height) made of voidless FRP has been manufactured and tested up to 150 keV.

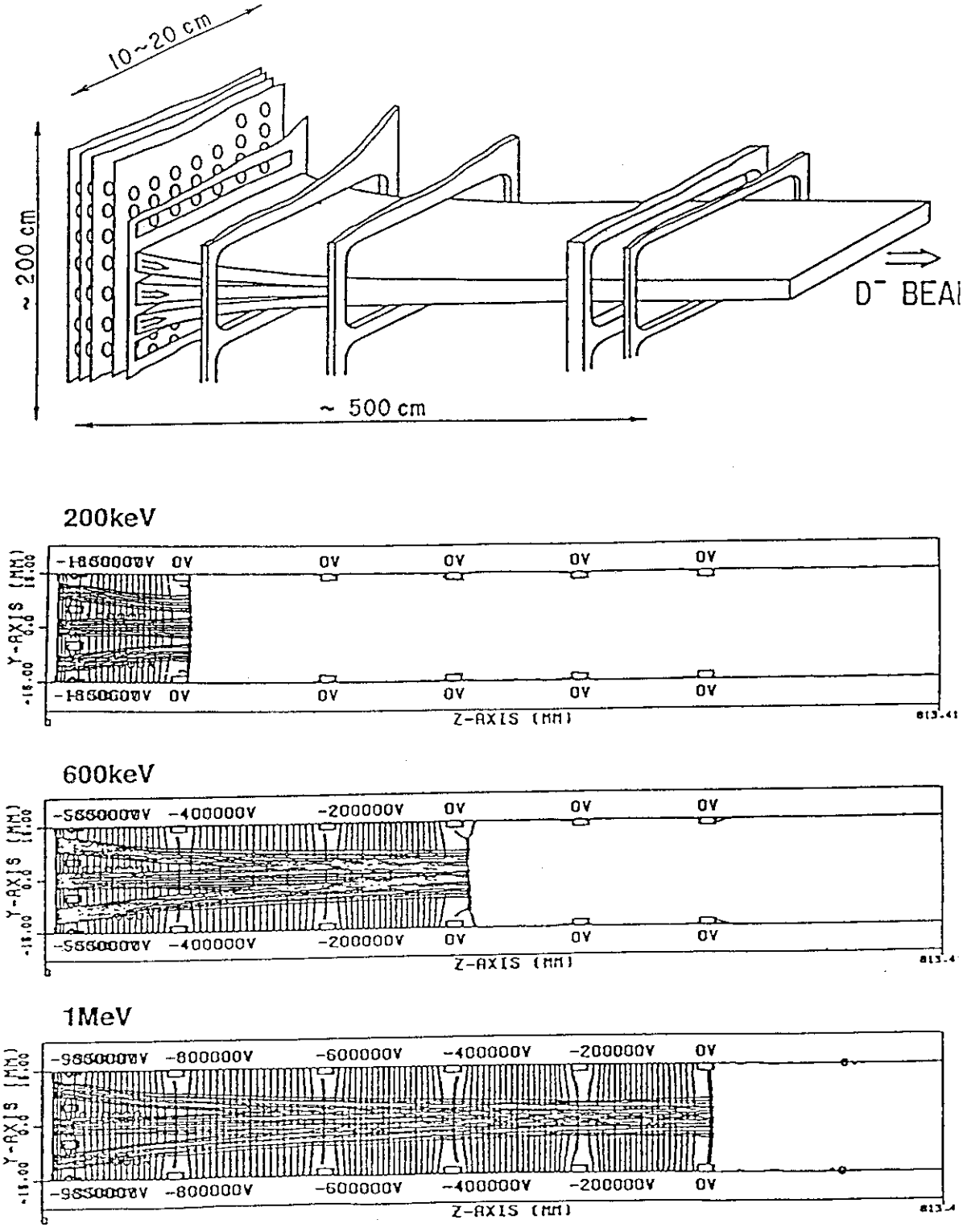

Fig. 3.1-5 A Schematic of the accelerator and an example of the beam trajectory in CCVV acceleration.

3.2 Beam Steering Mechanism

The beam steering mechanism is used to adjust the beam direction precisely into the injection port. The beam is steered mechanically by remote control, if necessary, during the beam pulse.

The major specifications are as follows;

1.	Type	: 2-Dimensional Steering Mechanism
2.	Dimensions	: about 3m high x 3m wide x 0.4m thick
3.	Inner Bore	: 2.0 m
4.	Materials	: Mild steel & stainless steel
5.	Weight	: 2 ton
6.	Steering Angle	: $\pm$ 20 mrad for both X- and Y-axis
7.	Steering Speed	: 0.1 mrad/s
8.	Durability	: 1000 cycles

A large diameter bellows is welded to flanges in both sides, and the distance between the flanges is variable by moter driving. The flanges are made of mild steel and μ-metal is installed inside of the bellows so as to shield the beam from residual magnetic field.

3.3 Source Disconnecting Valve

This valve is mounted between the beam steering mechanism and the vacuum vessel, and used when the ion source is removed for maintenance. This valve can be divided into two sections, each of which has a door with an inner bore of 2 meters. When the ion source is demounted, this valve is separated between the two sections. Since each door is closed and innert gas is filled in both the source and the vacuum vessel, the tritium gas and the activated materials does not leak out in the NBI room during the maintenance phase.

The major specifications are shown below:

1.	Dimensions	: about 4m h x 7m w x 0.5m t
2.	Inner bore	: 2.0 m
3.	Weight	: 40 ton
4.	Materials	: Aluminum alloy, SS, Mild steel & μ-metal
5.	Air Seal	: Aluminum or Viton
6.	Leak rate	: 1 x 10E-2 Pa.m^3/s for T_2
7.	Bakeout temperature	: 200°C
8.	Stroke	: 2.25 m
9.	Driving method	: Pressurized CO_2 gas at 10 atm.
10.	Open-close time	: 10 s
11.	Durability	: 100 cycles

The structure of the valve is shown in Fig.3.3-1. A part of the valve disk is made of mild steel and u-metal, so that the magnetic shield be continuous between the beam steering mechanism and the vacuum vessel.

From the manufacturing point of view, this valve does not require a particular technology.

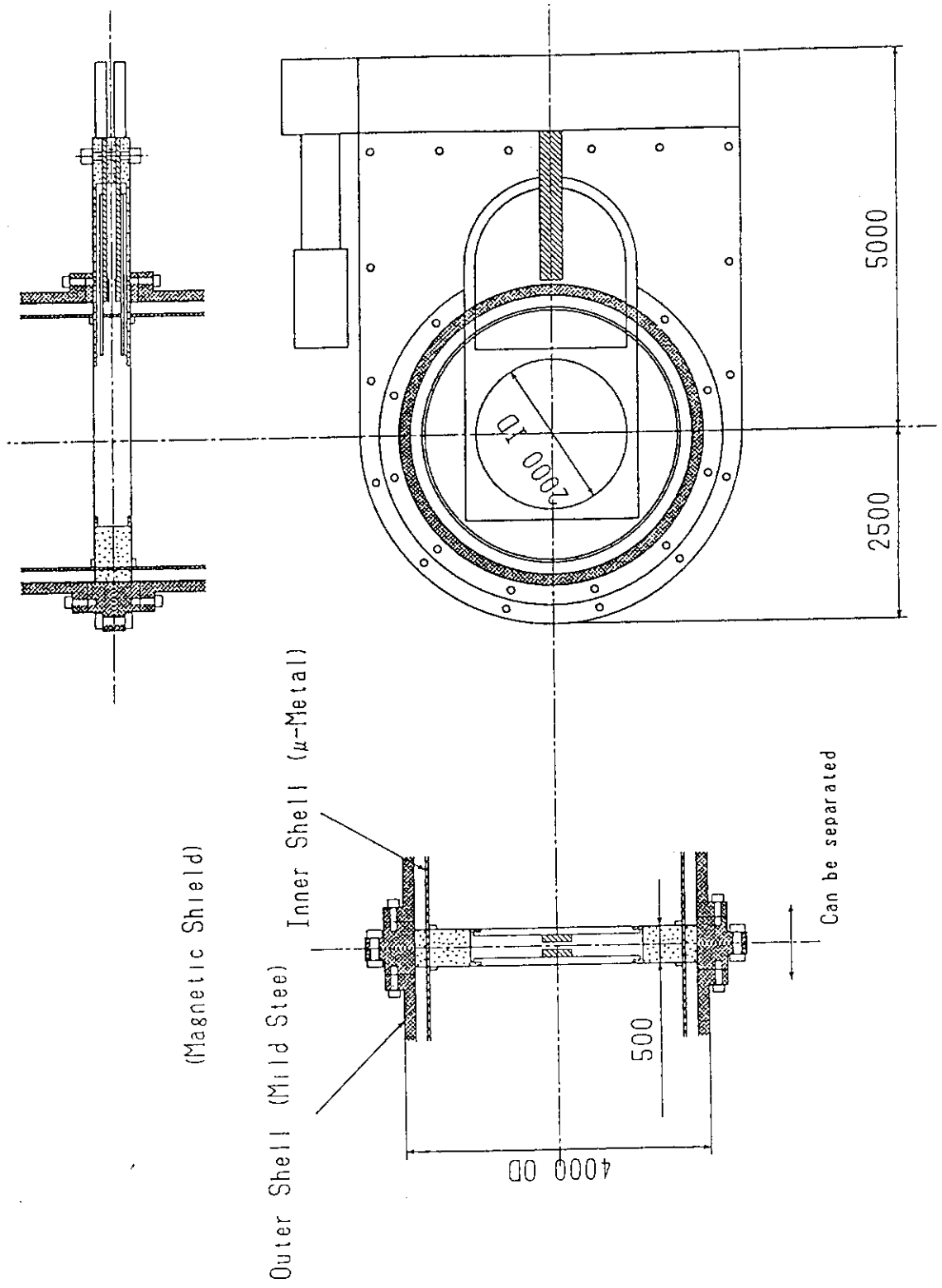

Fig. 3.3-1 Structure of the source disconnecting valve.

3.4 Beam Profile Controller

(a) Purpose of current profile control

In tokamak devices, control of plasma current profile is important from the viewpoints of beta enhancement, control of sawtooth oscillation, and suppression of major disruptions. This includes both detail control (e.g.,flattening the current in the neighbourhood of q=2 surface to suppress m=2 MHD activity) and bulk profile control (e.g., controlling q(o) and the internal inductance of the plasma). Beam profile controller in neutral beam system for ITER will be used for the bulk profile control.

(b) Concept of beam profile control

Figure 3.4-1 shows a schematic view of a neutral beam injector with the beam profile controller. Energetic negative deuterium or hydrogen ion beams extracted from a negative ion source are magnetically bent by a field produced by the coils of the beam profile controller, before entering in the neutralizing cell. Because the negative ions are easily stripped in collisions with neutral gas particles, the pressure in the region between the ion source and the neutralizer should be kept below about 0.02 Pa, making use of cryopanels with high pumping speed.

After passing through the profile controller, the negative ions enter in the neutralizer. Some of them are neutralized, and the other remains as negative ions or are converted into positive ions, after passing through the neutralizing cell. The residual ions will be magnetically or electrostatically bent to hit the ion dump. On the other hand, the neutralized particles go straight towards the tokamak, keeping the direction that the negative ions have had just before the neutralization.

In the way descibed above, the spatial intensity distribution of neutral beams at the torus position can be controlled by changing the electric current in the coils of the beam profile controller.

Since any change of operating parameters of the ion source is not necessary to change the beam profile, this system can control the beam profile at the torus without changing the neutral beam power level during one pulse of beam injection, if the size of injection port is sufficiently large, especially in vertical direction.

(c) Requirement to profile control

It is reqiured that the beam profile controller can form a hollow, a flat, and a peaked beam profiles at the torus plasma. Of these, a flat profile is preferable for a steady state operation in the technology phase of ITER, based on a numerical simulation study of current drive physics.

(d) Design of beam profile controller

Geometrical configuration of ITER NBI is shown in Fig.3.4-2.

Common dimensions of ITER NBI are as follows:

Size of injection port	: 800 mm wide, 3400 mm high, and 7800 mm long at most.
Size of one module	: 4000 mm in outer diameter, and about 17000 mm long.
Distance from the ion source to the definition point of tangency of injection	: 46500 mm
Vertical position of three ion sources	: 6500 mm (upper ion source) 0 mm (middle ion source) -6500 mm (lower ion source9
Angle between the axes of the middle ion source and the upper/lower ion sources	: 9.45 ^{o}

Other dimensions of ITER NBI proposed by JAERI are given below:

Grid size of accelerator	: 400 mm wide (140 mm wide x2) 1000 mm high.
Inner size of neutralizer	: 460 mm wide (200 mm wide x 2) 1300 mm high, and 6000 mm long.

Inner size of three drift tubes : 600 mm wide and 1800 mm high each.

Distance between the ion source and the neutralizer : 2500 mm

Considering these dimensions, we decide the dimensions of two coils of the beam profile controller as follows:

Shape of coils : race-track type
Size of coils : 500 mm wide and 1500 mm high each.
Cross-section of coil : 10 mm x 10 mm.
Distance from the ion source to the coils : 2800 mm

Limited by the height and the length of the injection port, ion beams emitted from the upper/lower ion sources can be magnetically bent only downwards/upwards, respectively, to change the beam intensity profile at the torus. Usually, ion beams from the middle ion source are not bent by the profile controller. However, if the vertically unsymmetrical beam profile is required by the physicists, the profile controller of the middle module will be energized to magnetically bend the ion beams upwards or downwards.

(e) Calculation of magnetic field distribution and beam trajectories

Distribution of magnetic field produced by the profile controller and trajectories of deuterium negative ion beams in the field are calculated by a computer code "NBI3DGFN" developed at JAERI.

Figure 3.4-3 shows the distribution of magnetic field vectors on the X-Y plane at Z = 30.5 m (center of the profile controller) for a coil current of 10000 AT. Direction of ion beams is along Z axis. Strength of the field in X direction (Bx) at X = 0, Y = 0 is 141 Gauss.

Figures 3.4-4 (a),(b), and (c) indicate the calculated beam trajectories projected on the X-Z, Y-Z, and X-Y planes, respectively. Beam energy of deuterium negative ions is assumed to be 1.3 MeV. As seen in the figures, the ion beams are not much diverged in both horizontal and vertical directions. That is, parallel beams emitted

from the ion source remains as almost parallel even after passing through the profile controller. Therefore, we may consider that all the ion beams extracted from one ion source are magnetically bent with a common deflection angle. For a coil current of 10000 AT, the common deflection angle is about 1 degree for the beam energy of 1.3 MeV.

(f) Examples of beam profiles at the torus position

Based on the discussion described above, the small-angle deflection of all the ion beams extracted from an ion source by the beam profile controller is nearly equivalent to tilting of the ion source itself around X axis.

Beam profiles at the definition point of injection tangency (Z = 46.5 m , see Fig.3.4-2) are calculated by a computer code "BEAMPROF", taking this equivalence into account. In the calculation, the grid area of 40 cm wide and 100 cm long of the source is divided into 2000 sections, each of which has an area of 2 cm wide and 2 cm long. A beamlet having Maxwellian intensity distibution with e-folding half width divergence angle of 5 mrad is emitted from the center of each small section. Axes of all the beamlets are assumed to be in parallel with each other.

If both the upper and the lower ion sources are tilted with the same angle, the crossing points (Z_{sp}) of the beam axes of the upper and the lower ion sources with the axis of the middle ion source change at the same time (see Fig.3.4.2).

Figures 3.4-5(a),(b),(c), and (d) show the vertical beam profiles at Z = 46.5 m for Z_{sp} = 35.3, 38.0, 39.6, and 46.5 m, respectively. A value of 1.0 E-04/cm^2 on the oridinate corresponds to a heat flux of 2.5 kW/cm^2 for the case of neutral injection power of 25 MW per module.

For Z_{sp} = 35.3 m, vertical beam profile is clearly divided into three parts, corresponding to the beams from the vertically stacked three ion sources. If the middle ion source is switched off, a vertically hollow profile will be realized.

For Z_{sp} = 38.0 m, the tails of the beams from three ion sources are overlapped with each other in the vertical direction.

For Z_{sp} = 39.6 m, vertical beam profile becomes a rather flat distribution even though it has three peakes.

For Z_{sp} = 46.5 m, the profile becomes a vertically hollow distribution with two peaks of high heat flux. This is because about

upper half of the beam from the upper ion source and about lower half of the beam from the lower ion source are scrapered by the injection port.

Figure 3.4-6 indicates the beam intensity contours at Z = 46.5 m for (a) Z_{sp} = 35.3 m, (b) Z_{sp} = 38.0 m, (c) Z_{sp} = 39.6 m, and (d) Z_{sp} = 46.5 m.

Figure 3.4-7 shows the geometrical beam loss calculated for the upper or the lower ion source as a function of Z_{sp}. As can be seen in this figure, the beam loss (and heat load) to the injection port increases rapidly for Z_{sp} below 35.0 m and above 40.0 m. For Z_{sp} between 35.0 m and 40.0 m, the geometrical beam loss of the upper or the lower ion source is only 3 to 5 %. To minimize the probability of failure in the injection port, the value of Z_{sp} should be kept between 35.0 m and 40.0 m. Therefore, it is difficult from an engineering point of view to obtain a peaked beam profile at the torus plasma, if we continue to use the present ITER NBI common dimensions. To obtain the peaked beam profile, the length of the injection port (7.8 m at present) or the angle of 9.45 ^{o} between the beam axes should be decreaed.

Deflection angle necessary to change Z_{sp} from the original value of 39.6 m to 35.0 m is calculated to be about 1.2 ^{o}. Thus, the maximum coil current of about 12000 AT is required to obtain the vertically hollow profile seen in Fig.3.4-5(a) by the profile controller.

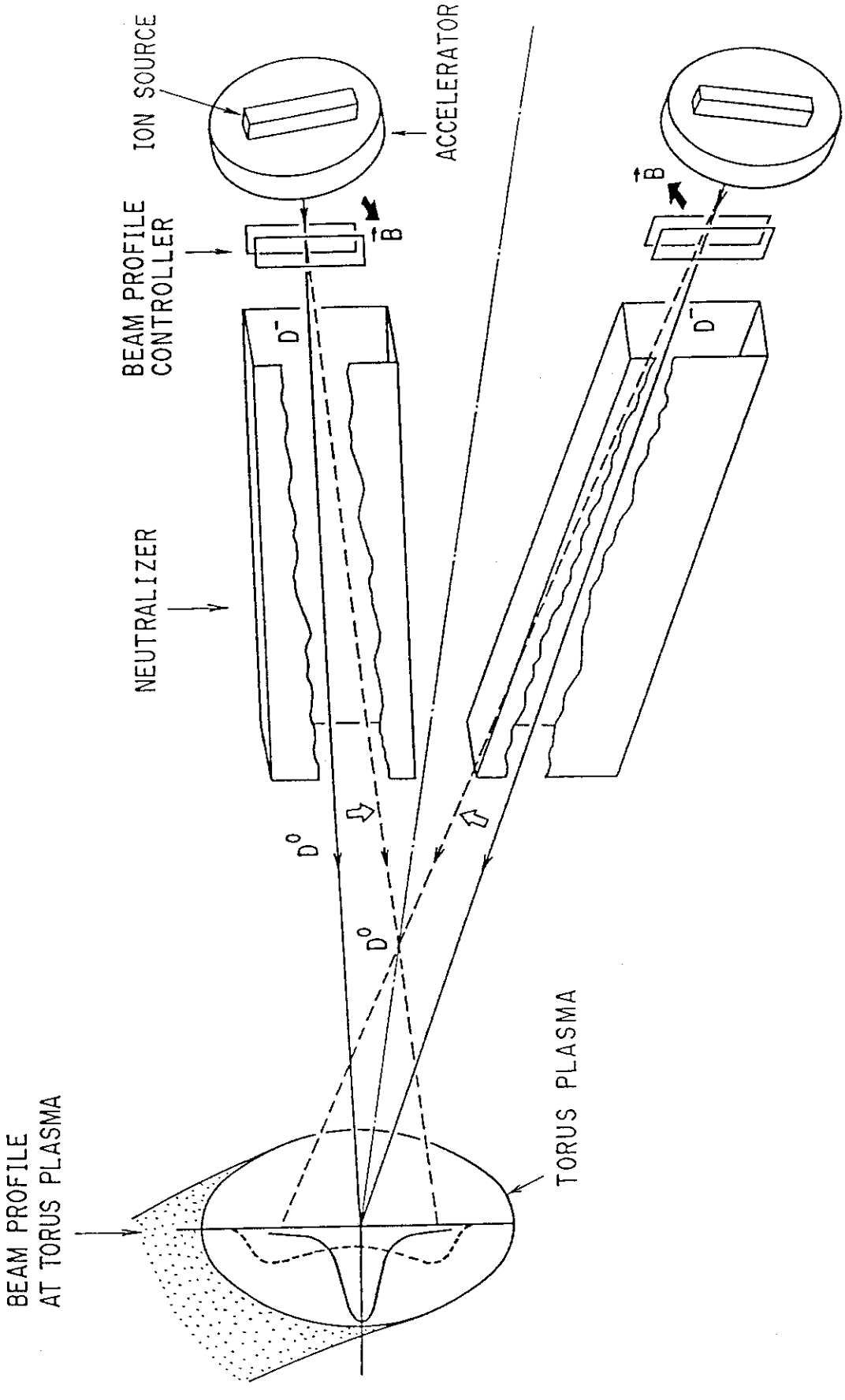

Fig.3.4-1 Schematic view of a neutral beam injector with the beam profile controller.

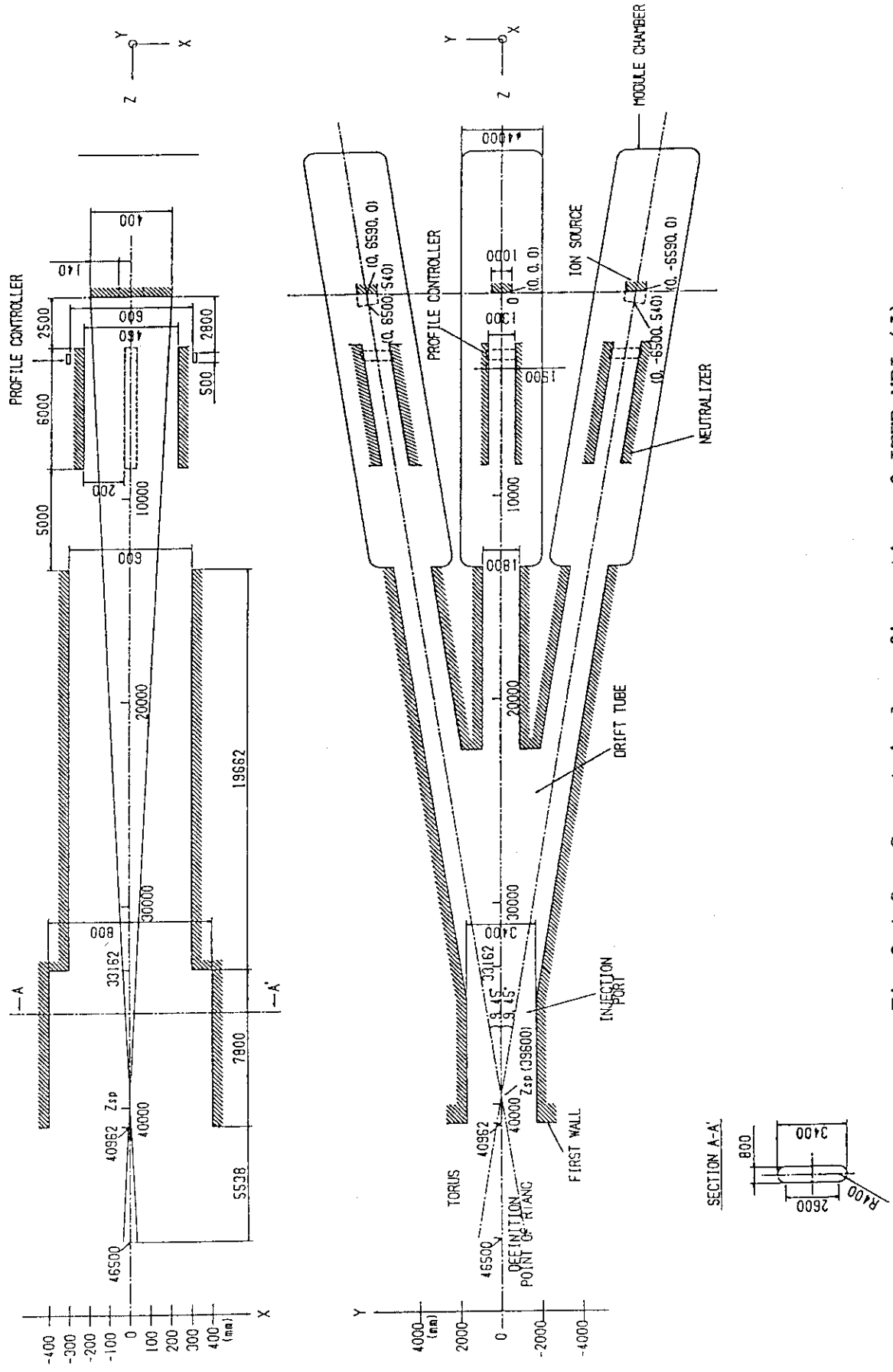

Fig.3.4-2 Geometrical configuration of ITER NBI (J).

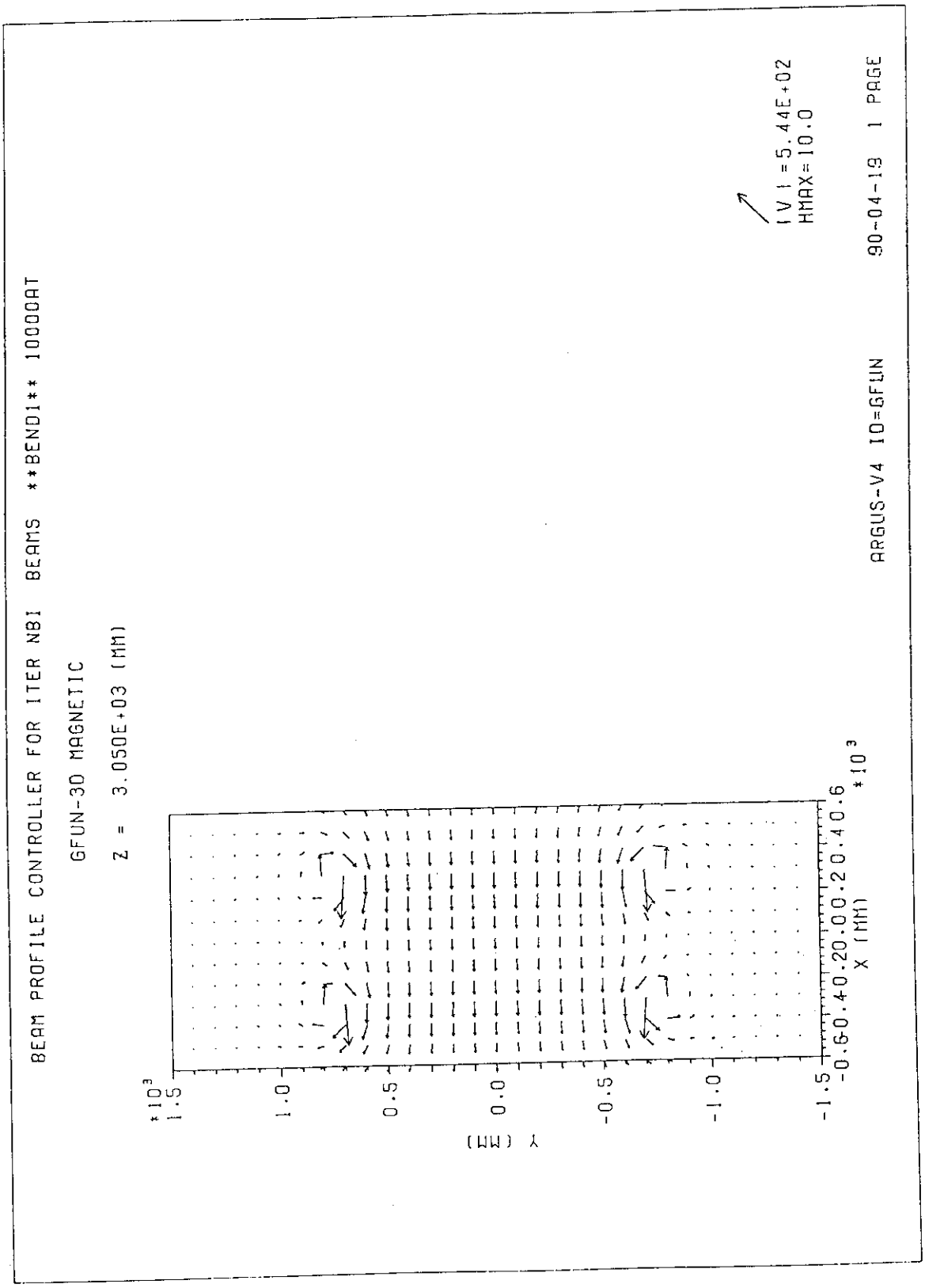

Fig.3.4-3 Distribution of magnetic field vectors on the X-Y plane at Z =3.05 m for a coil current of 10000 A.

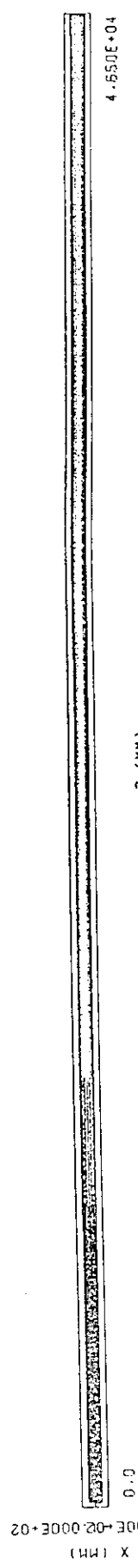

(a)

Fig.3.4-4(a) Calculated beam trajectories projected on the X-Z plane for a coil current of 10000 A.

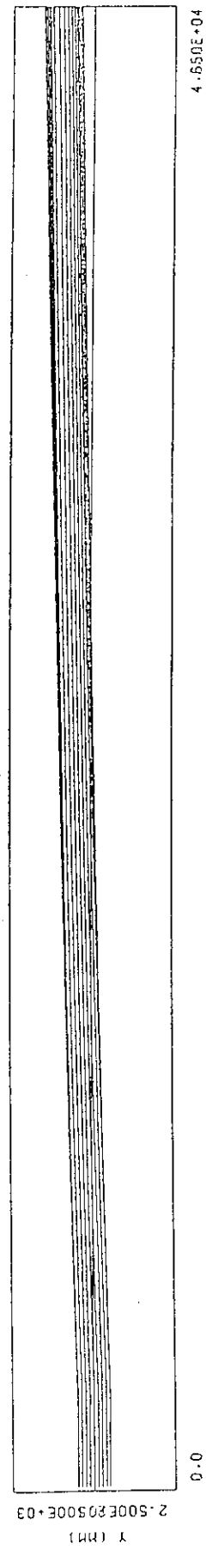

(b)

Fig.3.4-4(b) Calculated beam trajectories projected on the Y-Z plane for a coil current of 10000 A.

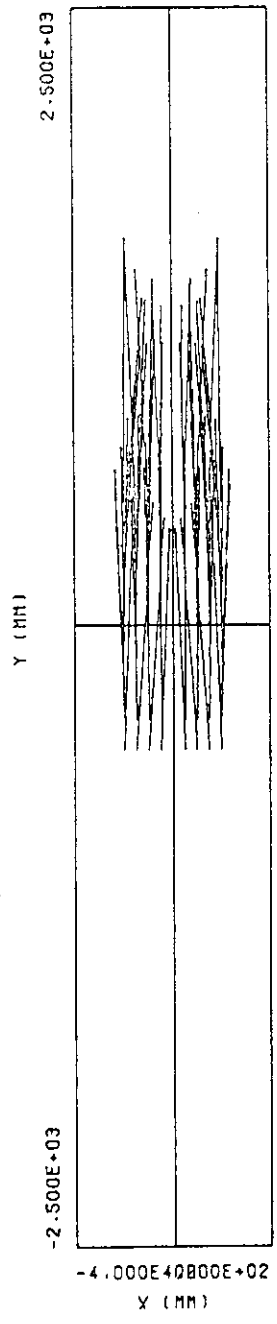

Fig.3.4-4(c) Calculated beam trajectories projected on the X-Y plane.

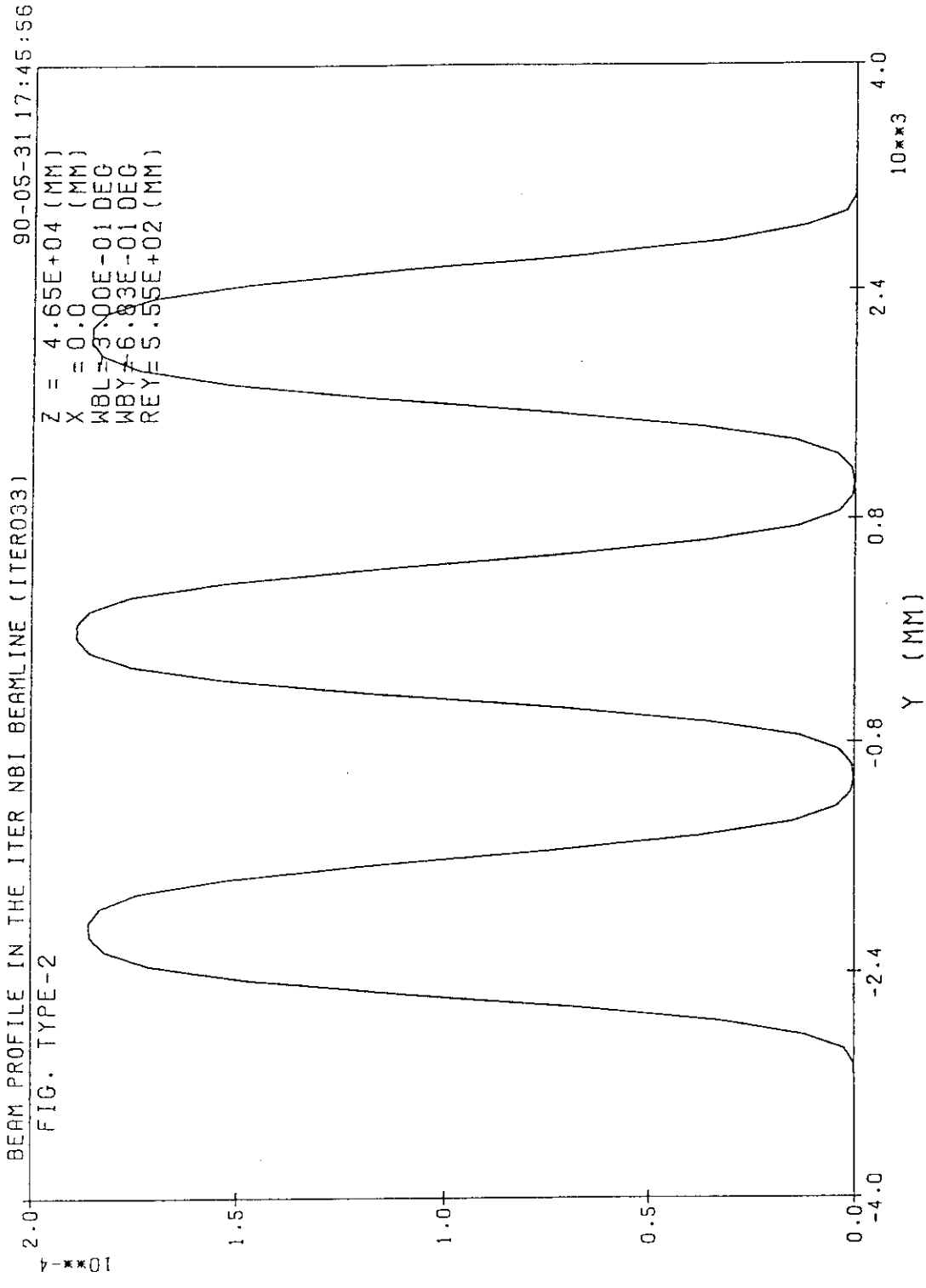

Fig. 3.4-5(a) Vertical beam profile at Z = 46.5 m for Z_{sp} = 35.3 m.

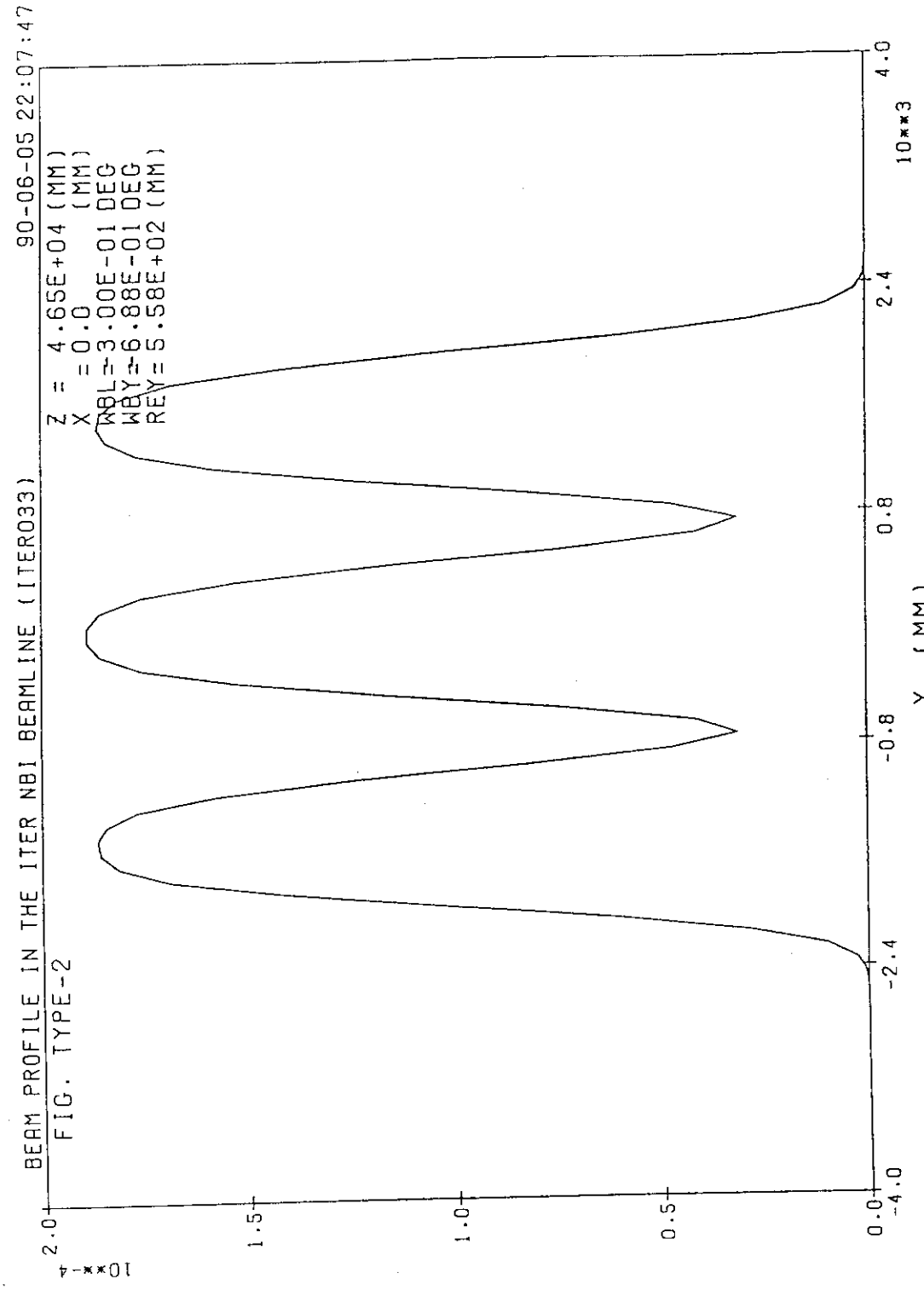

Fig. 3.4-5(b) Vertical beam profile at Z = 46.5 m for Z_{sp} = 38.0 m.

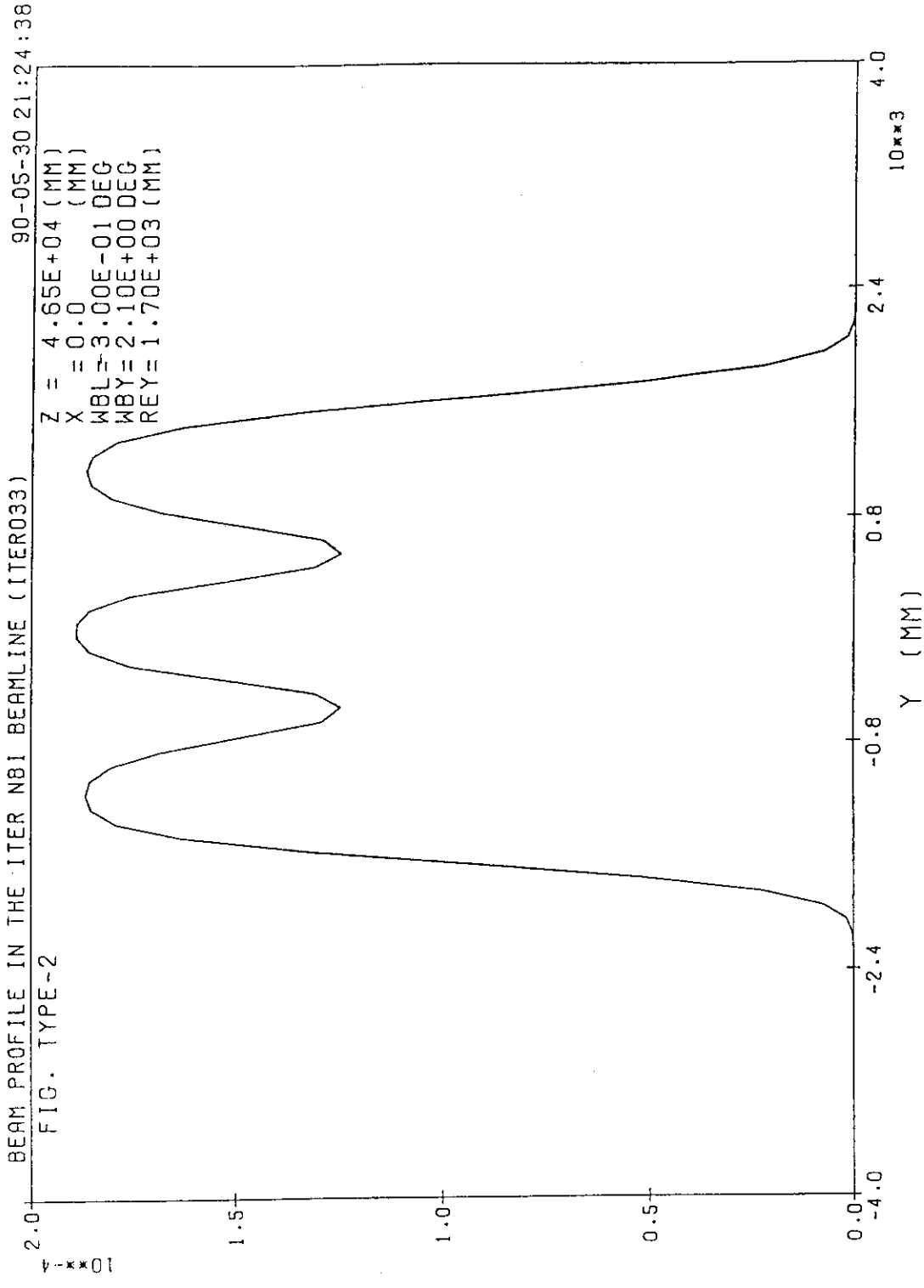

Fig. 3.4-5(c) Vertical beam profile at Z = 46.5 m for Z_{sp} = 39.6 m.

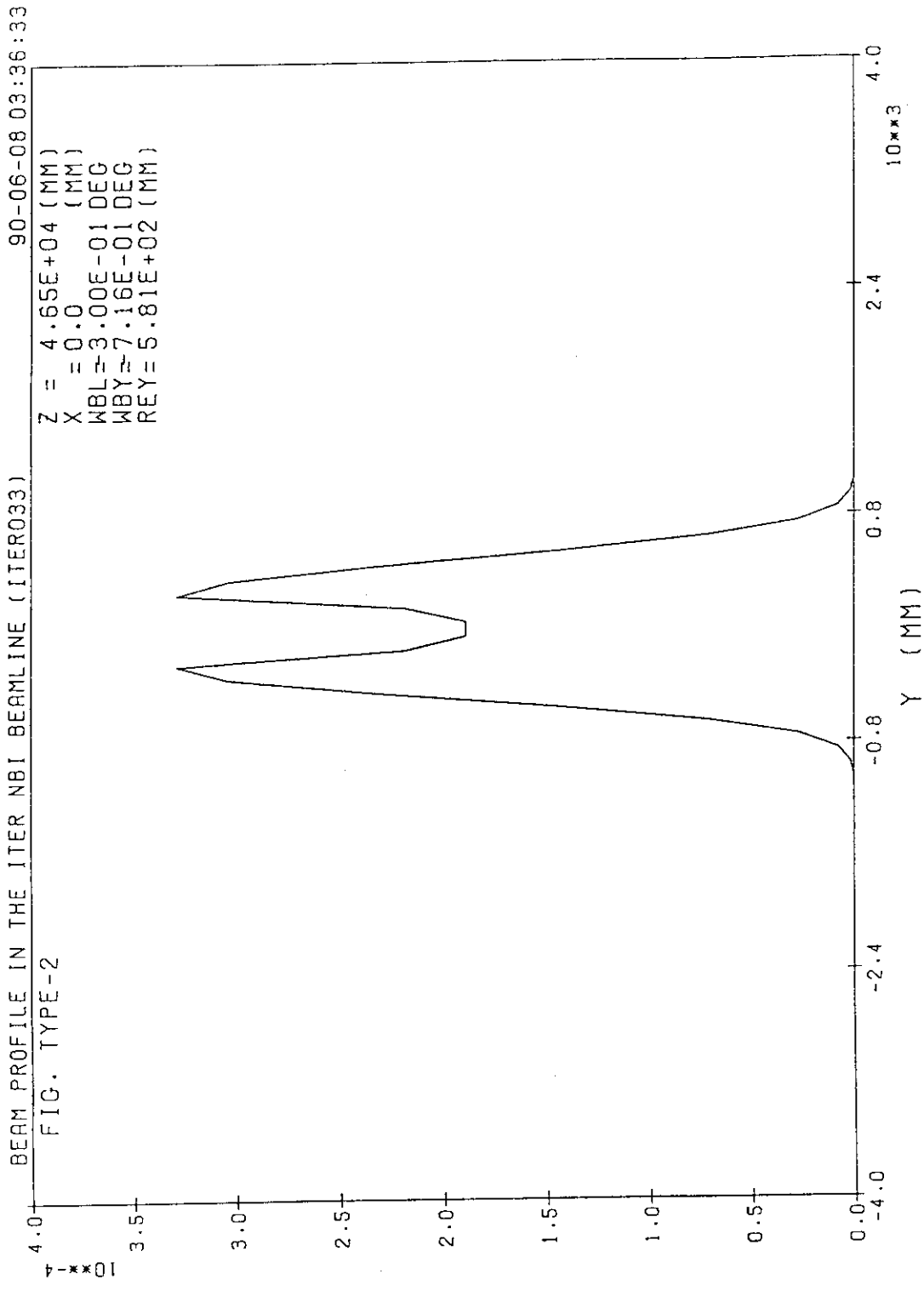

Fig. 3.4-5(d) Vertical beam profile at Z = 46.5 m for Z_{sp} = 46.5 m.

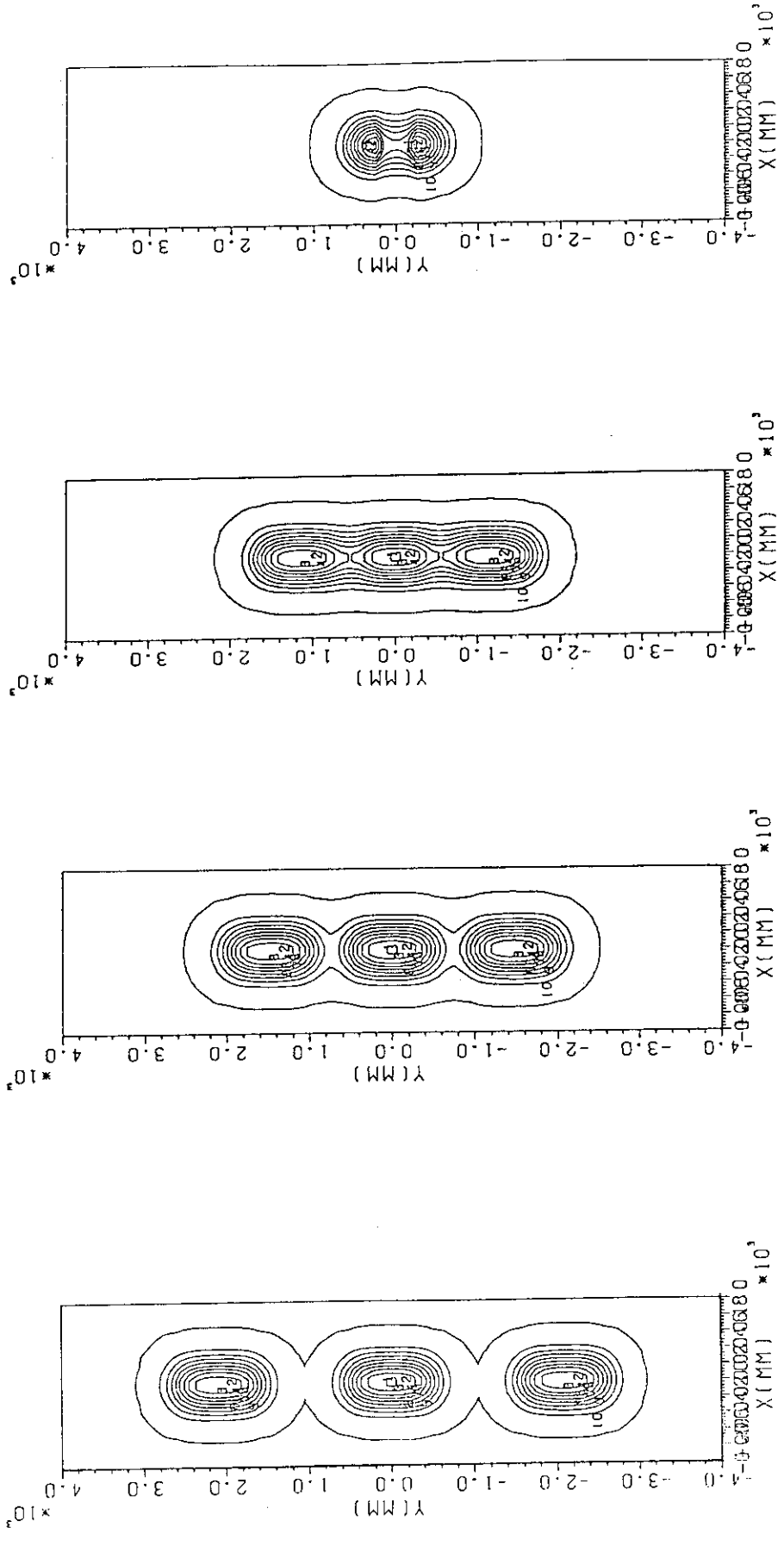

(a) Z_{sp}=35.3 m　(b) Z_{sp}=38.0 m　(c) Z_{sp}=39.6 m　(d) Z_{sp}=46.5 m

Fig.3.4-6 Beam intensity contour at Z = 46.5 m for (a) Z_{sp} = 35.3 m, (b) Z_{sp} = 38.0 m, (c) Z_{sp} = 39.6 m, (d) Z_{sp} = 46.5 m.

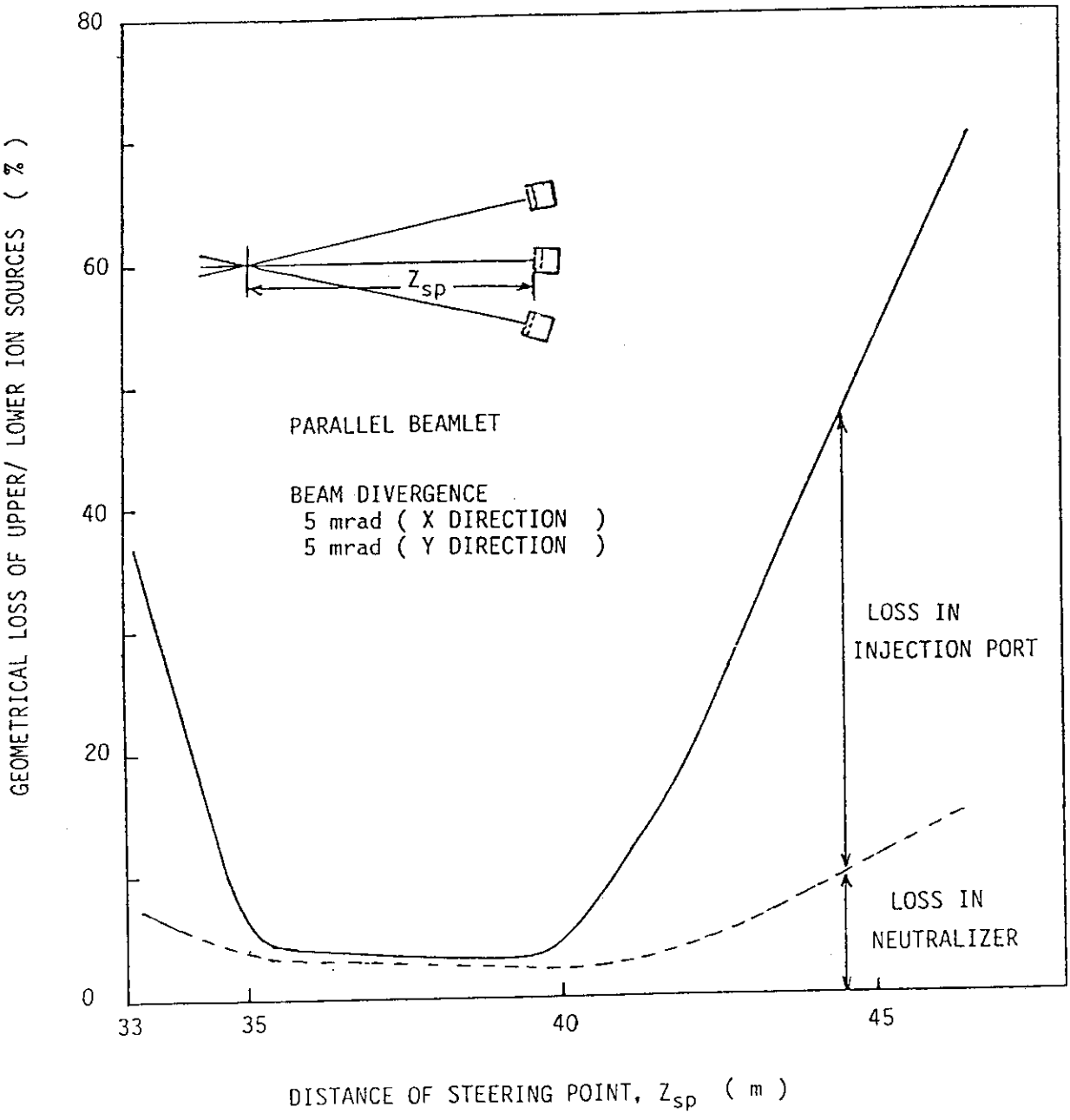

Fig.3.4-7 Geometrical beam loss calculated for the upper or lower ion source as a function of Z_{sp}.

3.5 Neutralizer

Specifications of the neutralizer are shown as follows;

Type	: Gas Cell	
Size	: (cross section)	20 cm x 130 cm
	(length)	600 cm
Number	: 2 slots per a beam line	
Material:	(outer) permalloy	
	(inner) copper	

A conventional gas cell is applied to convert negative ions to neutrals. The neutralizer is composed of two shells. The inner shell is made of water-cooled copper and serves as a beam scraper. The outer shell is made of permalloy to serve as an inner magnetic shield. The magnetic field in the neutralizer is reduced to 0.25 Gauss. The details is described in Section 3.11 (a).

In order to reduce the stripping loss of D^- ions without inducing the space charge blown-up, the pressure at the entrance of the neutralizer, namely, in the ion source room is determined to be 0.02 Pa. The pressure at the exit of the neutralizer, namely, in the beam dump room is determined to be 0.003 Pa to reduce the reionization loss below 5% of the neutral beam. As shown in Sub-section 2.4.3, the optimum line density for the neutralization of 1.3 MeV D^- beam is 1.7×10^{16} molecules/cm^2. To obtain the maximum neutralization efficiency, we need to supply the gas flow rate of 4.6 Pa.m^3/s into the neutralizer.

Using a 2D beam profile calculation code, the total heat load was estimated to be 0.4 MW at the beam divergence angle of 5 mrad.

3.6 Ion Deflection System

The D^+ and D^- ions, which are not converted to neutrals in the neutralizer, are deflected by the deflection coil system. A pair of coils is placed at the exit of the neutralizer. Under the conditions that (1) the maximum heat flux on the beam dump is below 20 MW/m^2 and (2) the length of the beam dump along the beam axis is around 3 m, the deflection system was optimized as shown below;

Geometry	: 1.2 m x 3.0 m rectangular
Distance between the coils	: 2 m
Ampere turn	: 400 kAT

Figure 3.6-1 shows the orbits of D^+ and D^- beams. The magnetic field is applied perpendicularly to the beam, so that the residual ion beams are separated to D^+ and D^- ions and guided to the beam dumps mounted on both side of the beam axis. The length of beam dump of 3m is sufficient to receive all the beams.

On the basis of this beam orbit, the heat flux on the beam dump was calculated. Though the current of D^- beam is less than that of D^+ at the optimum line density for the 1.3 MeV D^- beam as shown in Fig.2.4-12, we calculated the heat flux by assuming both currents to be same. From the standpoint of safety margin, a higher beam current was used, which corresponds to the current of D^- beam of 3.85A. Figure 3.6-2 shows the heat flux on the beam dump. The maximum heat flux is 14 MW/m^2. This heat flux can be handled using the present technology on high heat flux components such as a externally-finned swirl tube.

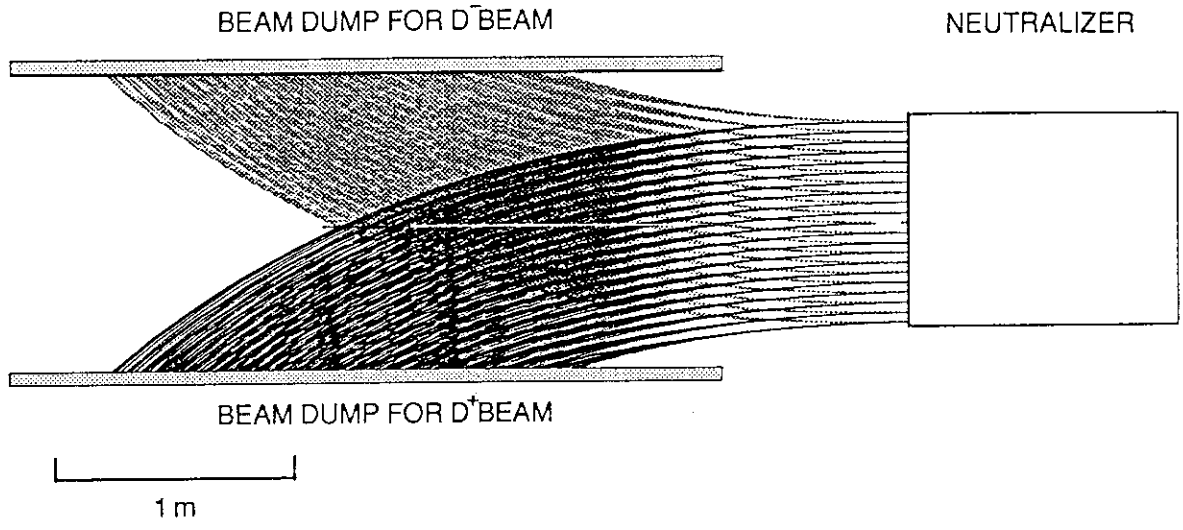

Fig.3.6-1 Beam orbits of D^+ ions and D^- ions deflected by the deflection coil system.

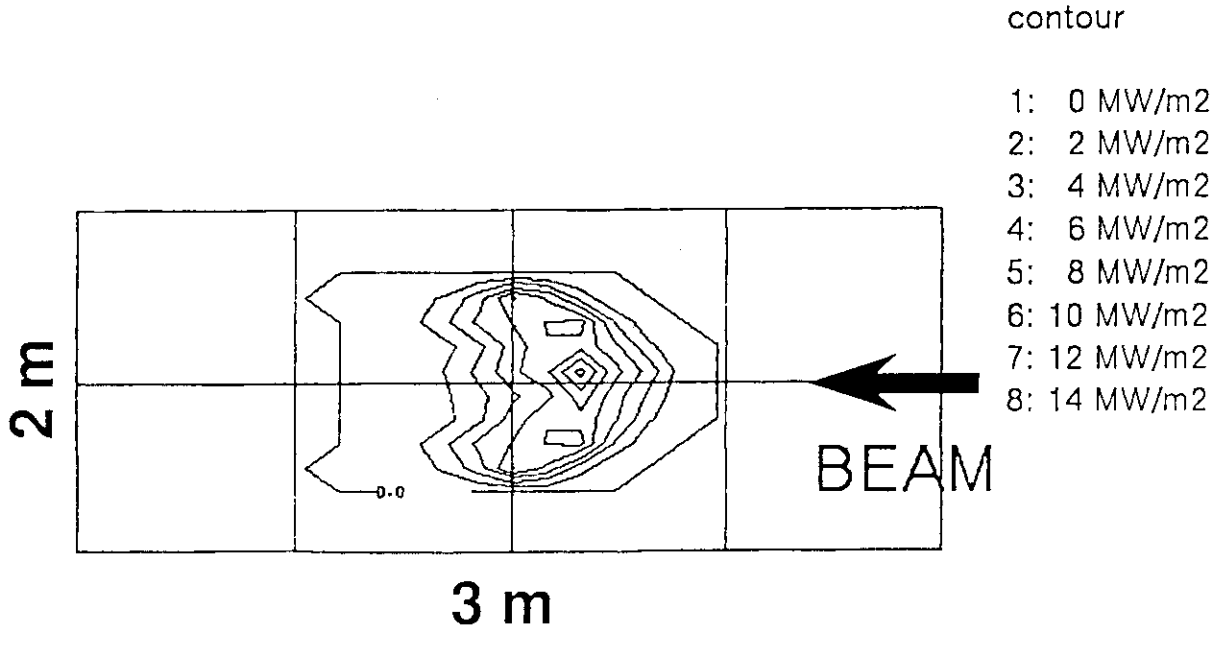

Fig. 3.6-2 Distribution of the heat flux density on the beam dump using a 1.3 MeV, 3.85 A deuterium beam.

3.7 Ion Beam Dump

The 1.3 MeV D^+ or D^- beams which are not converted to neutrals in the neutralizer are deflected, and then are dissipated thermally on the beam dump. Though the damage on the beam dump caused by high energy beams depends on the heat load, sputtering and bristering.

At first, we estimated the damage by the heat load. Maximum heat flux on the beam dump is 14 MW/m^2 as shown in Fig.3.6-2. Taking the safety factor of 2, the heat flux for the beam dump is 30 MW/m^2. In order to bear the high heat flux of 30 MW/m^2, the externally-finned swirl tube is used as a cooling channel of the beam dump. At JAERI, the externally-finned swirl tube has already been tested. The specifications of the tested tube are as follows.

(Dimensions)
- outer diameter : 10 mm
- inner diameter : 7 mm
- twist ratio : 2.5
- (The twist ratio is defined as the length to 180 degree rotating divided by the inner diameter.)

(Materials) : 0.2 % Ag+OFCu

Figure 3.7-1 shows the dependence of the critical heat flux on the axial flow velocity for different inlet water pressure[1]. The critical heat flux tends to increase with the axial flow velocity. On the basis of this experimental result, the flow velocity is required to be 7 m/s which corresponds to the flow rate of 15 l/min/tube. This suggests that the beam dump can be fabricated using the presented technology.

In the second place, the damage by the sputtering was estimated. Maximum ion flux on the beam dump is 13.4×10^{15} ions/cm^2.s, which corresponds to 30 MW/m^2. The sputtering yield at the beam energy of 1.3 MeV, which is calculated in Appendix, is 3.88 $\times 10^{-3}$ atoms/ion. Therefore, the sputtered atoms are 2.88×10^{13} atoms/cm^2.s. According to the operating scenario shown in Fig.5.4-3, the sputtered depth per year is 3.9×10^{-3} cm. It shows that there is no problem on the damage by the sputtering during the operation. However, the damage by the bristering is not estimated here.

Reference

[1] M. Araki, et al.: To be published.

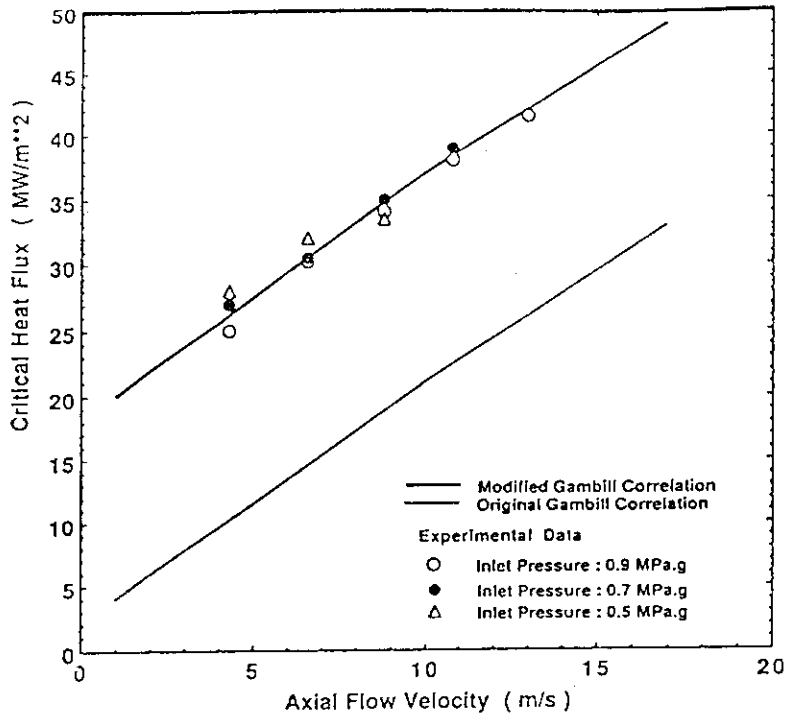

Fig.3.7-1 Dependece of the critical heat flux on the axial flow velocity in changing inlet pressure.

3.8 Cryopumps

(a) Design conditions

Design conditions for ITER NBI (J) are as follows;

Cryopump for ion source room

Pumping speed	: 400 m^3/s for D_2
Gas flow rate to the pumps	: 10.9 $Pa.m^3/s$
Operation period	: 2 weeks continuously

Cryopump for beam dump room

Pumping speed	: 1200 m^3/s for D_2
Gas flow rate to the pumps	: 3.34 $Pa.m^3/s$
Operation period	: 2 weeks continuously

(b) Type of cryopump and pumping speed per unit area

Considering the space prepared for the cryopumps and the required pumping speeds, louver blind type cryopumps are adopted for both the cryopumps for ion source room and beam dump room. Pumping speed of this type of cryopump per unit area facing to the beam path is

$$250\ m^3/s/m^2 \quad \text{for } H_2,$$
$$\text{and } 175\ m^3/s/m^2 \quad \text{for } D_2.$$

(c) Design of cryopump for ion source room

Required area of the pump facing to the beam path is given as,

$$S = 400 / 175 = 2.3\ m^2.$$

We set the height of the cryopanels to be 2 m, considering spatial limitation of the ion source room and determine the pitch between the cryopanels in the louver blind structure to be 0.3 m. Then, the dimension of a unit pump facing to the beam path is determined to be 2 m high and 2 m long, taking the geometrical condition of the ion source room into account.

For continuous operation of the pump, a pair of unit pumps, each of which has an area of 2 m x 2 m facing to the beam path, are installed on both sides of the beam, and each unit pump is divided into two; a half in operation phase, and the other half in refreshing phase or cool down phase, changing the roles in turn.

There are two conditions to determine the time interval for the refreshment of one half unit;

1) Pressure of deuterium gas when desorbed from the panels should be below the lower pressure limit of hydrogen explosion when mixed with air (1700 Pa).
2) Permissible tritium inventory on the cryopanals would be below 1g per module of beamline.

Considering that the inner volume of vacuum vessel of one module is about 150 m^3, the amount of deutrium gas absorbed on the cryopanels is limited,by condition 1), below the value given by,

$$Q = 1700 \text{ Pa} \times 150 \text{ m}^3 = 2.55 \times 105 \text{ Pa m}^3.$$

Time necessary for the cryopump for ion source room to reach the above value is calculated as,

$$t = 2.55 \times 10^5 / 10.9 = 2.3 \times 10^4 \text{ s} = \text{about 6 hr.}$$

Tritium flow rate from the torus to the ion source room was calculated to be 1×10^{-3} g/hr, assuming that neutral gas pressure at the periphery of the torus plasma during ITER operation is 2×10^{-4} Pa. Time necessary for the cryopump for ion source room to reach the permissible level of tritium inventory is calculated as,

$$t = 1 / 1 \times 10^{-3} = 10^3 \text{ hr.}$$

Thus, the time interval for the refreshment of the cryopump for ion source room is determined by condition 1) to be 6 hr.

(d) Design of cryopump for beam dump room

Required area of the pump facing to the beam path is calculated, in a similar way to that of the cryopump for ion source room, as,

$S = 1200 / 175 = 6.8\ m^2$.

The dimension of a unit pump facing to the beam path is set to be 2.5 m high and 4.3 m long.

For continuous pumping, a pair of unit pumps are installed on both sides of the ion dump, and each unit is divided into two half units, similar to the cryopump for ion source room.

Figure 3.8-1 shows one unit of the cryopump for beam dump room. One half of the unit is closed by the movable shutter for refreshment, and the other half is opened for operation. The shutter has rollers and is driven on the rail with rack and gear mechanism.

The amount of deuterium gas absorbed on the cryopanels is limited below the same value as that given for the cryopanels for ion source room. Time for the cryopanels for beamdump room to reach the limit value is calculated as,

$$t = 2.55 \times 10^5 / 3.34 = 7.7 \times 10^4 s = 21\ hr.$$

Tritium flow rate from the torus to the beamdump room was calculated to be 0.022 g/hr, assuming that neutral gas pressure at the periphery of the torus plasma is 2×10^{-4} Pa. Time necessary for the cryopump for beam dump room to reach the permissible level of tririum inventory is given as,

$$t = 1 / 0.022 = 45\ hr.$$

Thus, the time interval for the refreshment of the crtyopump for beam dump room is determined by condition 1) to be 21 hr.

(e) Heat load during steady state of operation

Heat loads to the cryopumps during steady state are calculated under the following conditions;

1) Temperature of surfaces cooled by liquid nitrogen is 100 K.
2) Surfaces cooled by liquid helium are all surrounded with liquid nitrogen cooled surfaces.
3) Probabilty of thermal radiation emitted from materials at room

temperatur to penetrate the louvers is assumed to be 0.3 %.

4) Emissivities of the louver and the cryopanel are 0.9 and 0.1, respectively.
5) Surface temperature of the cryopanels is 3.7 K.

Heat loads due to thermal radiation from surrounding surfaces, heat conduction through mechanical connections, heat conduction by neutral particles, condensation heat,and nuclear heating are calculated for the cryopump for ion source room in steady state operation. The results are summarized in Table 3.8-1. The values in the table are for one module.

Based on the values in Table 3.8-1, total heat load to all the cryopumps of 9 modules are calculated as,

$$P = (49.4 + 58.1) \times 9 \times 1.3 = 1258 \text{ W},$$

where a numerical factor of 1.3 is multiplied in order to consider the ambiguity of heat loads. If we let total length of transfer tubes from the helium refrigerator to the cryopumps about 600 m, heat load to the transfer tubes is calculated as,

$$600 \text{ m} \times 0.5 \text{ W/m} = 300 \text{ W}.$$

Thus, the total heat load to the whole cryopump system for NBI during steady state operation is evaluated to be 1600 W.

(f) Heat to be removed during cool down phase

As described in (c), the time interval for refreshment of the cryopump for ion source room is 6 hr. We assume that 1 hr is used for warm up and 5 hr for cool down of the cryopanels. The cryopanels will be warmed up to 77 K and cooled down to 3.7 K. We use the value of specific heat of aluminium at 40 K ($C = 3 \times 10^{-2}$ J/gK) for calculation. Weight of aluminium cryopanels of one unit pump for ion source room is evaluated to be 320 kg. Then, heat to be removed from the bulk of aluminium is calculated as,

$$Q = C(T1 - T2)W$$
$$= 3 \times 10^{-2} \times 73 \times 320 \times 10^{3} = 700800 \text{ J},$$
$$P = 700800/(3600 \times 5) = 39 \text{ W}.$$

Heat loads due to thermal radiation, heat conduction through mechanical connections, and nuclear heating can be considered to be the same as those in steady state operation. Thus, total heat load to be removed from the cryopanels for ion source room during cool down phase is given as,

(39 + 12 + 12 +6) x 1.3 = 90 W per module,

where a numerical factor 1.3 is for the ambiguity.

The time interval for refreshment of the cryopump for beam dump room is 21 hr as described in (d). We assume that 2 hr is used for warm up and 19 hr for cool down of the cryopanels. Weight of aluminium cryopanels of one unit pump for beam dump room is evaluated to be 900 kg. Then heat to be removed from the bulk of aluminium is calculated as,

$$Q = 3 \times 10^{-2} \times 73 \times 900 \times 10^{3} = 1971000 \text{ J},$$
$$P = 1971000 / (3600 \times 19) = 29 \text{ W}.$$

Heat loads due to thermal radiation, heat conduction through mechanical connections, and nuclear heating are considered to be the same as those in steady state. Thus, total heat load to be removed from the cryopanels for beam dump room during cool down phase is given as,

(29 + 22 + 16 + 16) x 1.3 = 110 W per module.

Hence, total heat load to the whole cryopump system for NBI during cool down phase is evaluated to be as,

(90 + 110) x 9 = 1800 W.

(g) Helium gas pressure in the beamline

A part of helium produced in fusion plasma will backstream into the beamline of neutral beam injector. However, cryocondensation pumps, which are used to evacuate the beamline, do not have any ability to pump helium gas. Therefore, helium partial pressure in the beamline will be equal to that at the periphery of the torus plasma.

Helium fraction in the main plasma is defined as,

$$f_{He} = \frac{n_{He}}{n_D + n_T}.$$

For ITER case, f_{He}=0.1 is assumed. Total neutral pressure at the periphery of the torus plasma is evaluated to be 2 x 10^{-4} Pa for ITER[1]. Assuming that the helium partial pressure at the periphery of the torus plasma is proportional to f_{He}, the helium partial pressure in the beamline can be estimated as,

$$P_{He} = 2 \times 10^{-4} \text{ Pa} \times 0.1 = 2 \times 10^{-5} \text{ Pa}.$$

This is about 1 % of total pressure in the drift duct of neutral beam injector and will not have any significant influences on the performance of the neutral beam injector.

Helium gas in the torus will be evacuated by compound cryopumps or turbomolecular pumps. From a viewpoint of vacuum system, the beamline is connected to the torus. Therefore, helium gas backstreaming from the torus into the neutral beam injector will not accumulate in the beamline. Consequently, any pumps to evacuate helium gas in the beamline will not be necessary.

Reference

[1] Cohen and Hopman:ITER Internal Letters,ITER-IL-HD-4-9-11(1989).

Table 3.8-1 Heat load per module to the cryopanels during steady state operation

	CRYOPUMP FOR ION SOURCE ROOM	CRYOPUMP FOR BEAM DUMP ROOM
THERMAL RADIATION	12.0 W	22.2 W
HEAT CONDUCTION THROUGH MECHANICAL CONNECTION	12.0	16.0
HEAT CONDUCTION BY NEUTRAL GAS	9.6	0.96
CONDENSATION HEAT	9.8	3.0
NUCLEAR HEATING	6.0	16.0
TOTAL	49.4 W	58.1 W

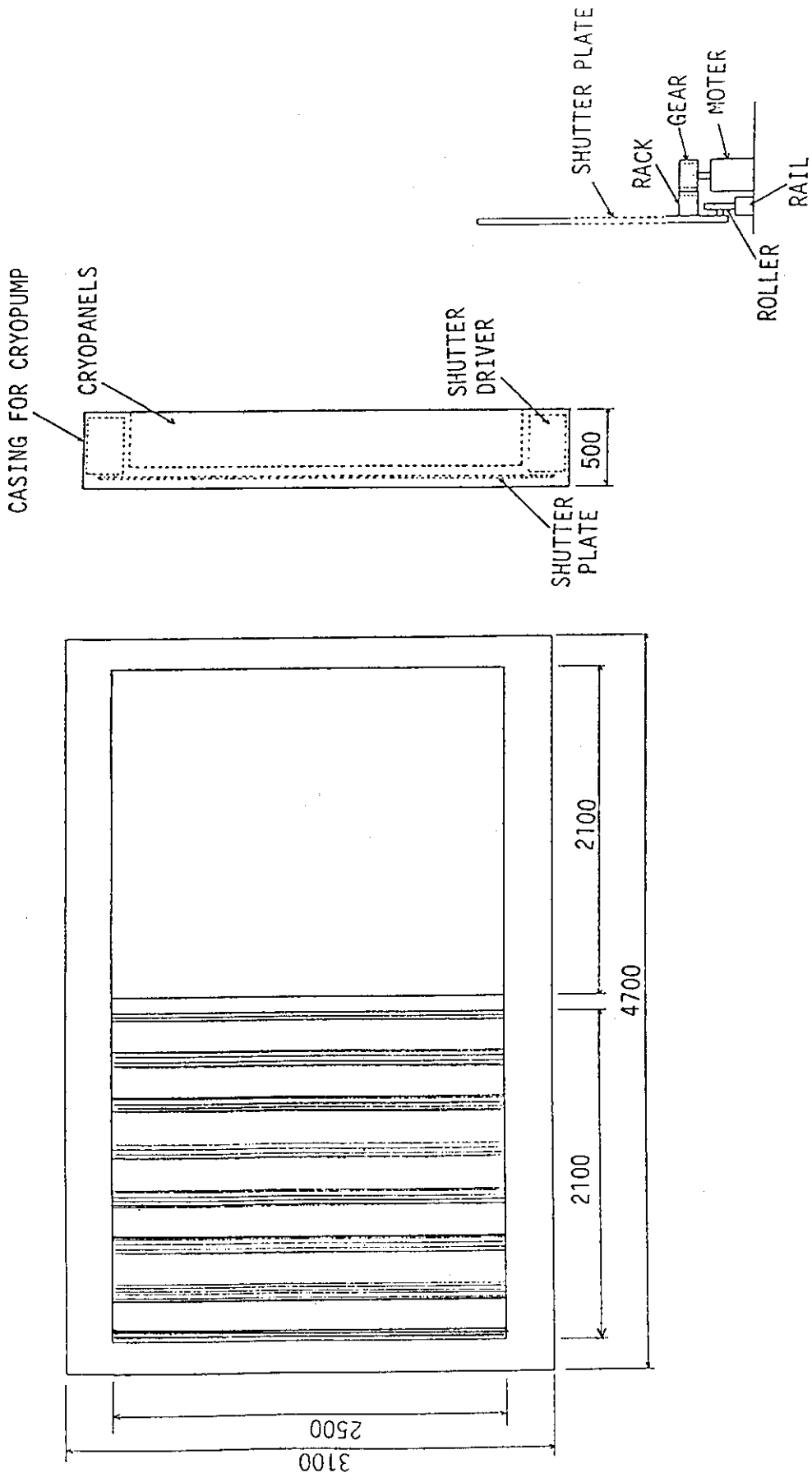

Fig. 3.8-1 One unit of cryopump for beam dump room.

3.9 Vacuum Vessel

Vacuum vessel of beamline module is divided into two; vacuum vessel for ion source unit and vacuum vessel for beamline unit.

(a) Vessel for ion source unit

Dimension : 4.0 m in outer diameter, 5 m long.
Material : mild steel.
Weight : 60 ton (for 10 cm thick mild steel).

Functions :

1) vessel for pressurized SF_6 gas (4 to 5 atm).
2) outer shell of magnetic shield for ion source.
3) a part of radiation shield.
4) container to prevent spreading of radioactivated materials.

Ports :

1) port for connection/disconnection of electric cables, water pipes, and deutrium gas to the ion source.
2) port for connection/disconnection of SF_6 gas feed/evacuation lines for electric insulation.

(b) Vacuum vessel for beamline unit

Dimension : 4.0 m in outer diameter, 12 m long.
Material : mild steel.
Weight : 130 ton (for 10 cm thick mild steel).

Functions :

1) vacuum vessel.
2) outer shell of magnetic shield for neutralizer.
3) a part of radiation shield.
4) container to prevent spreading of radioactivated materials.

Ports :

1) ports for connection/disconnection of liquid helium, gas helium, and electric cables to the cryopumps for ion source room and for beam dump room.
2) port for connection/disconnection of water pipes, electric cables, and deuterium gas to the neutralizer.
3) port for connection/disconnection of electric cables, and water pipes to the beam profile controller.
4) port for connection/disconnection of water pipes to the ion dump.
5) port for connection/disconnection of electric cables and water pipes to the solenoid coils.
6) port for connection/disconnection of electric cables, water pipes, and pneumatic service lines to the calorimeter.
7) ports for windows and for connection/disconnection of electric cables for various beam monitors.

3.10 Large Metal Seal Gate Valve

This valve is mounted between the beamline module and the NBI port, and used when the beamline module is removed for maintenance or the vacuum in the reactor and the beamline module is separated. This valve is composed of two sub-valves, each of which has an opening of 60 cm wide by 180 cm high. When the beamline module is demounted, this valve is separated between the two sub-valves. Since each sub-valve is vacuum-tight, the tritium gas and the activated materials does not leak out in the NBI room during the maintenance phase. In addition, the reactor and the NBI system can be operated independently when the valve is clased.

The major specifications are shown below:

1.	Dimensions	: about 2.5m h x 3m w x 0.8m t
2.	Opening	: 1.8m h x 0.6m w
3.	Weight	: 10 ton
4.	Materials	: Aluminum alloy, SS
5.	Vacuum Seal	: SS diaphragm
6.	Leak rate	: 1 x 10E-7 Pa m^3/s for T_2
7.	Bakeout temperature	: 200°C
8.	Stroke	: 0.8 m
9.	Driving method	: Pressurized CO_2 gas at 10 atm.
10.	Open-close time	: 10 s
11.	Durability	: 100 cycles

The structure of the valve is shown in Fig.3.10-1. The most characteristic feature of this valve is that the vacuum seal is conducted by a couple of rectangular diaphragm plate rings with a differential pumping system between them. From the manufacturing point of view, this valve does not require a particular technology.

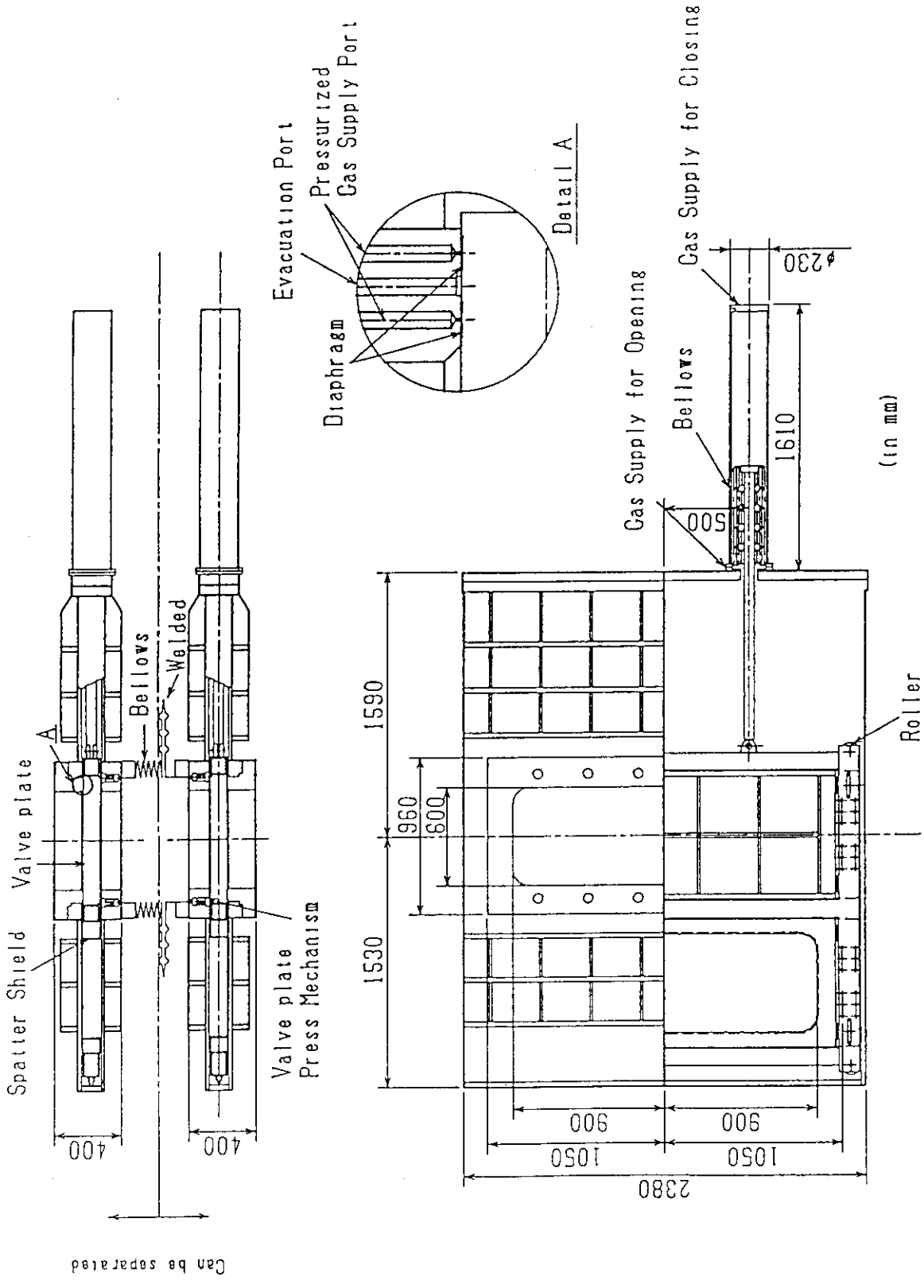

Fig. 3.10-1 Large metal seal gate valve.

3.11 Magnetic Shield

(a) Determination of permissible magnetic field

In the NBI module, the following components should be magnetically shielded;

i) negative ion source (plasma generator),
ii) accelerator,
iii) beam profile controller,
iv) neutralizer.

In our design, the position of the beam profile controller is common to that of the neutralizer. Therefore, the magnetic shield for the beam profile controller is common to that for the neutralizer.

Before starting the design of magnetic shields, we should determine permissible level of the external magnetic field in each component.

The permissible level of the field for a magnetic multipole plasma generator was expeimentally evaluated to be about 5G [1], so that plasma density distribution in the source may be uniform over the beam extraction area of the plasma grid. Although this permissible value is for a positive ion source, we assume that this value is also valid for the negative ion source of the ITER NBI.

Displacement angle of the ion beam in the accelerator due to a uniform magnetic field perpendicular to the beam axis is given as [2],

$$\theta_A = \frac{\dfrac{eL_A^2 B_A^2}{MV}}{\sqrt{1 - \left(1 - \dfrac{eL_A^2 B_A^2}{MV}\right)^2}} \qquad (1)$$

where θ_A :displacement angle during the acceleration (rad),
B_A :strength of the uniform magnetic field in the accelerator(T),
L_A :acceleration gap length(m),
M :mass of the ion (kg),
V :acceleration voltage of the beam(V).

In general, the magnetic shield is designed to sufficiently satisfy the following condition;

$$1 >> \frac{eL^2B^2}{MV} \qquad (1 >> (\frac{L}{\rho_i})^2). \qquad (2)$$

Therefore, the Eq.(1) can be simply expressed as,

$$\theta_A = (\frac{e}{2MV})^{1/2} L_A B_A. \qquad (3)$$

In a similar way, displacement angle of the ion beam in the neutralizer due to a uniform magnetic field perpendicular to the beam axis is given by,

$$\theta_N = (\frac{e}{2MV})^{1/2} L_N B_N$$

where

θ_N :displacement angle in the neutralizer(rad),
B_N :strength of the uniform magnetic field in the neutralizer(T),
L_N :neutralizer length (m).

Thus, total deflection angle due to the magnetic field becomes,

$$\theta = \theta_A + \theta_N = (\frac{e}{2MV})^{1/2} (L_A B_A + L_N B_N). \qquad (4)$$

We will design the magnetic shields such that the magnetic field in the accelerator is almost equal to that in the neutralizer;i.e.,$B_A = B_N$. Then, Eq.(4) becomes,

$$\theta = (\frac{e}{2MV})^{1/2} B_A (L_A + L_N). \qquad (5)$$

We set the permissible displacement angle of the beam in horizontal direction at the exit of the injection port to be + 1 mrad(46.5 m tan(1mrad) = 4.65 cm) because the increase of geometrical loss due to this horizontal displacement of the beam is lower than 1 %(see Fig.2.4-9). Hence, the following condition should be satisfied in the neutralizer and the accelerator of the ion source;

$$\theta \leqq 10^{-3} \text{ rad.} \qquad (6)$$

Substituting the following values into Eqs.(5) and (6),

$L_A + L_N = 9.2$ m,
$V = 1.3 \times 10^6$ V,

$$M = 2 \times 1.673 \times 10^{-27} \text{ kg},$$

we obtain,

$$B_A \leqq 2.5 \times 10^{-5} \text{ T} = 0.25 \text{ G}.$$

That is, we will design the magnetic shield so that external field in the area of the accelerator of the ion source and the neutralizer may become lower than 0.25 G.

As can be seen in Fig.3.1-1, the plasma generator is enclosed with the structure of the accelerator and closely contacts with the accelerator. Therefore, from a viewpoint of magnetic shielding, it is very difficult to divide this space into two regions. That is, if the accelerator is magnetically shielded to the similar level to the neutralizer, the plasma generator is automatically shielded to the same level as the neutralizer, even though the permissible level of the magnetic field for the plasma generator is much higher than that for the accelerator and the neutralizer.

(b) Design of magnetic shield for neutralizer

Stray magnetic field from the ITER tokamak is about 120 G and about 70 G at the exit and the entrance of the neutralizer, respectively. Direction of the field is almost perpendicular to the beam. Then, target value of shielding factor of the magnetic shield for neutralizer is determined as,

$$S = 120 / 0.25 = 480.$$

This shielding factor is too high to be achieved by one shell type magnetic shield. Thus, we adopt 2 shell type structure of magnetic shield. To prevent the shield from magnetic saturation, we select mild steel as the material of the outer shell. To reduce weight and space of the magnetic shield, we select permalloy as the material of the inner shell.

Outer diameter of the injector module is limited to 4 m, in the ITER NBI common design. Thus, in order to design the module as compact and as light as possible , it is effective that the outer shell of magnetic shield serves as the vacuum vessel of the beamline unit, too. We adopt this concept.

For the outer shell made of mild steel not to be magnetically saturated, the next inequality should be satisfied;

$$2R_2 B_{ext} \leqq t_2 B_{in,sat}(\text{Fe}) \qquad (7)$$

where

R_2 : outer radius of the outer shell(cylindrical shape)
t_2 : thickness of the outer shell
B_{ext} : strength of external magnetic field
$B_{in,sat}(Fe)$: saturation magnetic flux density of mild steel.

Substituting the following values into Eq.(7),

R_2 = 200 cm
B_{ext} = 120 G
$B_{in,sat}(Fe)$ = 21500 G,

we obtain,

$$t_2 \geq 2.23 \text{ cm.}$$

That is, to prevent the outer shell from magnetic saturation, thickness larger than 2.23 cm is necessary. Considering the ambiguity of 3D effect of magnetic shield structure, we take a safety factor of 2 for magnetic saturation. Thus, we determine,

$$t_2 = 4.5 \text{ cm.}$$

In the inner space of the outer shell , the external field is reduced by a factor of

$$1 + S_2 = 1 + (\mu_2 t_2 / 2R_2) = 4.4,$$

where μ_2 is the permeability of mild steel and μ_2 = 300 was used for calculation. Thus, field strength in the inner space of the outer shell is estimated as,

$$120 / 4.4 = 27 \text{ G.}$$

For the inner shell made of permalloy not to be magnetically saturated, the next inequality should be satisfied;

$$(R_2 - t_2) \times 27 \text{ G} \leq t_1 B_{in,sat}(perm) \qquad (8)$$

where t_1 : thickness of the inner shell
$B_{in,sat}(perm)$: saturation magnetioc flux density of permalloy.

Substituting $B_{in,sat}(perm)$ = 7000 G, we obtain

$$t_1 \geq 0.8 \text{ cm.}$$

This means that thickness of the inner shell made of permalloy should be larger than 0.8 cm to prevent magnetic saturation. We take a safety factor of 2 for magnetic saturation. Thus, we determine

t_1 = 1.6 cm.

Cross-section of the neutralizer is a rectangle with inner dimension of 46 cm wide and 130 cm high. Then we asasume the cross-sectional shape of the inner shell to be a rectangle with outer dimension of 65 cm wide and 150 cm high. This rectangle can be approximated by a circle of 112 cm ($2R_1$) in diameter, which has the same cross-sectional area as that of the rectangle. Then, the shielding factor of the inner shell is evaluated as,

$$S_1 = \mu_1 t_1 / 2R_1 = 357,$$

where μ_1 is the permeability of permalloy and u_1 = 25000 was used for calculation.

At the final, the shielding factor of the shield for neutralizer is calculated as,

$$S = 1 + S_1 + S_2 + S_1 x S_2 \left(1 - \left(R_1/R_2 \right)^2 \right)$$
$$= 1481.$$

This valu is sufficiently higher than the target value (S = 480).

(c) Design of magnetic shield for ion source(plasma generator and accelerator)

Stray magnetic field from the tokamak is about 60 G and 50 G at the bottom and the top of the ion source, respectively. Then, target value of shielding factor of the magnetic shield for ion source is determined as,

S = 60 / 0.25 = 240.

Similar to the magnetic shield for neutralizer, 2 shell structure is adopted. For the same reasons as those of the magnetic shield for neutralizer, mild steel and permalloy are selected as the materials of the outer and the inner shells, respectively.

In case of the magnetic shield for ion source, the outer shell of the shield should serve as the vessel of pressurized gas. That is, SF_6 gas at 4 to 5 atm is filled in the space between the ion source and the shells, for electrical insulation between the ion source at high potential (1.3 MV) and the shells at earth potential.

Outer diameter of the outer shell is limited to 4 m($2R_2$). To keep continuity between the outer shells for neutralizer and for ion source, the thickness of the outer shell of the ion source shield is determined to be 4.5 cm(t_2), even though this thickness is too large to prevent magnetic saturation.

In the inner space of the outer shell, the external field is reduced by a factor of 4.4 which was calculated in (b). Then, field strength in the inner sapce of the outer shell is estimated as,

60 / 4.4 = 14 G.

For the inner shell made of permalloy not to be magnetically saturated, the inequality similar to Eq.(4) should be satisfied;

$$(R_2 - t_2) \times 14\ G \leq t_1 B_{in,sat}(perm).$$

Thus, we obtain,

$$t_1 = 0.4\ cm.$$

The outer diameter of the accelerator at high potential is 2.5 m in our design. To hold electrical insulation between the components at high potential (1.3 MV) and the inner shell at ground potential, an insulating distance larger than 40 to 60 cm might be required even though the pressurized SF_6 gas is filled in the space. Thus, we set the outer diameter of cylindrical inner shell to be 3.6 m($2R_1$).

If we select a safety factor of 2 for magnetic saturation of permalloy, t_1 becomes 0.8 cm. In this case, shielding factor of the inner shell is calculated as ,

$$S_1 = \mu_1 t_1 / 2R_1 = 55.$$

Then,shielding factor of the shield for ion source as a whole is evaluated as,

$$S = 1 + S_1 + S_2 + S_1 \times S_2 (1 - (R_1/R_2)^2)$$
$$= 93.$$

This value is much lower than the target value (S=240). After some trials, we find the solution which satisfies the target value. That is , if we set

$$t_1 = 2.2\ cm,$$

the shielding factor of the shield for ion source is calculated as,

$$S = 255.$$

(d) Summary of designs

The designed values are summarized in Table 3.11-1 and the cross-sectional views of the magnetic shields for ion source and for neutralizer are shown in Figs.3.11-1 and 3.11-2, respectively.

References

[1] S.Tanaka et al.;Rev.Sci.Instrum.57,145(1986).
[2] S.Matsuda et al.;Japan Atomic Energy Research Institute Report, JAERI- M7655(1978).

Table 3.11-1 Summary of designed values of magnetic shields for ITER NBI.

	SHIELD FOR NEUTRALIZER	SHIELD FOR ION SOURCE
MAX. EXTERNAL FIELD	120 G	60 G
TARGET SHIELDING FACTOR	480	240
DESIGNED SHIELDING FACTOR	1480	255
THICKNESS OF OUTER SHELL (MILD STEEL)	4.5 cm	4.5 cm
THICKNESS OF INNER SHELL (PERMALLOY)	1.6 cm	2.2 cm

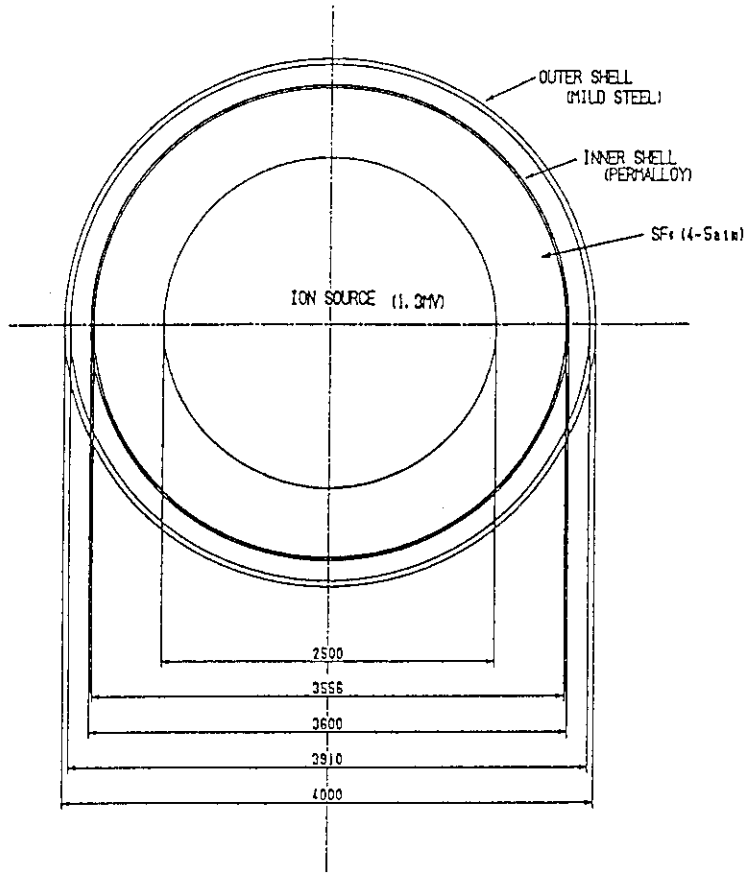

Fig.3.11-1 Cross-sectional view of the magnetic shield for ion source.

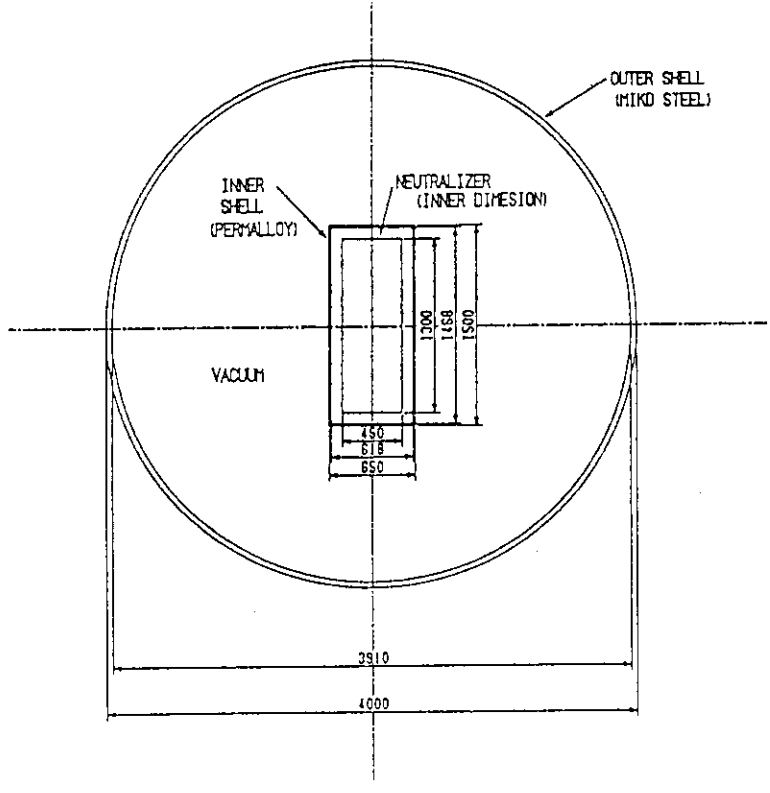

Fig.3.11-2 Cross-sectional view of the magnetic shield for neutralizer.

3.12 Neutron Shield

Through the neutronics calculation conducted in FY89, following requirements were embossed for the beamline;

i) The flux of high energy neutrons is very high along the beamline axis, since there is no obstacle in it. In order to stop and attenuate the neutrons, a neutron dump should be equipped on the back of the ion source.

ii) A part of the dumped neutrons are reflected backward to the beamline. To decrease the reflected neutron flux, the source mounting flange and the partition in the beam line, i.e. walls placed perpendicular to the beamline axis, were taken to be thick enough.

iii) Some of the neutrons are scattered toward the transverse direction by the accelerator grids and the source back plate. However, this transverse neutron flux have to be reduced so as not to activate wall of the NB room (See section 5.2). Thus the thickness of the vacuum chamber will be increased (10 cm -) as a primary shield of the high energy neutrons.

iv) The other option to reduce the transverse neutron flux is to surround the beamline by a separated neutron shield such as a water pool or B_4C liner. This design may have an advantage of easy maintenance. The beamline design as a neutron container should be decided by a results of the neutronics calculations being developed.

4. ELECTRICAL SYSTEM

Figure 4.1-1 shows a schematic diagram of ITER-NBI power supply system. It consists of acceleration power supply, ion source power supply system, surge protection system and high voltage transmission line. Ion source power supply system is installed in the high voltage table (HVT) and is used at the potential of the acceleration power supply output. Acceleration power supply, ion source power supply system and ion source are connected by SF_6 gas insulated cable duct. Surge blocker and reactor-resister elements are used to suppress the surge energy and current when electrical breakdowns occur in ion source.

4.1 Acceleration Power Supply System

Acceleration power supply accelerates the negative ions up to 1.3 MeV. This power supply has 6 outputs corresponding to the accelerator grids (Fig.4.1-1). Voltages for the acceleration gaps can be varied individually. When the breakdown occurs in the accelerator, outputs are turned off immediately. Specifications of the acceleration power supply are shown below:

1. Voltage	:	1200,1000,800,600,400,200 kV
2. Current	:	18 A for 1200 kV output 1 A for others
3. Ripple	:	10 %p-p
4. Rise time	:	0.2 sec
5. Cutoff time	:	0.2 ms
6. Pulse length	:	DC

Acceleration power supply consists of 6 power supplies connected in series (Fig.4.1-1). Each power supply has same output of 200 kV, 18 A except the insulation voltage. These power supplies are inverter type power supplies without DC switches [1]. A power supply consists of converter, inverter, insulating transformer and rectifier. Converter controls the output voltage and inverter cuts off the output when breakdown occurs.

Output of inverter is rectangular and rectifier circuits are multi-phased to eliminate the DC filter. Frequency of inverter is pre-

ferred to be high , however it is determined to be 500 Hz from a manufacturing point of view.

In a cascade transformer system, insulation is easy. However, total capacity of the transformers is large. Output voltage of each stage cannot be controlled independently and the ratio of voltages varies with current. On the other hand, the capacity of the transformers is small and output voltage of each stage can be controlled independently in non-cascade transformer system. From these point, the latter system is adopted even though insulation is not easy.

Output of 1.2 MV is connected to HVT through the reactor with the parallel resistor to suppress the surge energy and the surge current. Intermediate outputs are connected to the accelerator through the resistors.

Reference

[1] M. Mizuno et al., " Inverter type high voltage DC power supply for negative-ion based neutral beam injectors, " Proc. of 13th. Symp. on Fusion Engineering, Knoxville, Oct. 2-6, 1989, pp.574-577.

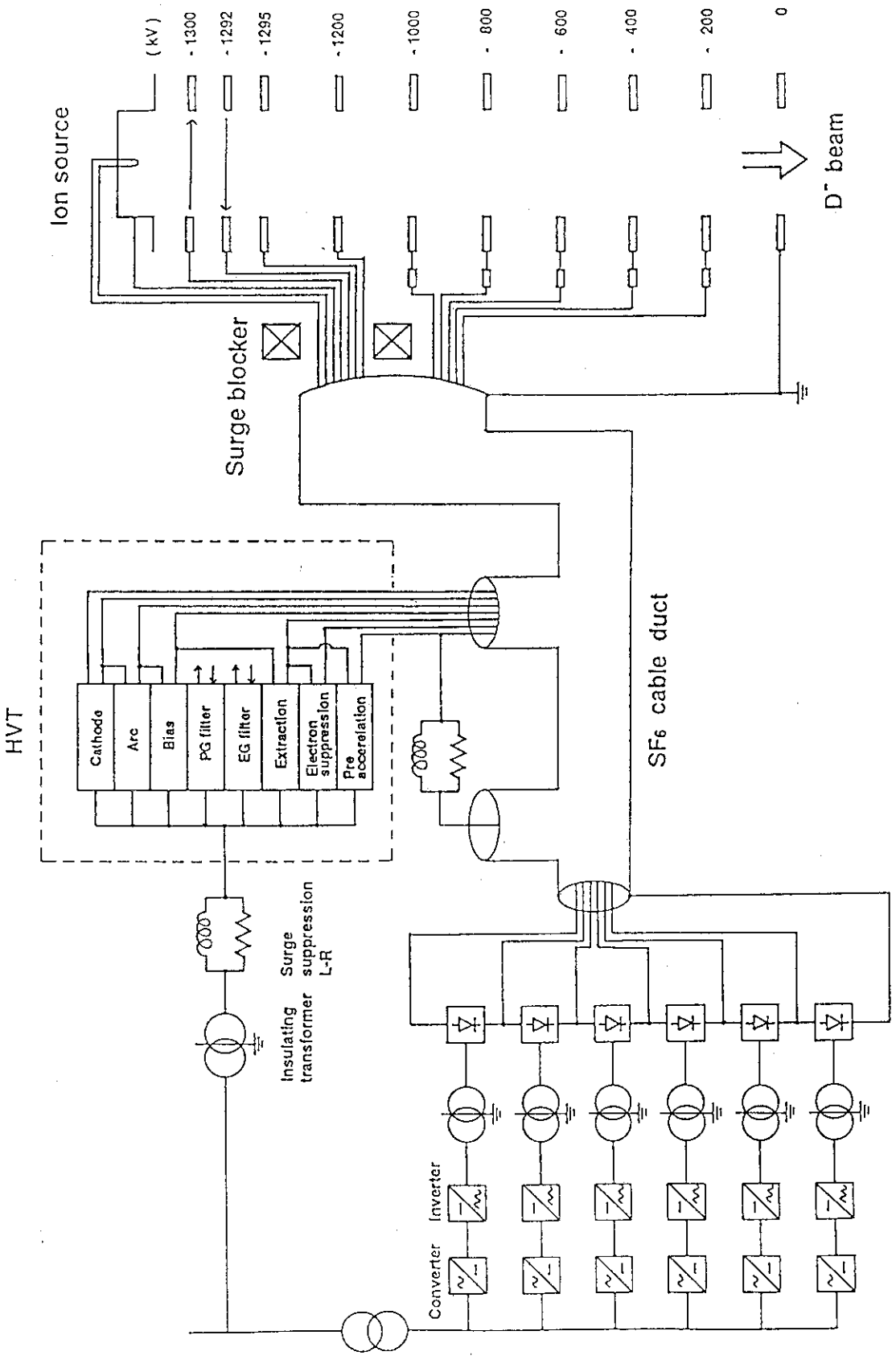

Fig.4.1-1 Schematic diagram of ITER-NBI power supply system.

4.2 Ion Source Power Supply System

Ion source power supply system consists of power supplies for negative ion production and those for beam extraction. Negative ions are accelerated up to 100 keV by this power supply system. Specifications of power supplies are shown in Table4.2-1.

These power supplies are installed in the HVT, which is located in the room filled with SF6 gas. Electric power is fed by the insulating transformer. When breakdowns occur in the accelerator, arc, extraction, electron suppression and pre-acceleration power supplies are turned off immediately, while cathode, bias, PG filter and EG filter power supplies are not turned off.

Outputs of PG filter and EG filter power supplies are converted to DC currents of 4000 A and 2000 A respectively near the ion source.

Table 4.2-1 Specifications of power supplies

	Output voltage	Output current	Pulse length	Duty factor	Ripple (%p-p)	Rise time (sec)	Cutoff time (μs)
Cathode	15 V	6000A	DC	1	3	3	-
Arc	100 V	3000 A	DC	1	3	0.2	100
Bias	10 V	300 A	DC	1	3	1	-
PG filter	400 V (AC 3-phase)	60 A	DC	1	-	1	-
Extraction	10 kV	60 A	DC	1	5	0.2	100
Electron suppression	5 kV	12 A	DC	1	5	0.2	100
EG filter	400 V (AC 3-phase)	30 A	DC	1	-	1	-
Pre-acceleration	100 kV	18 A	DC	1	5	0.2	100
Acceleration	1200 kV	18 A	DC	1	10	0.2	200

4.3 Surge Protection System

It has been experimentally confirmed that not only the suppression of surge energy, but also the reduction of surge current when breakdowns occur in the accelerator are very important to protect both the ion source and the power supply system itself[1][2]. Therefore, the surge current and the input energy to the ion source have to be suppressed under 1 kA and several joules, respectively[3][4]. Figure 4.1-1 shows the schematic diagram of the ITER NBI power supply system. The surge energy flows from stray capacitance which exist at high voltage area. In the power supply system, an insulating transformer of the source plasma power supply has the biggest stray capacitance. Therefore, a surge suppression reactor with paralleled resistors must be utilized for suppression of surge current and energy. In the present power supply system, there are some winding coils which correspond to each power supply of filament, arc, etc., in the insulating transformer. Such transformer has large stray capacitance, because the area of high voltage region is wide. To reduce the stray capacitance of the insulating transformer, we proposed to use one big insulating transformer and to distribute the power at the high voltage[4]. Utilizing such method, stray capacitance can be reduced and it becomes easy to use the surge suppression reactor. Therefore, the size of a surge blocking core (surge blocker) can be reduced. In short the core can be designed to absorb only the stored energy which exist at the high voltage part of the system except the insulating transformer.

Further, we investigated the core materials which have a high saturation magnetic flux to reduce the core size. The result shows that it is possible to reduce core size by using amorphous cores[5]. These materials have high saturation magnetic flux of larger than 12kG. The size of the high quality surge blocker becomes 1/2 to 1/3 of the size of the present surge blocker made of ferrite core whose saturation magnetic flux is 3kG.

References

[1] H.M.Owren et al, Proc. 12th Symp. on Fusion Technology, Julich, 1982, p.455.
[2] K.Watanabe et al., JAERI-M 86-104, 1986 (in Japanese).
[3] Y.Ohara et al.,Proc. 12th Symp. on Fusion Eng.,Monterey,1987,p.298.
[4] K.Watanabe, Proc. Symp. on Negative Ion Sources and Their Applications, KEK Tsukuba, 1988,p.147.
[5] M.Mizuno et al.,Proc.13th Symp.on Fusion Eng., Knoxville,1989,p.574.

4.4 High Voltage Transmission Line

Outputs of power supplies are in high potential of over 1 MV. In the air, large space is required for the insulation. To reduce the space, SF_6 gas insulation is adopted in most of the equipments. Equipments are connected by the cable ducts insulated by the pressurized SF_6 gas. Specifications of the cable duct are as follows:

1. Diameter of outer duct : 1230 mm (Inner diameter)
2. Diameter of inner duct : 520 mm x 1, 200 mm x 4
3. Pressure of SF6 gas : 5 bar (abs)
4. Insulator : Epoxy

The structure of the cable duct is shown in Fig.4.4-1. Inner ducts corresponds to the outputs of acceleration power supply. Outputs of ion source power supplies are transmitted through the inner duct of -1200 kV. Insulation design is based on the data shown below:

1. Flash over voltage V_f of SF_6 gas is given by

$$V_f = 89pdf \ (kV)$$

where

p : SF_6 gas pressure (atm)
d : gap length (cm)
f : ratio of average electric field strength to maximum one

2. Maximum electric field strength is limited to 70% of the value mentioned above in consideration of spacer efficiency of 0.7.

As the pressure of SF_6 gas in HVT room is about 1 bar (abs), bushings are required. Bushings are made of FRP and are around 2 m long.

Cooling water for the ion source and the accelerator grids is also transmitted through the cable duct accompanied with the electric feeders. Cooling water is fed to each inner duct through insulated pipes in the power supply room.

Coaxial shell structure is not adopted from a manufacturing point of view. Feeding of cooling water is also difficult in the coaxial shell structure.

The design of the insulation is affected largely by the dusts and the surge voltage. It is important to reduce the dusts at the installation and to suppress the surge voltage.

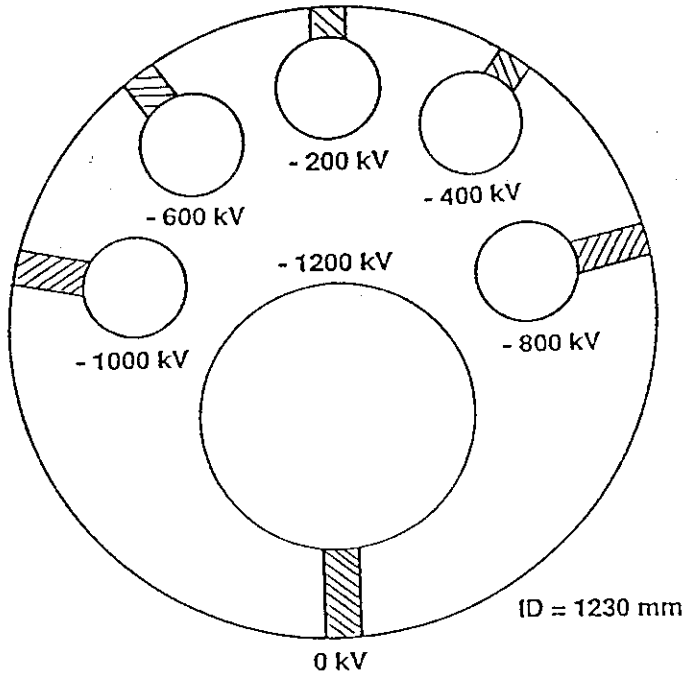

Fig. 4.4-1 Cross section of non-coaxial SF_6 cable duct

4.5 Auxiliary Power Supply System

Power supplies for the profile controller and the ion deflector supply the currents of the coils. Output currents of these power supplies are around 1 kA and fast control is not required.

Power supply for the profile controller controls the output current according to the beam profile and the beam energy.

Power supply for the ion deflector controls the output current according to the beam energy. Sweeping of the current maybe required to reduce the heat load on the ion dump.

4.6 SF_6 Gas Handling System

Large amount of SF_6 gas is utilized in the NBI system for high voltage insulation. Functions required for SF_6 gas handling system is as follows:

1. Gas circulation for the cooling and the dehumidification.
2. Gas evacuation in the maintenance of the ion source etc.

Analysis of the gas may be required to monitor corona discharge.

5. NEUTRON SHIELD

We have considered an overview of NB neutronics in FY89; The generation rate of the DD neutron and tritium in the beamline have been estimated on the basis of J. Kim's model. The tritium flow rate from the torus has also been evaluated as a function of pressure in the torus. Furthermore, a series of neutronics calculations in the beamline have been performed to evaluate the activation problem. Then the induced RI yields for some functional materials, like Cs, Ba, Co, etc have been estimated.

In FY90, the considerations on the neutronics is being developed with the basis obtained in FY89. The purpose is concentrated on the followings:

i) Consistency with ITER torus neutronics
(ITER neutronics & safety concept, calculation coordinate)

ii) Reasonable neutronics design
(layout, maintenance, optimization)

iii) Establishment of neutronics calculation procedure

5.1 ITER Neutronics Concept

Two guidelines have been introduced by Maki[1].

i) In the ITER, as a nuclear reactor, each device surrounding the torus should have a radiation shield individually.

We should provide NB room, containing ion source and beamline, as a radioactive boundary. After DT operation, it is basically prohibited to enter NB room even if the ITER is shutdown. All the maintenance have to be treated by remote handling. The power supply and auxiliary rooms will be designed so as to be freely accessed. Namely, the wall of the NB room is the biological shield.

ii) On C&R to decide the construction, it will not be accepted if the ITER produce so much amount of induced activities. The ITER has to be designed so as to minimize the fusion radioactive waste with a perspective of its moth ball.

Although concrete used for the building is an important member of the radiation shield, the activation of NB room wall have to be suppressed to be a modest level. A permissible level for such a structural material may be below 10^{-6} Ci/cm^3 as a low level radioactive waste. Thus the activation of the wall is limited from a view point of decommission. Then shield for high energy neutron should be mounted around the beamline, instead of the concreat wall, in order to minimize its activation.

Reference

[1] K. Maki et.al.: Japan Atomic Energy Research Institute Report, JAERI-M90-046 (1991).

5.2 ITER NBI Neutron Shield Concept

The peculiarity of the NB configurations from an aspect of the neutronics is summarized in Fig. 5.2-1.

First of all, each NB system have a big opening (0.8 m x 3.4 m) in the torus vacuum vessel as an injection port, which will allow 14 MeV neutrons flow into the NB system. This wide and high opening facing DT burning plasma will result in a high neutron fluence in the NB beamline.

Following the port is a high drift duct that dimensions are $8m^{h}$ x $21m^{l}$. In order to reduce the activation in the torus hall, big neutron shield is required around the drift duct. It should also be noticed that tritium will diffuse into the NB system from scrape off region of the torus, since the pressure in the duct is maintained high vacuum as equivalent to that of torus in order to prevent re-ionization loss of the NB.

Then inside of the NB room, the neutron and the tritium flow into a main body of the NB system, i.e. the beamline. By a high neutron flux, beamline component may be activated considerably. Tritium will be accumurated on cryopump, with a potential of leakage and permiation into cryogenic systems. Both of them will be troublesome for maintenance of the beamline necessary several times during the life.

The ion source, the heart of the system, looks at the burning plasma directly. Namely, it is exposed by high flux of 14 MeV neutron, which may result in a high level of activity production. Although the ion source requires periodic maintenance, it may be impossible to approach to it for several monthes or more.

Thus the biggest peculiarities of the NB system from an aspect of the neutronics are summarized as follows:

i) Big opening as a injection port requires a shield for the NB system equivalent to that in the torus cryostat.

ii) Direct neutron flux toward the ion source may yield a high level and much amount of the induced radioactivities in the ion source and the beamline.

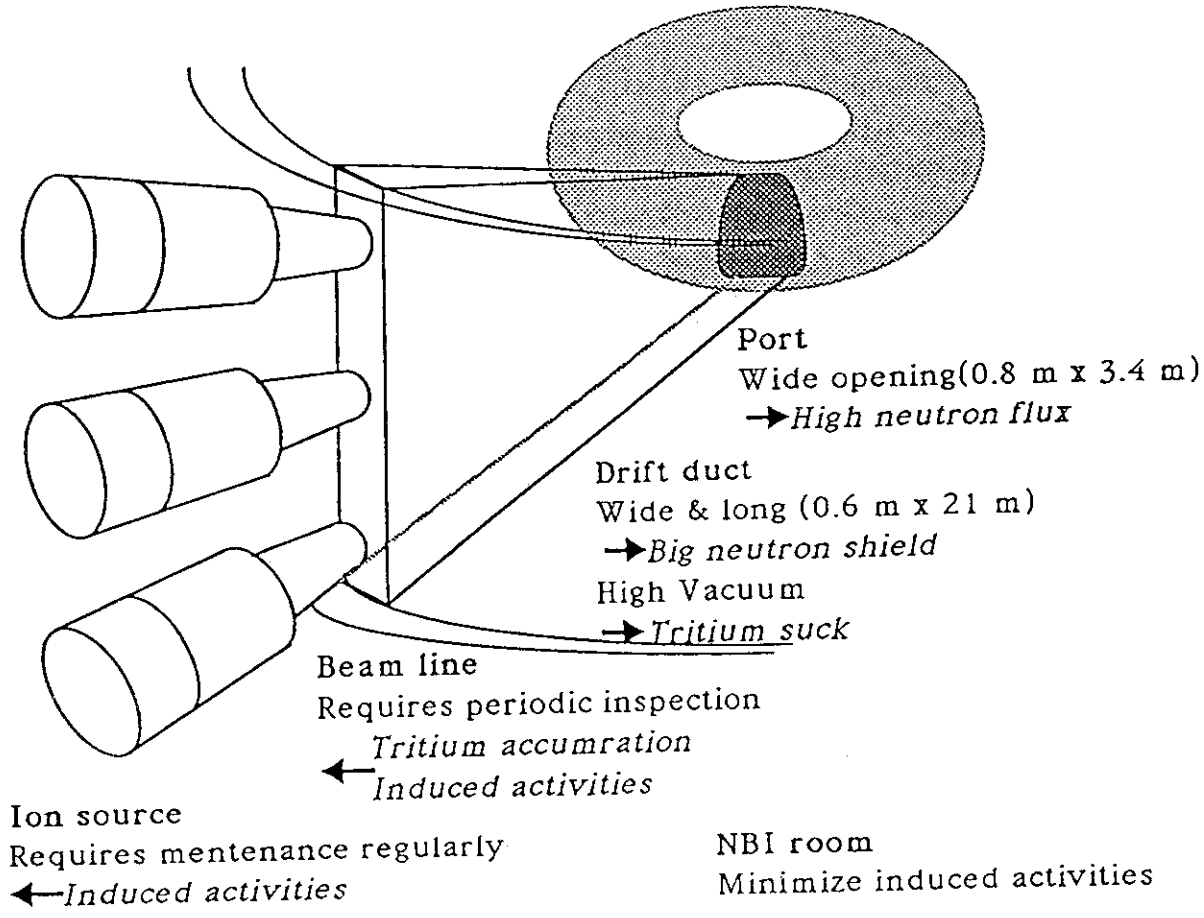

Fig. 5.2-1 An illustration of the peculiarity of the ITER/NBI neutronics.

5.3 Neutronics Circumstances around the NBI System

5.3.1 Neutron Flux from the Torus

2D and 3D neutronics in the region shown in Fig. 5.3-1 (2D case) and Fig. 5.3-2 (3D case) have been calculated by Maki et. al.[1] The results obtained both calculations are illustrated in Fig. 5.3-3. This is a total neutron flux distributions along the axis of the NB drift duct. Since the difference of the neutron fluxes obtained by 2D and 3D calculations is small, it was made clear that the 2D model is a good approximation for the neutronics calcuration in the NB drift duct. The narrow width of the drift duct allows 2D modeling enough approximation. Thus the neutron flux in the drift duct is limited by the width (0.6 m), and expanding the port and the duct width will cause the crucial increase of the neutron flux. Thus 2D calculation in the duct gives a sufficient informations for the following calculations.

A summary of the calculations is shown in Table 5.3-1. The neutron fluxes at the entrance of the NB room (2800 cm from the torus axis) are 7.7×10^{10} n/cm^2 (total), 2.2×10^{10} n/cm^2 (14 MeV), and 5.1×10^{10} n/cm^2 (0.1 MeV). These values are utilized for calculations in the NB room.

Reference

[1] K. Maki et.al.: Japan Atomic Energy Research Institute Report, JAERI-M90-046 (1991).

Table 5.3-1 Neutron and gamma ray flux; The results obtained by a three dimensional computation (MCNP).

Distance from Point A (cm)	14 MeV Neutron (n/cm2)	0.1 MeV Neutron (n/cm2)	Total Neutron (n/cm2)	Primary Gamma (n/cm2)	Secondary Gamma (n/cm2)
0.0	———	———	———	———	———
300.0	1.608 x 10^12	1.048 x 10^13	2.798 x 10^13	2.335 x 10^12	9.316 x 10^12
800.0	3.159 x 10^11	1.313 x 10^12	2.925 x 10^12	3.327 x 10^11	8.865 x 10^11
1300.0	1.173 x 10^11	3.496 x 10^11	6.908 x 10^11	1.096 x 10^11	1.943 x 10^11
1800.0	5.479 x 10^10	1.760 x 10^11	2.800 x 10^11	4.668 x 10^10	7.664 x 10^11
2300.0	3.559 x 10^10	8.947 x 10^10	1.724 x 10^11	2.523 x 10^10	3.181 x 10^10
2800.0	2.166 x 10^10	5.059 x 10^10	7.648 x 10^10	1.546 x 10^10	1.547 x 10^10

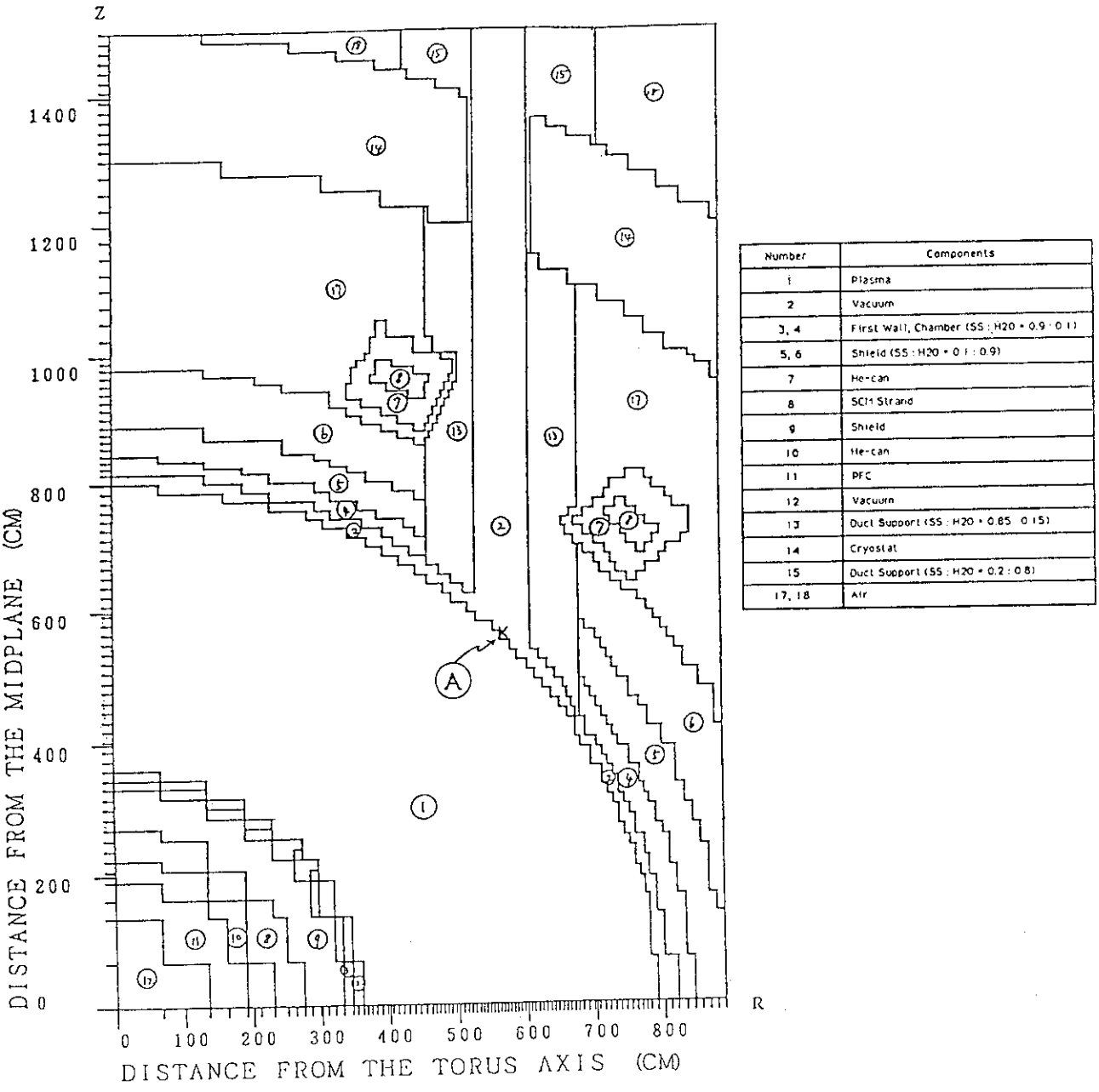

Number	Components
1	Plasma
2	Vacuum
3, 4	First Wall, Chamber (SS : H20 = 0.9 : 0.1)
5, 6	Shield (SS : H20 = 0.1 : 0.9)
7	He-can
8	SCM Strand
9	Shield
10	He-can
11	PFC
12	Vacuum
13	Duct Support (SS : H20 = 0.85 : 0.15)
14	Cryostat
15	Duct Support (SS : H20 = 0.2 : 0.8)
17, 18	Air

Fig. 5.3-1 A model of NBI drift duct for two dimensional computation.

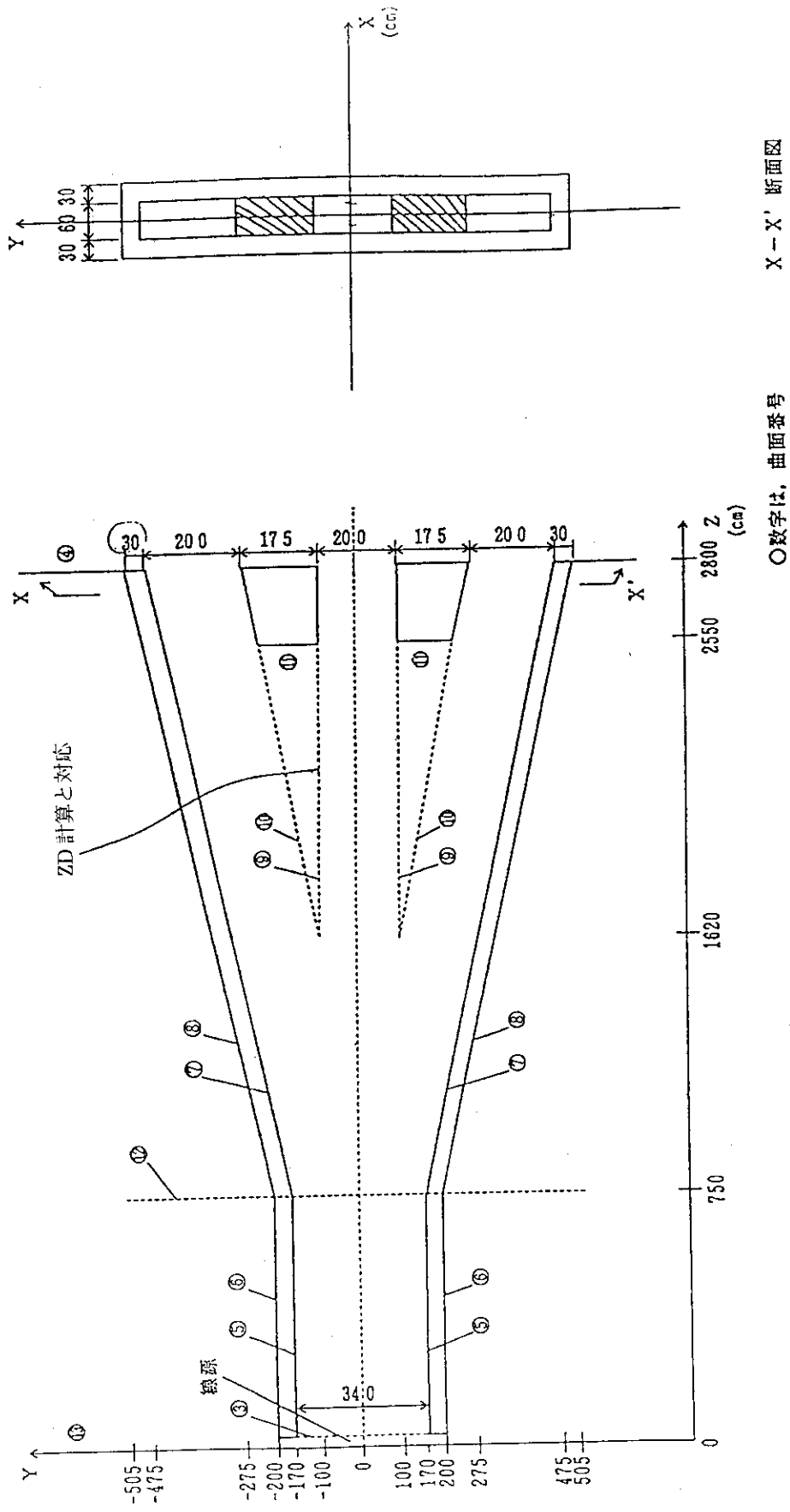

Fig. 5.3-2 A model of NBI drift duct for three dimensional computation.

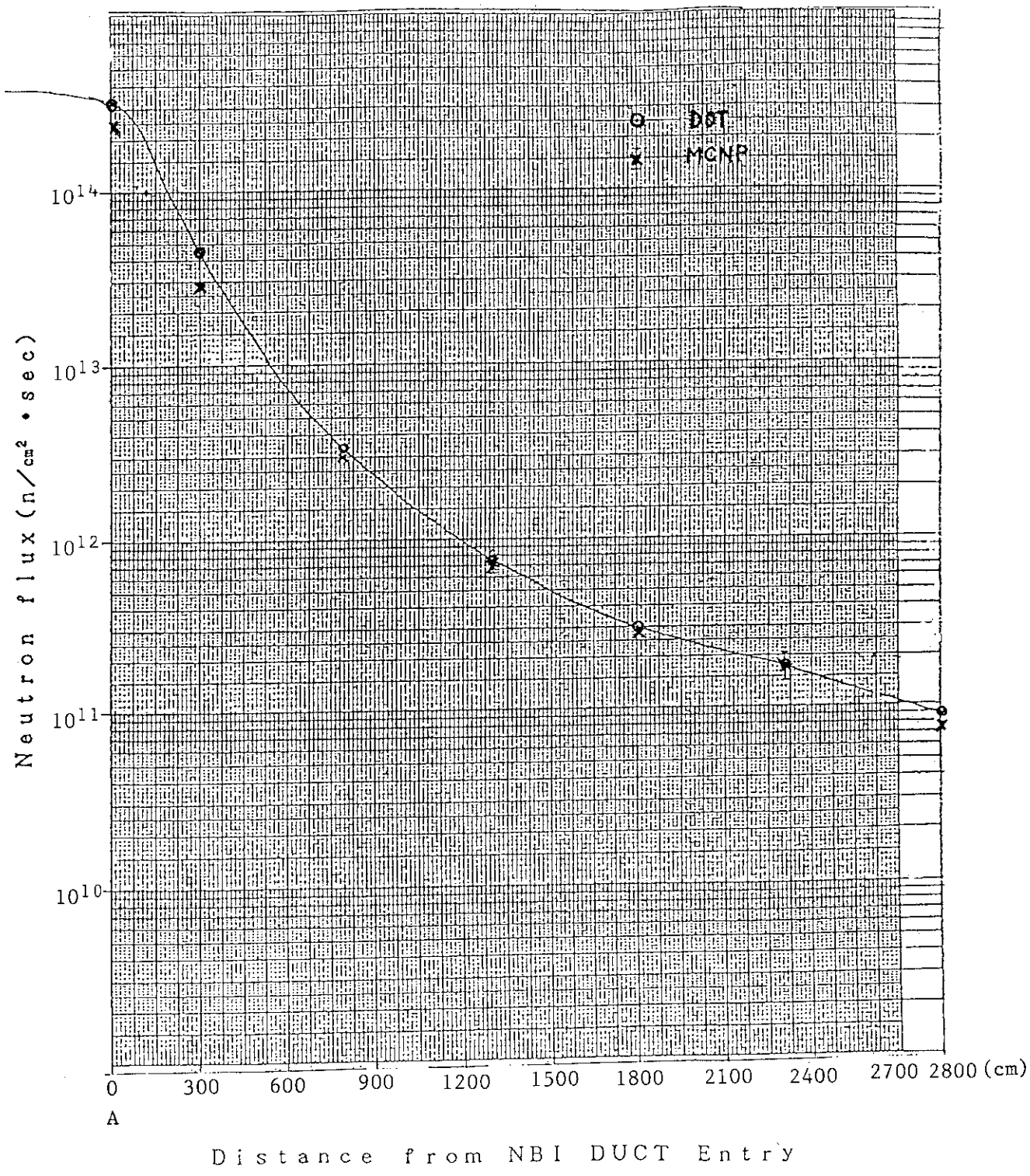

Fig. 5.3-3 Total neutron flux distribution; a comparison of the results obtained by 2D and 3D computations.

5.3.2 Tritium Flow from the Torus[1]

Tritium gas flow from the torus was evaluated from a consideration of tritium gas flow given by the geometrical configuration of beamline and the pumping speed of ITER NB common design proposed by JAERI.

As the result, we obtained the following relations and values;

(Q_{T2} to cryopump in ion dump room) = 23 P_T(Pa m^3/s)

(Q_{T2} to cryopump in ion source room) = 1.1 P_T(Pa m^3/s)

where Q_{T2} is the tritium gas flow rate in Pa.m^3/s, and P_T (Pa) is the tritium gas partial pressure at the scrape off region of the torus. This relations are shown in Fig. 5.3-4.

Reference

[1] S. Tanaka, Presented at ITER NBI Design Joint Work, Feb.26-Mar.2 (1990), Garching.

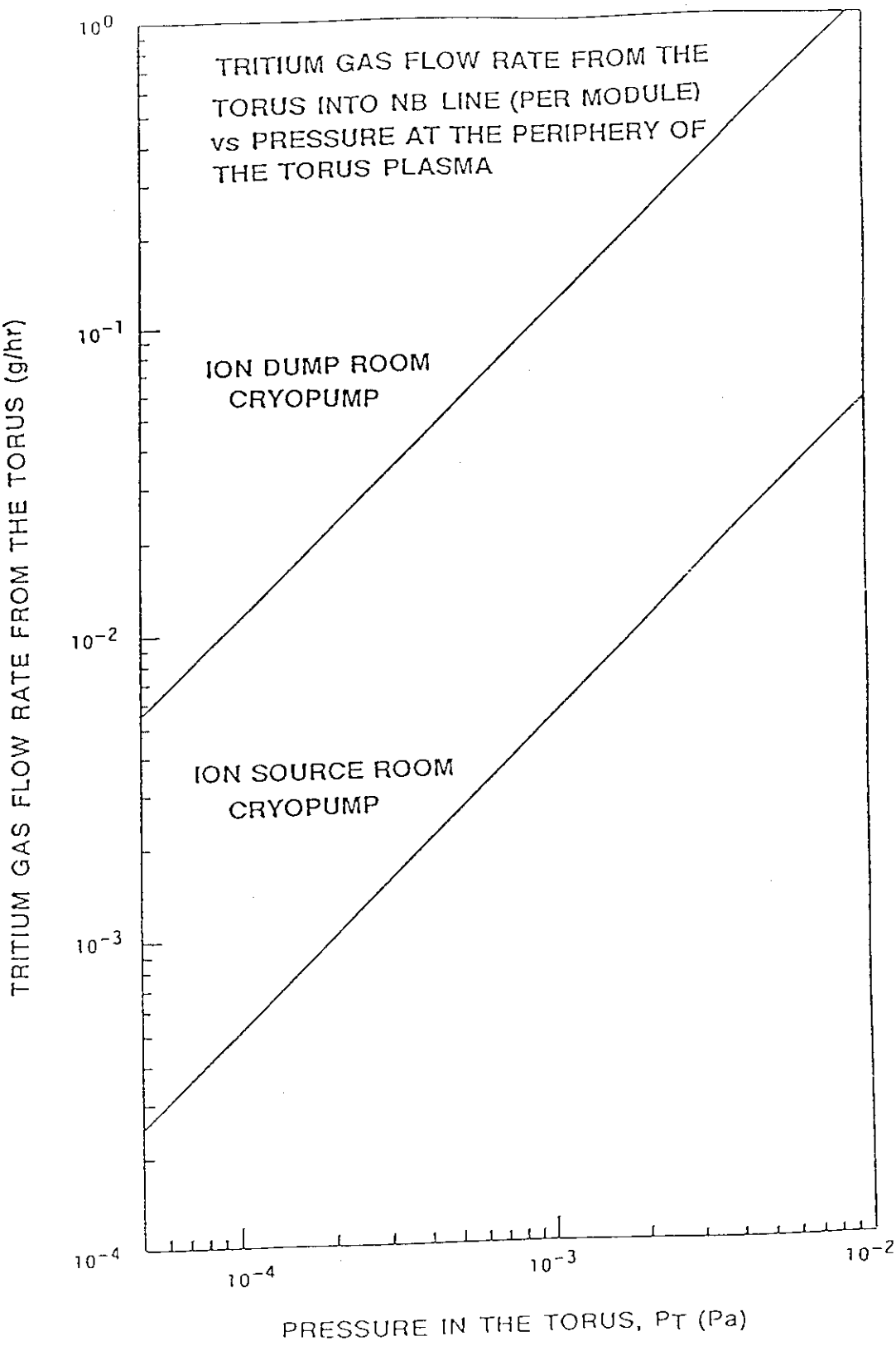

Fig. 5.3-4 Relations between tritium gas flow rate and the partial pressure in the torus.

5.3.3 Neutron and Tritium Production in the Beamline

DD Neutron and tritium yield (N&T) in the beamline has been estimated with a base of J. Kim's model[1].

Assumptions adopted in the model are following;

i) N&T are proportional to beam current. So, N&T is calculated for 1 A deuterium beam. The particle flux, n_b, of the 1 A beam is given as follows:

$$n_b = 6.24 \times 10^{18} \text{ D/s}$$

ii) From the results reported in Ref. 1, deuterium concentration in copper target is assumed to be constant value, C_D, over the deuterium range at the saturated condition;

$$c_D/n_{Cu} = 1/50$$

Hence,

$$c_D = 1.70 \times 10^{22} \text{ D/cm}^3$$

iii) Cross section of $D(d,n)^3He$ or D(d,p)T reactions are taken from Ref. 2.

iv) Energy loss process of deuterium in copper target is taken into account from stopping power data in Ref. 3.

Neutron yield (n) or tritium yield (n_T) is given by the folmura;

$$n_n \text{ or } n_T = n_b\, c_D \int_0^R \sigma_n \text{ or } \sigma_T(E(x))dx$$

Results obtained by the calculation are summarized as follows;

Neutron

in beam dump: 4×10^{12} n/As

in neutralizer: 9×10^{9} n/As

Tritium

from beam dump: 1×10^{12} T/As

from neutralizer: 9×10^{9} T/As

The results are also shown in Fig. 5.3-5 and 5.3-6 for neutron and tritium yield, respectively, as a function of the beam energy. These values give a few order of magnitude smaller flux or flow rate than that from the torus mentioned in section 5.3.1 and 5.3.2.

References

[1] J. Kim, Nucl. Instrum. Meth. 145 (1977) 9-17

[2] "Atomic data for controlled fusion research", ORNL-5207

[3] H.H. Anderson and J.F. Ziegler, "Hydrogen stopping powers and ranges in all elements", Pergamon Press

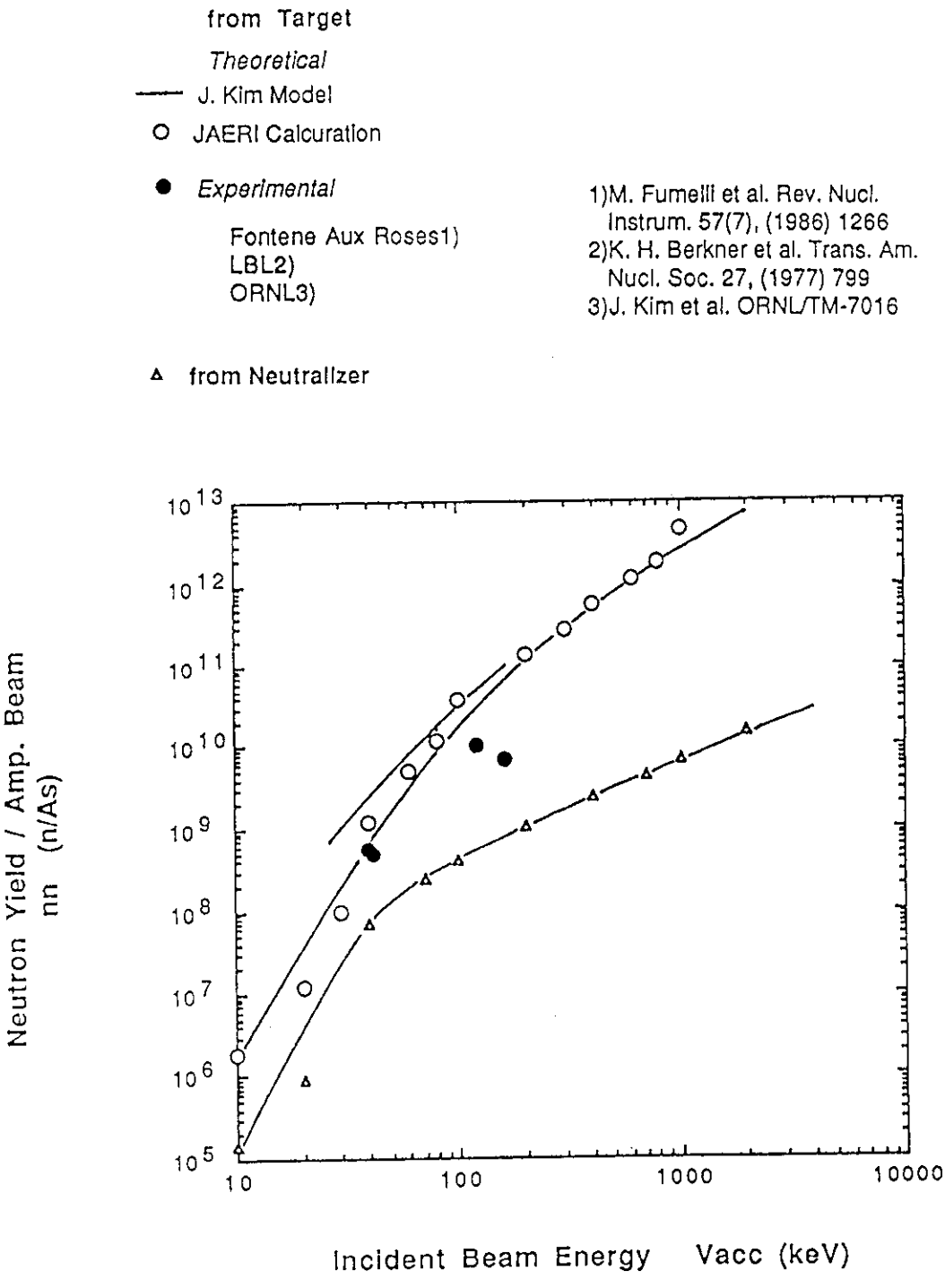

Fig. 5.3-5 DD neutron yield from beamline.

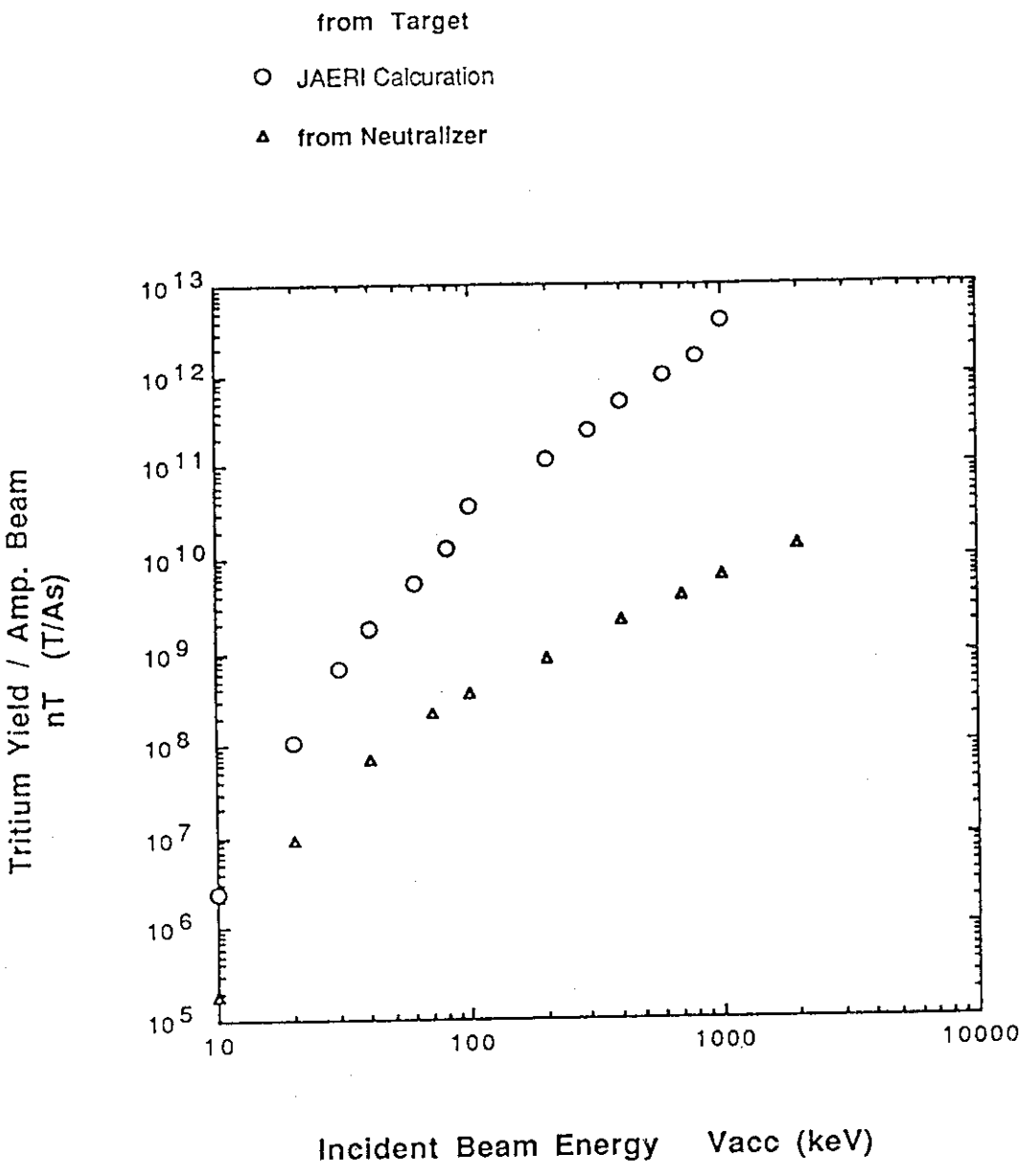

Fig. 5.3-6 Tritium yield from beamline.

5.4 Neutronics Calculation

5.4.1 Calculation Procedure

A flow of the neutronics calculation is illustrated in Fig. 5.4-1. Inputs of the calculation, drawn on a dark hatched square in the figure, have been obtained from the consideration described above. Then the neutronics computation is conducted to consider the neutron flow from the torus and the activation of the NB system.

In the present calculations, DOT3.5[1] code have been used for two dimensional transport computation of the neutron and gamma ray. For the transmutation calculation, CINAC-V4[2], which was developed at Hitachi Ltd., has been utilized and linked with the transport computations.

References

[1] RSIC Computer Code Collection, "DOT III: A Two-Dimensional Discrete Ordinate Transport Code", CCC-209, Radiation Shielding Information Center.

[2] H. Fukumoto, J. Nucl. Sci. and Tech, 23/2 (1986), 97

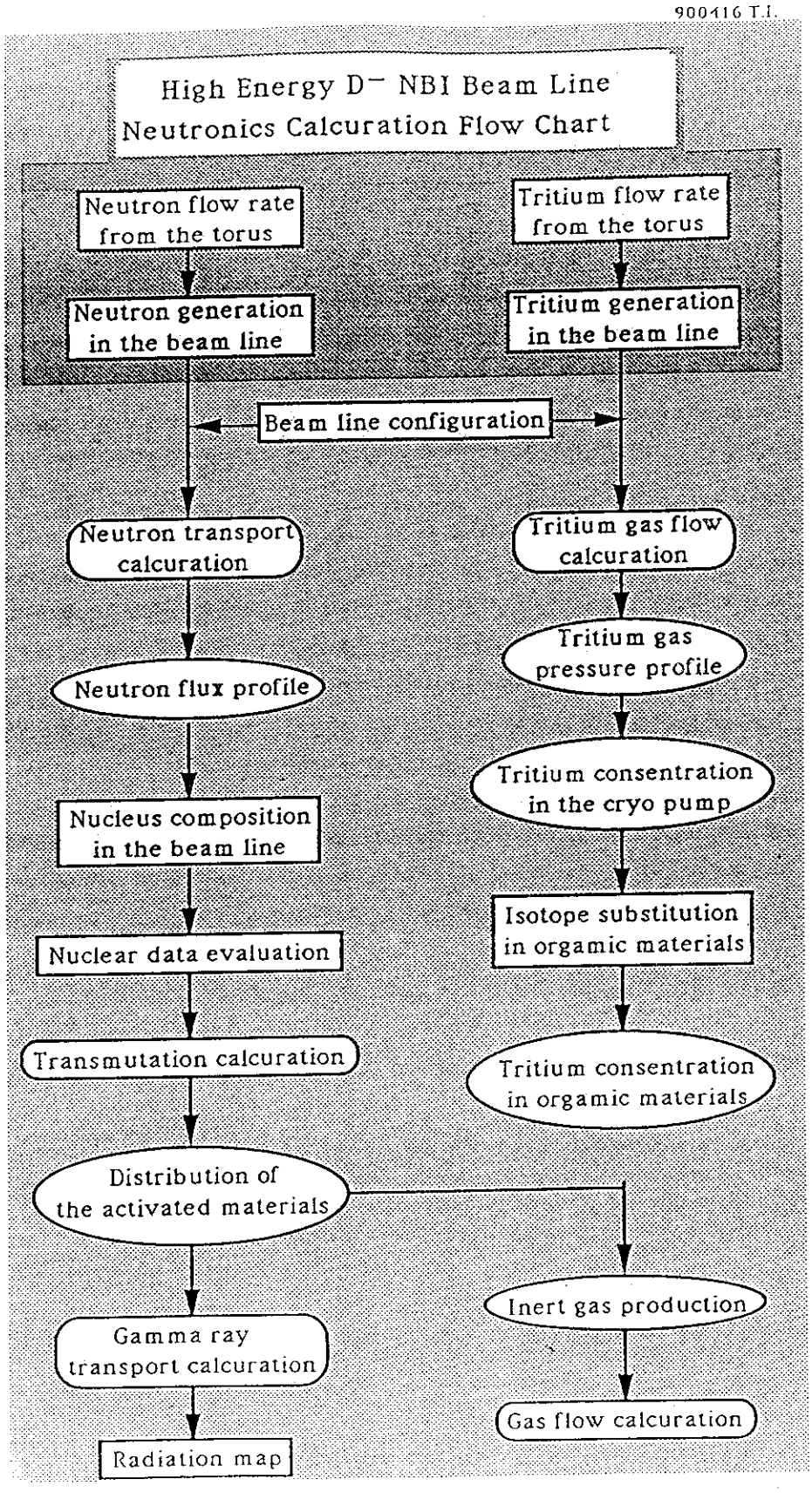

Fig. 5.4-1 A flow chart of the neutronics calculation for high energy D^- NBI beamline.

5.4.2 Modeling of the NBI room

For the two-dimensional calculation, the NB system was modified to be a cylindrical symmetry, which was a proper modeling for the cylindrical beamline. An example used for activation analysis is shown in Fig. 5.4-2. (note that this configuration is slightly different to that of the ITER NB system.) The modeling method for each component is as follows;

i) The inner diameter of a component was taken to be the same as the closest distanse between the inner surface and the beamline axis.

ii) The volume and the density of the component was conserved in the model.

iii) Consequently, the outer diameter could be decided.

iv) In some cases such as acceleration grids, the volume in the model was taken to be the same as the accelerator column, then the density of the compornent was deluted by mixing the grid materials and void (vacuum).

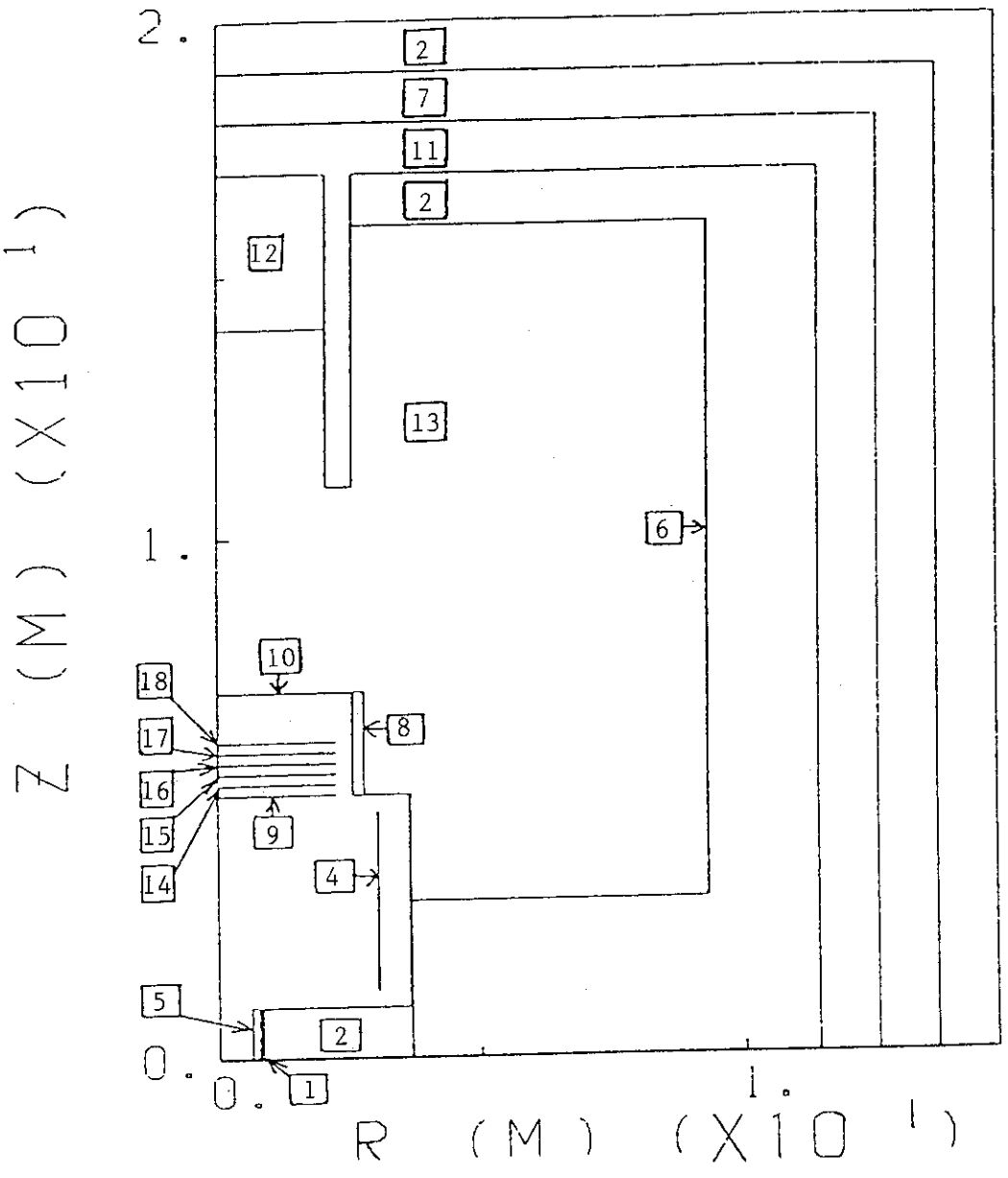

Fig. 5.4-2 An example of the model for two dimensional neutronics calculations; The ion source room was modeled to clindrical symmetry.

5.4.3 Neutronics in the Ion Source Room

The activation of cesium/barium deposited grids was evaluated in the first. Since the NB system, especially the ion source, is exposed to high energy and fluence of neutrons as described in section 5.2, it is indispensable that the component is activated. The next thing to do is to consider how the induced activities are reduced. From view points of maintenance and decommissioning, we do not worry about the production of radioactive nuclei with short life. The critical point is the production of the long life (more than a few weeks) radioactives.

(1) Assumption

The assumptions applied in the calculation is as follows:

i) Monoenergetic neutrons (14 MeV or 2.45 MeV) flow into the ion source room. Namely, only the direct neutrons entering the room without any reflection or attenuation was considered. The flux at the entrance of the room was simply evaluated by assuming isotropic radiation of the neutrons carrying the ITER fusion power (1000 MW). Also the neutron divergent angle was estimated from the beamline configuration. The values are shown below.

Neutron flux

2.5×10^{9} n/cm^2 (14 MeV)

1.0×10^{10} n/cm^2 (2.45 MeV)

Divergent angle

1.3 degree

ii) Fig. 5.4-2 illustrates the two dimensional (cylindrical) model for the ion source room, which was used only for evaluating the activation. Special features applied in the model are;

a) In order to attenuate the direct neutron flux penetrating the ion source, a neutron dump was placed on the back.

b) Functional materials such as samarium, cobalt (magnets), cesium, and barium were mixed in each grids separately. Since the amounts of the materials are strongly dependent

on the ion source design, they were assumed to be 0.1 g/cm^3 for each materials at present.

c) The void outside of the beamline was filled with SF_6 and the air to evaluate the activation, though the gas have slight stopping/attenuation power.

iii) Operation scinario was assumed as shown in Fig. 5.4-3. The activation history was calcurated after the two years operation.

(2) Neutron flux distribution

Fig. 5.4-4, 5.4-5, and 5.4-6 show the results obtained by the neutron transport computation of DOT 3.5. Fig. 5.4-4 is the 2.45 MeV neutron distribution corresponding to the ITER DD operation, i.e. The neutron source was 2.45 MeV monoenergetic. Fig. 5.4-5 and 5.4-6 were that for 14 MeV neutron source corresponding to the DT operation.

From these neutron distributions, followings should be minded;

i) Most of the direct neutrons entering the room flow straight-forward and dumped in the neutron dump. Consequently, high energy neutron flux is very high along the beamline axis, since there is no obstacles in the beamline.

ii) Then, a part of dumped neutrons are reflected to the beamline backward.

iii) Some of the neutrons are scattered by the accelerator grids and the source back plate toward the radial direction. They form an peninsula of higher neutron flux on a side between the ion source and the dump.

(3) Induced radioactivity

Induced activity of copper and molybdenum, as an example for main materials of the ion source, is shown in Fig. 5.4-7 and 5.4-8, respectively, as a function of the time after the two year operation. The general feature of the history is summarized as follows;

i) A threthold of the activation reaction is below 2.45 MeV for most of the materials used in the NBI. So the intensity of

the induced activity will not change even in DD operation. The intensity is mostly dependent on the neutron flux rather than the energy of the fusion neutron.

ii) As a characteristic of the fusion induced radioactives, generally speaking, the half life $T_{1/2}$ is shorter than that of fission product. In case of copper, the induced activity of ^{62}Cu and ^{64}Cu are dominant just after the shut down. However, they are reduced exponentialy and become negligible within 10^6 s, i.e. two weeks.

A point should be noticed is production of ^{60}Co as a daughter of copper. Since the half life of ^{60}Co is long (5.27 years), copper parts used in a high flux of 14 MeV neutron region may not be recommended.

Let us take a look at cesium. The induced activity of cesium is shown in Figs. 5.4-9 for 2.45 MeV and 14 MeV neutron. Although cesium is famous as a harmful fission product (like ^{137}Cs; its half life is 30.17 years), the nuclei will not be transmuted by the fusion neutron. A problem is ^{134}Cu ($T_{1/2}$=2.062 years), however, the radioactivity is two order of magnitude smaller than ^{60}Co transmuted in copper, and the total amount is much smaller. The other problem is a production of xenon radioactives (^{133}Xe) by an irradiation of 14 MeV neutrons. Xenon, an inert gas, will be evacuated by the vacuum system and released to an environment easily, though the amount is small and the half life is only 5.29 days.

Barium may be worse (see Fig. 5.4-10): ^{133}Xe and ^{135}Xe, long life nuclei, will be transmuted.

As for samarium and cobalt, materials of SmCo permanent magnet, the history is shown in Fig. 5.4-11 and 5.4-12, respectively. The long life nuclei are ^{51}Sm, ^{58}Co, and ^{60}Co.

The amounts of each materials were assumed to be 0.1 g/cm^3 in each grids at present. Because the amount of the magnets or the Cs/Ba consumption rate are strongly dependent on the ion source design. In the next step, it is required to calculate the gamma ray intensity profile in the room by fixing the ion source specifications.

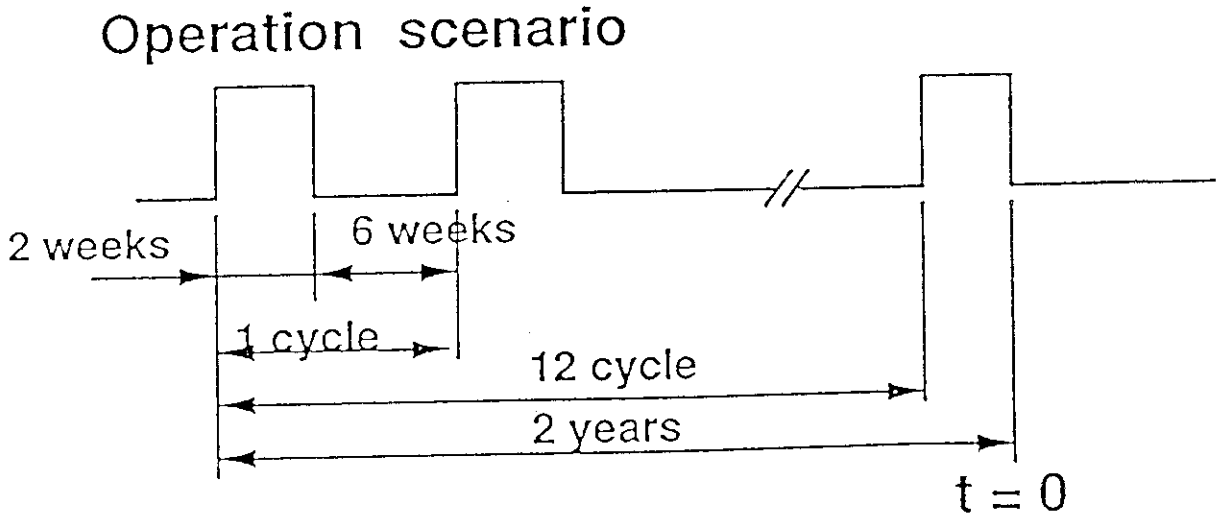

Fig. 5.4-3 Operation scenario assumed in the FY89 calculations.

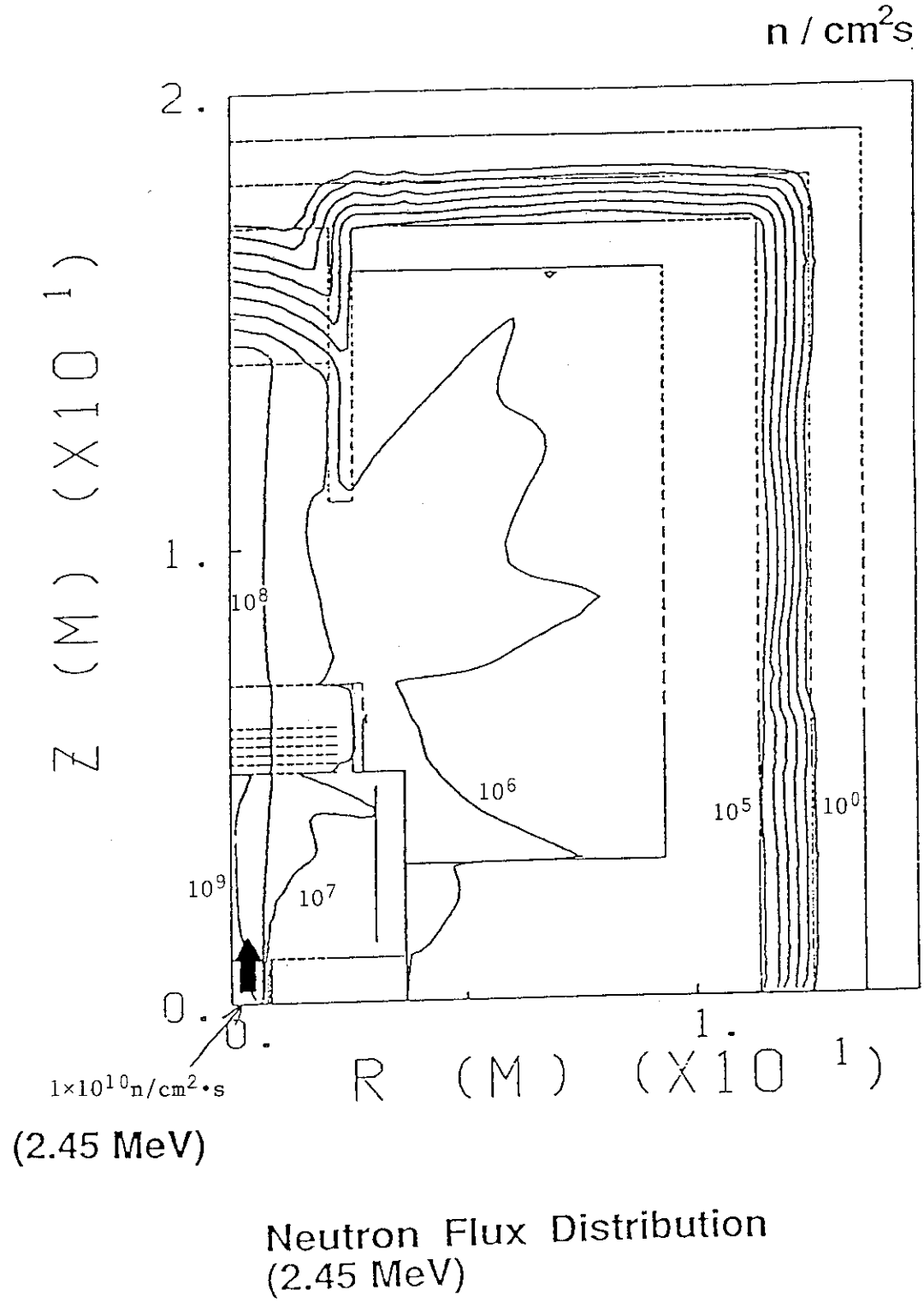

Fig. 5.4-4 Flux distribution for 2.45 MeV neutrons; DD neutrons were injected from the entrance of the vacuum chamber mounting the ion source.

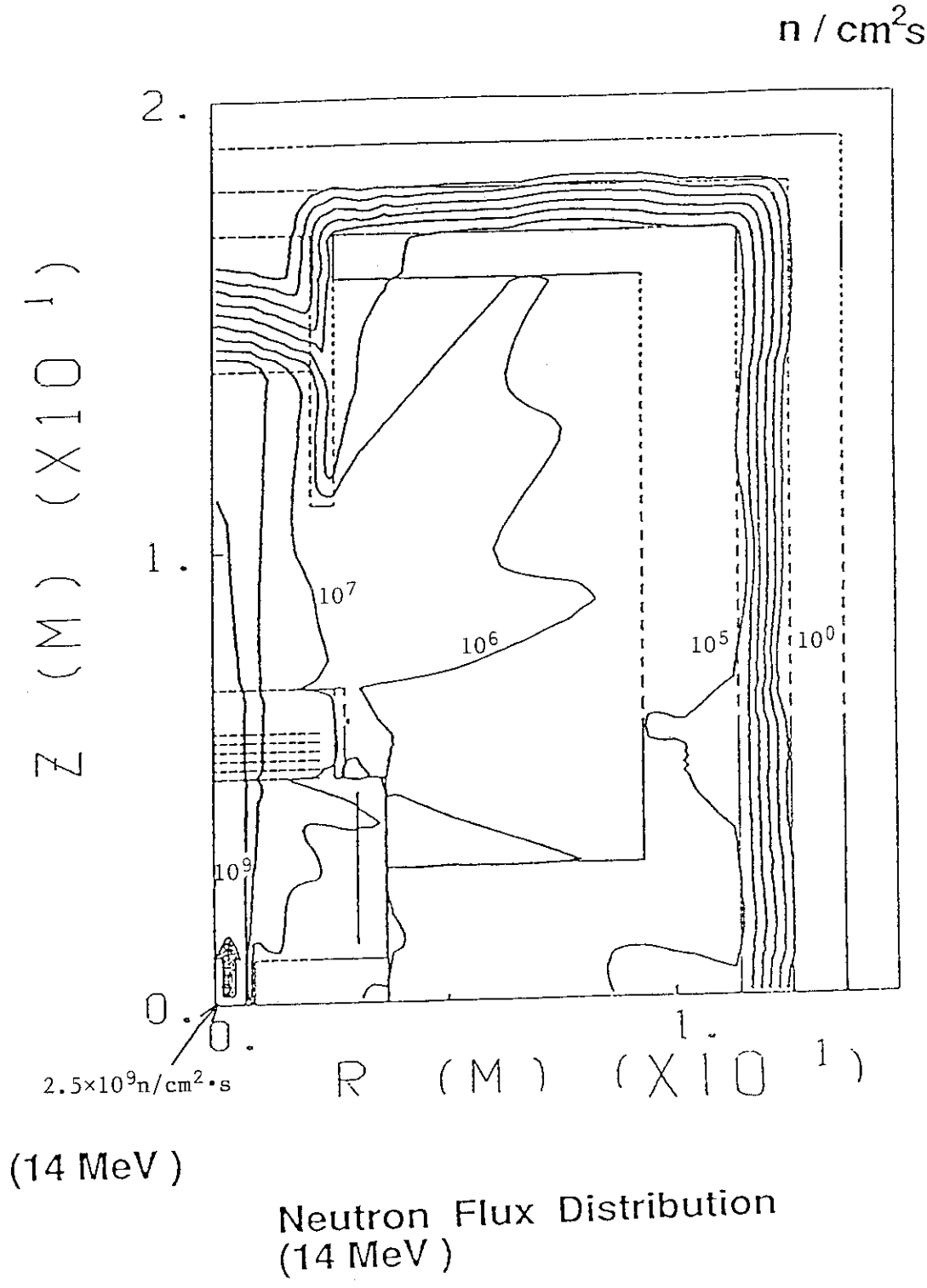

Fig. 5.4-5 Flux distribution for 14 MeV neutrons; DT neutrons were injected from the entrance of the vacuum chamber mounting the ion source.

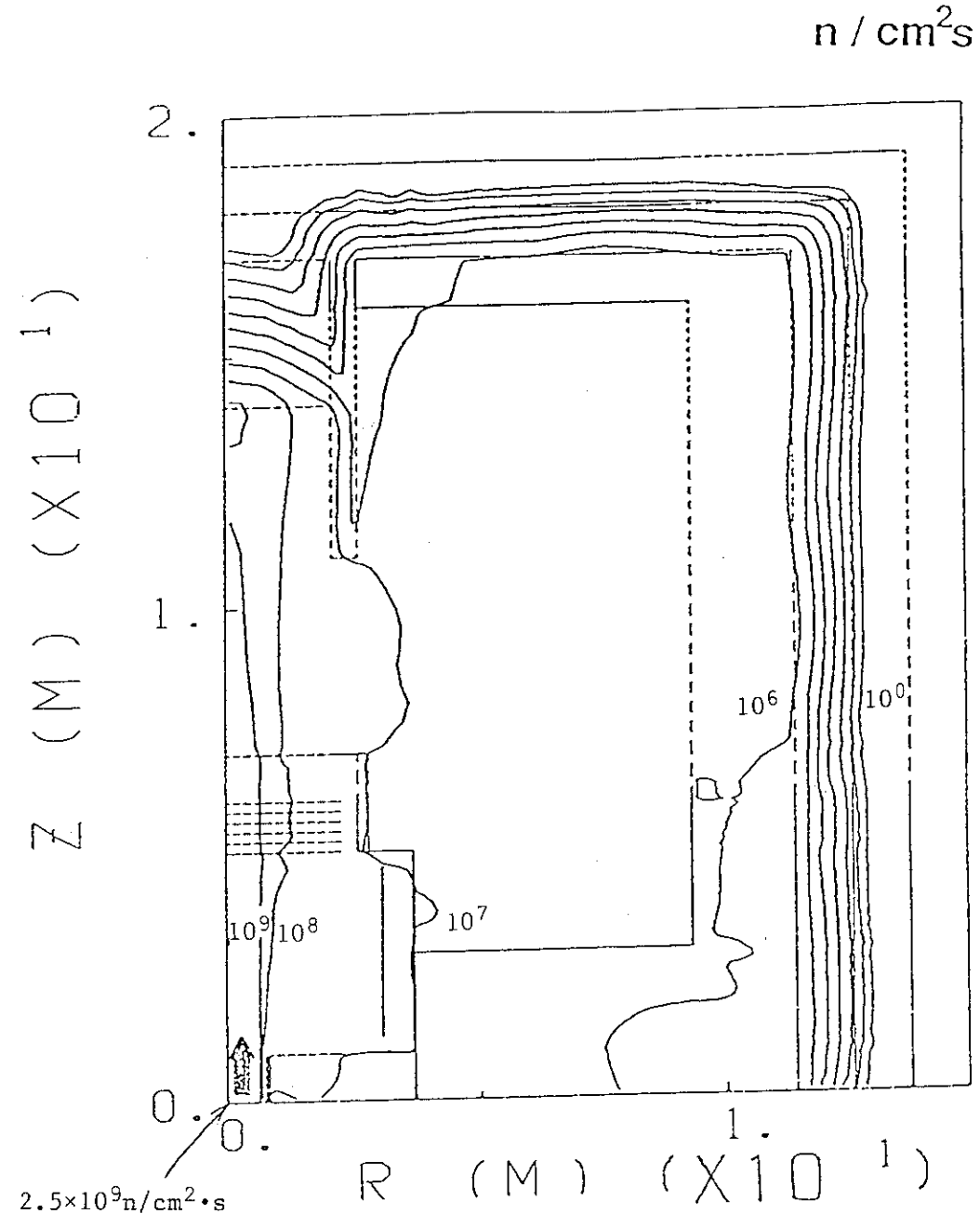

(14 MeV)

Neutron Flux Distribution
(above 1 MeV)

Fig. 5.4-6 Flux distribution for neutrons above 1 MeV; DT neutrons were injected from the entrance of the vacuum chamber mounting the ion source.

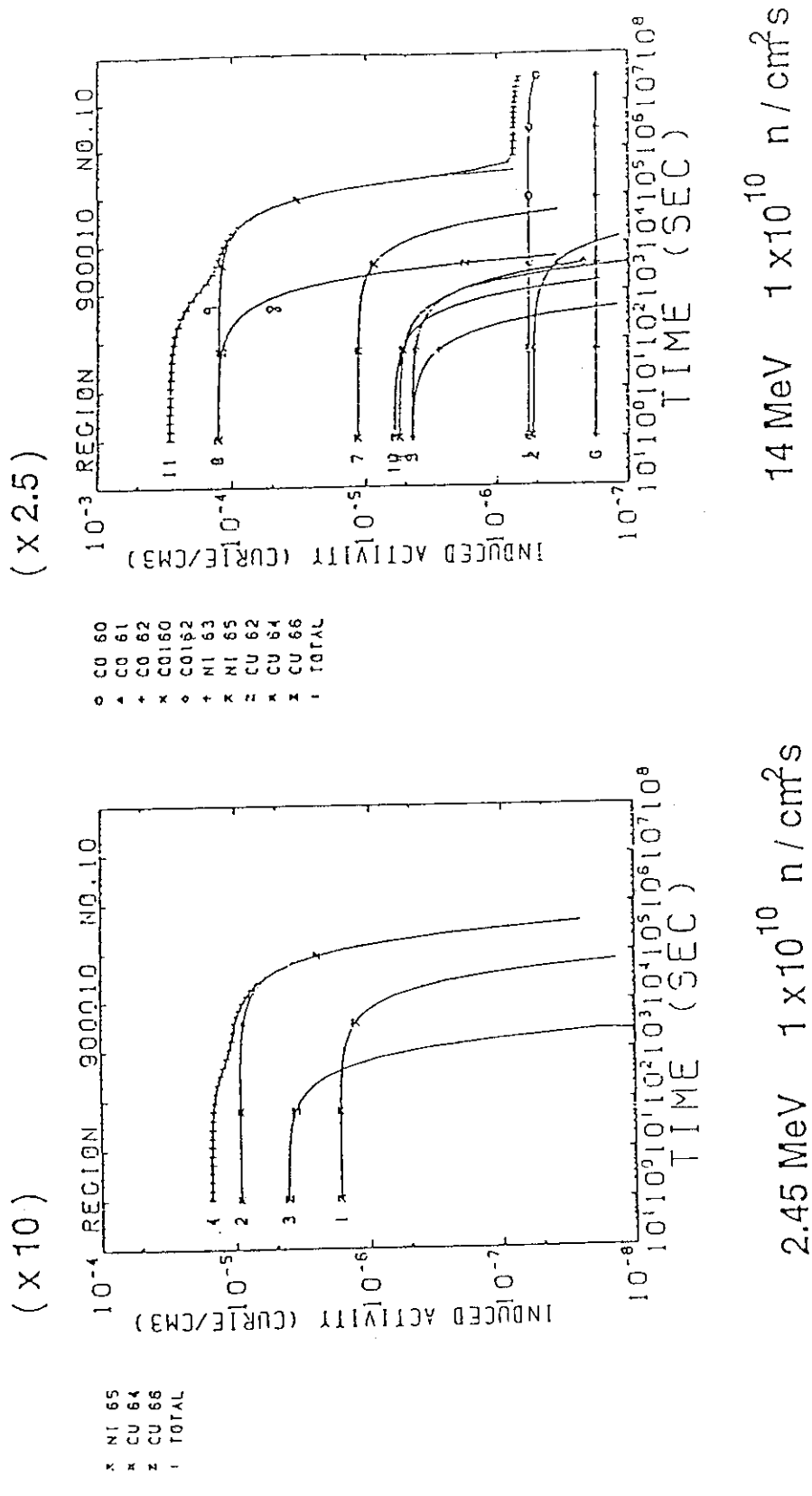

Fig. 5.4-7 The history of induced radioactivities transmuted from copper.

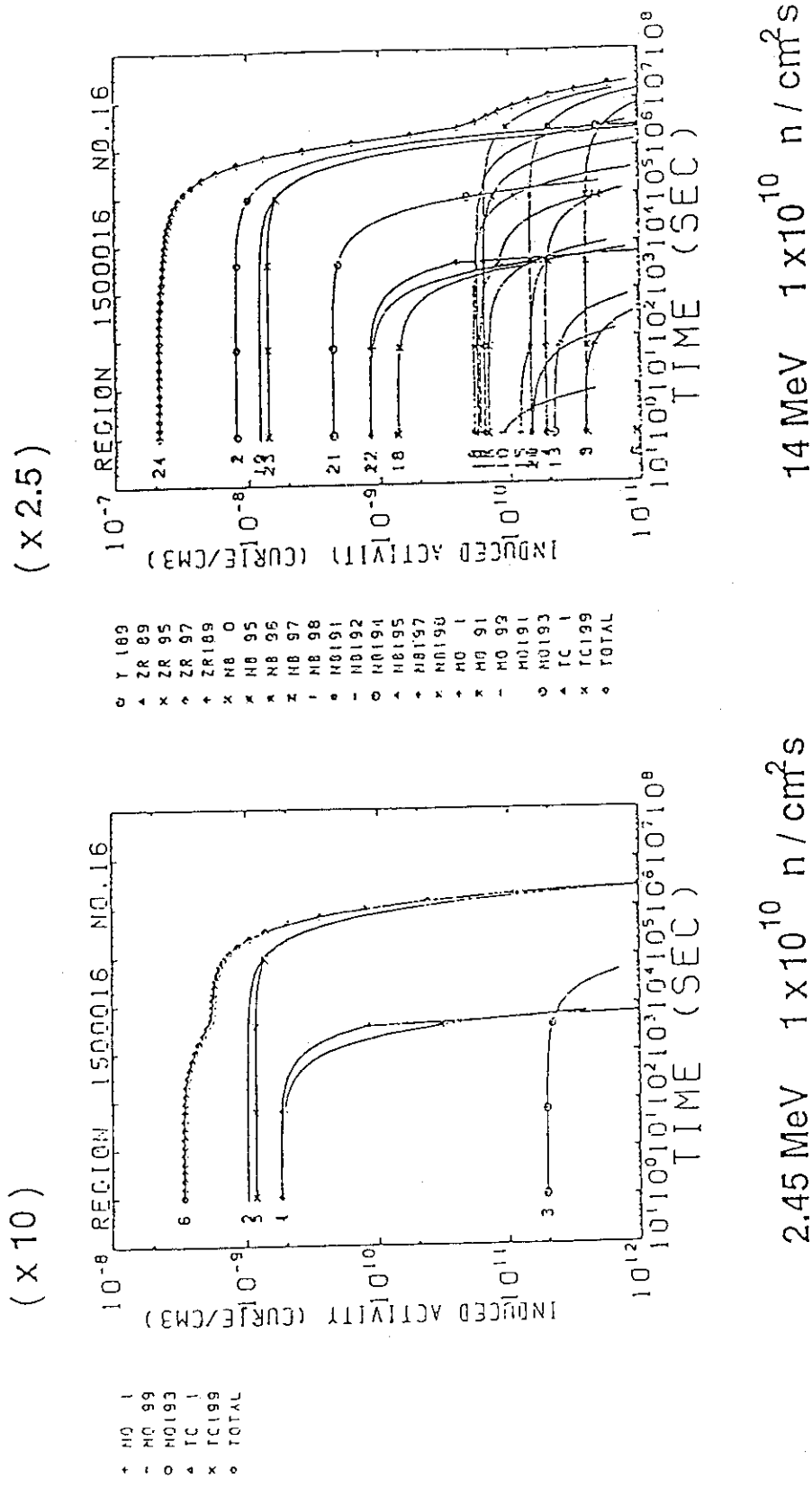

Fig. 5.4-8 The history of induced radioactivities transmuted from molybdenum.

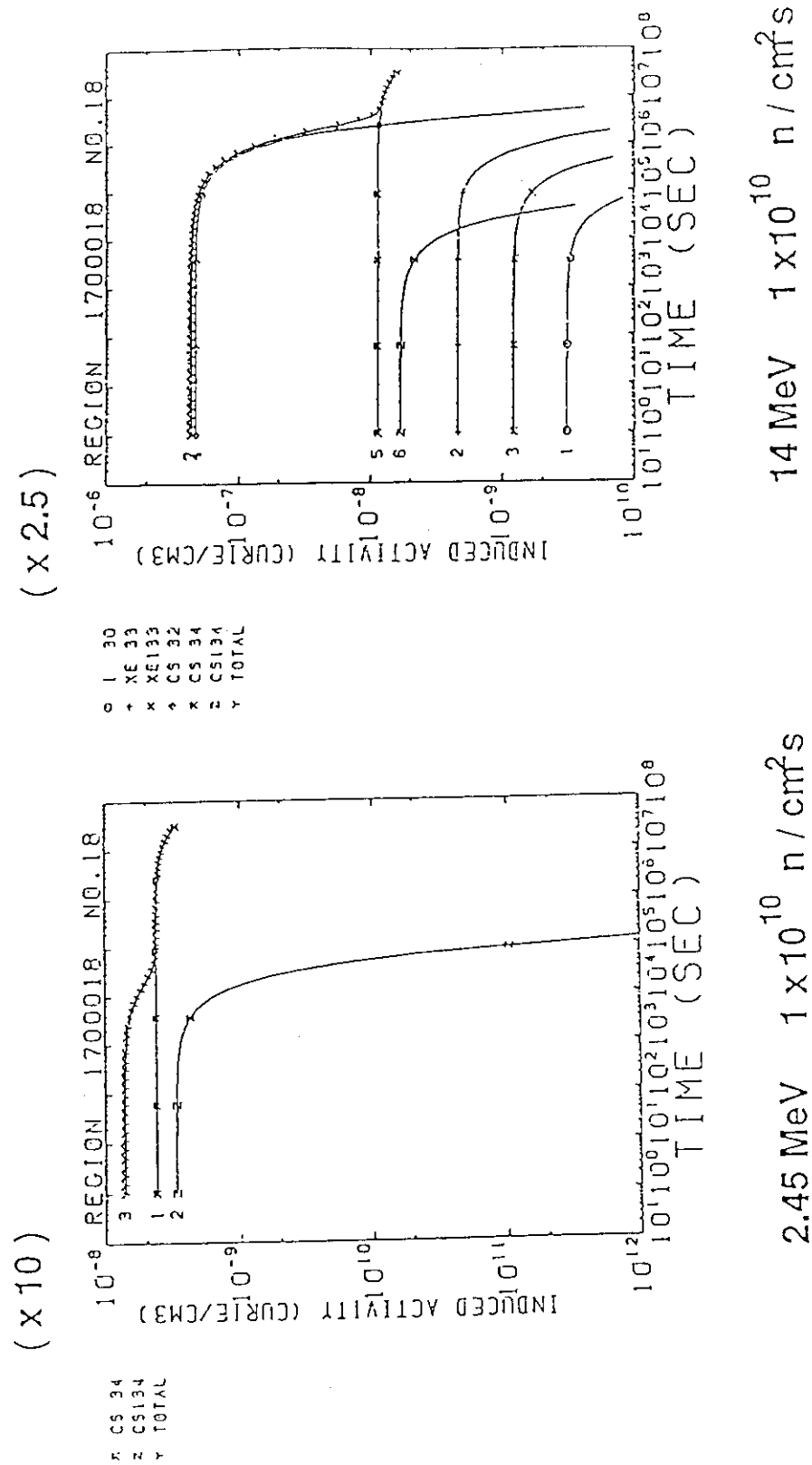

Fig. 5.4-9 The history of induced radioactivities transmuted from cesium.

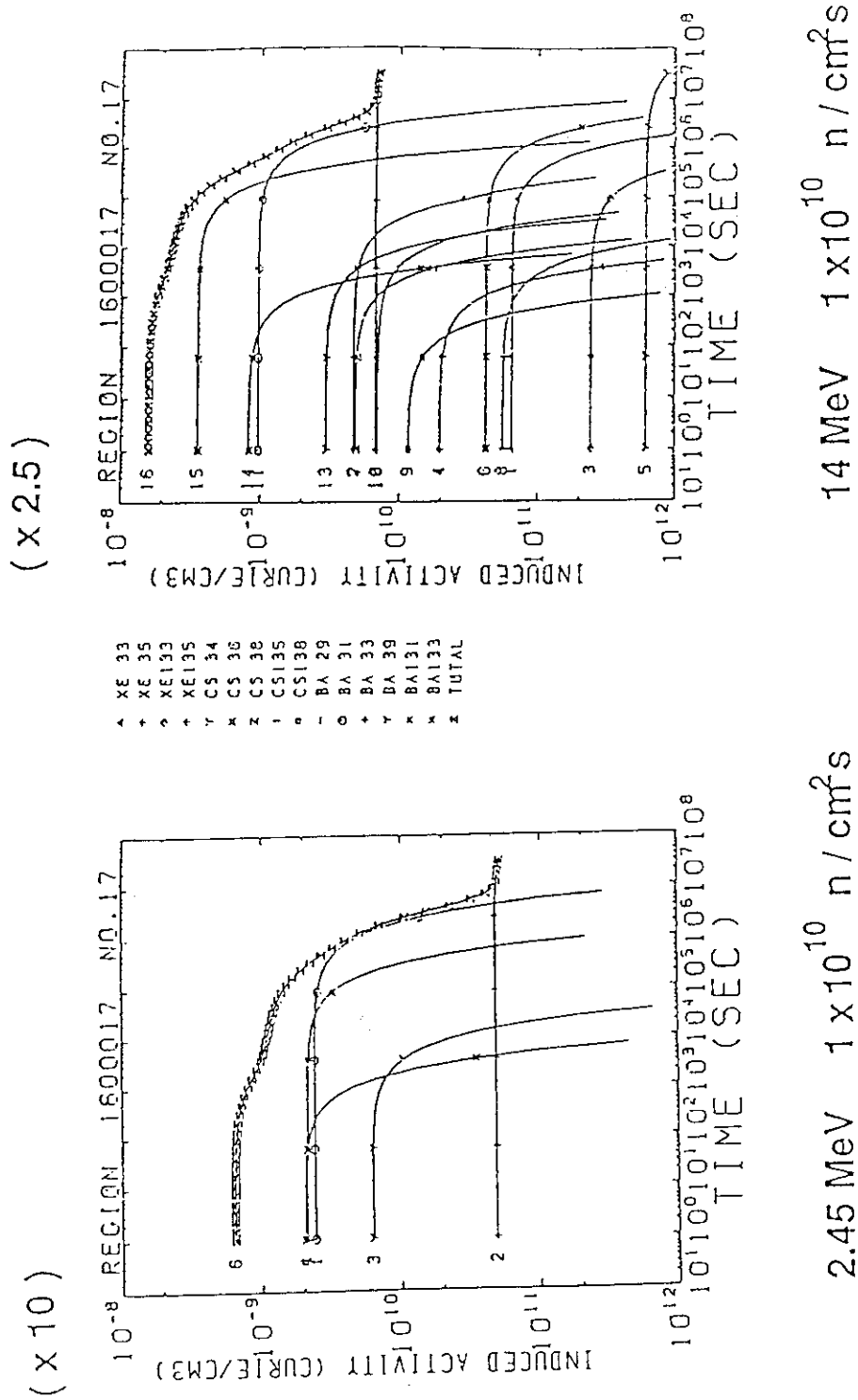

Fig. 5.4-10 The history of induced radioactivities transmuted from barium.

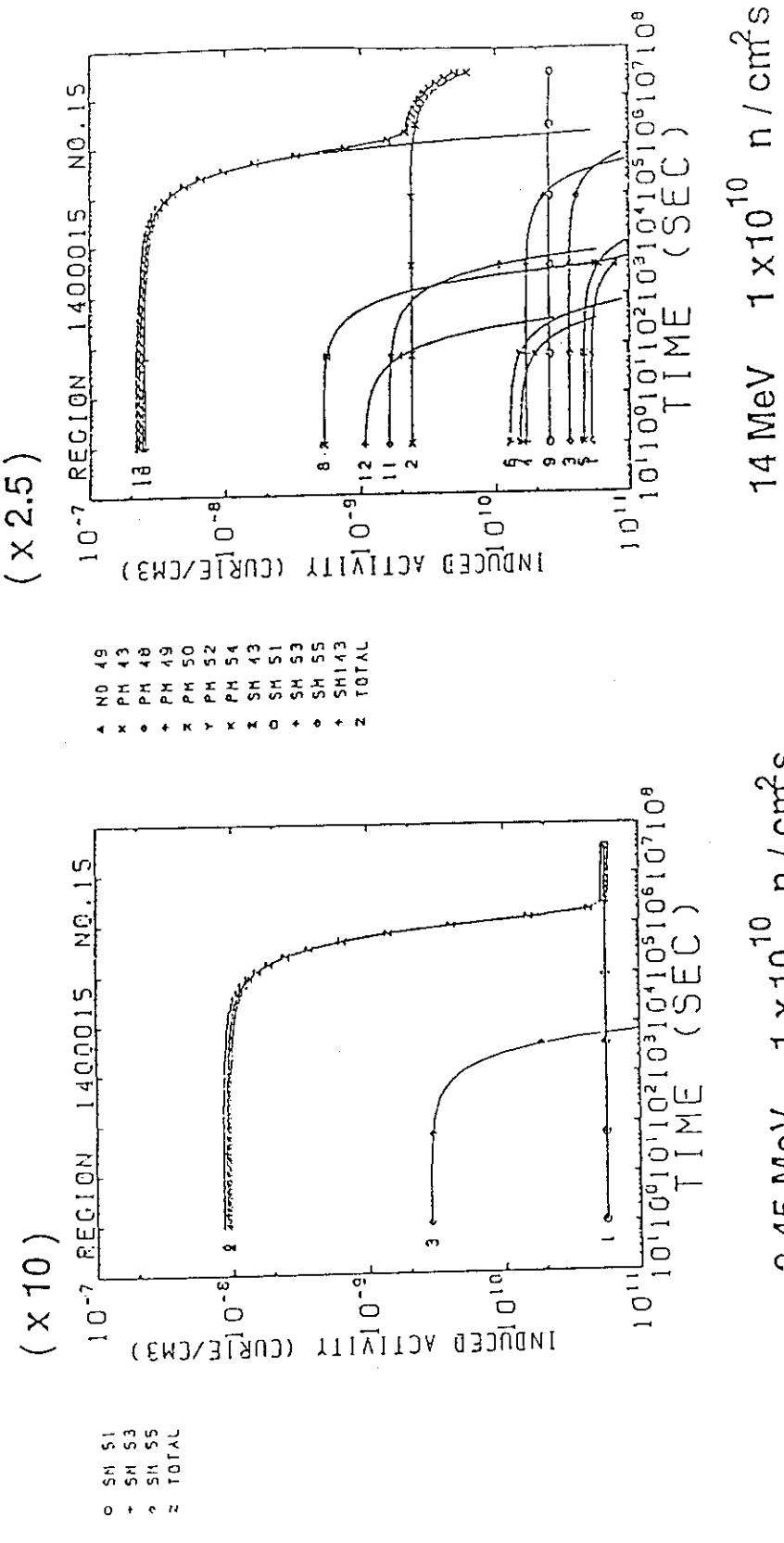

Fig. 5.4-11 The history of induced radioactivities transmuted from samarium.

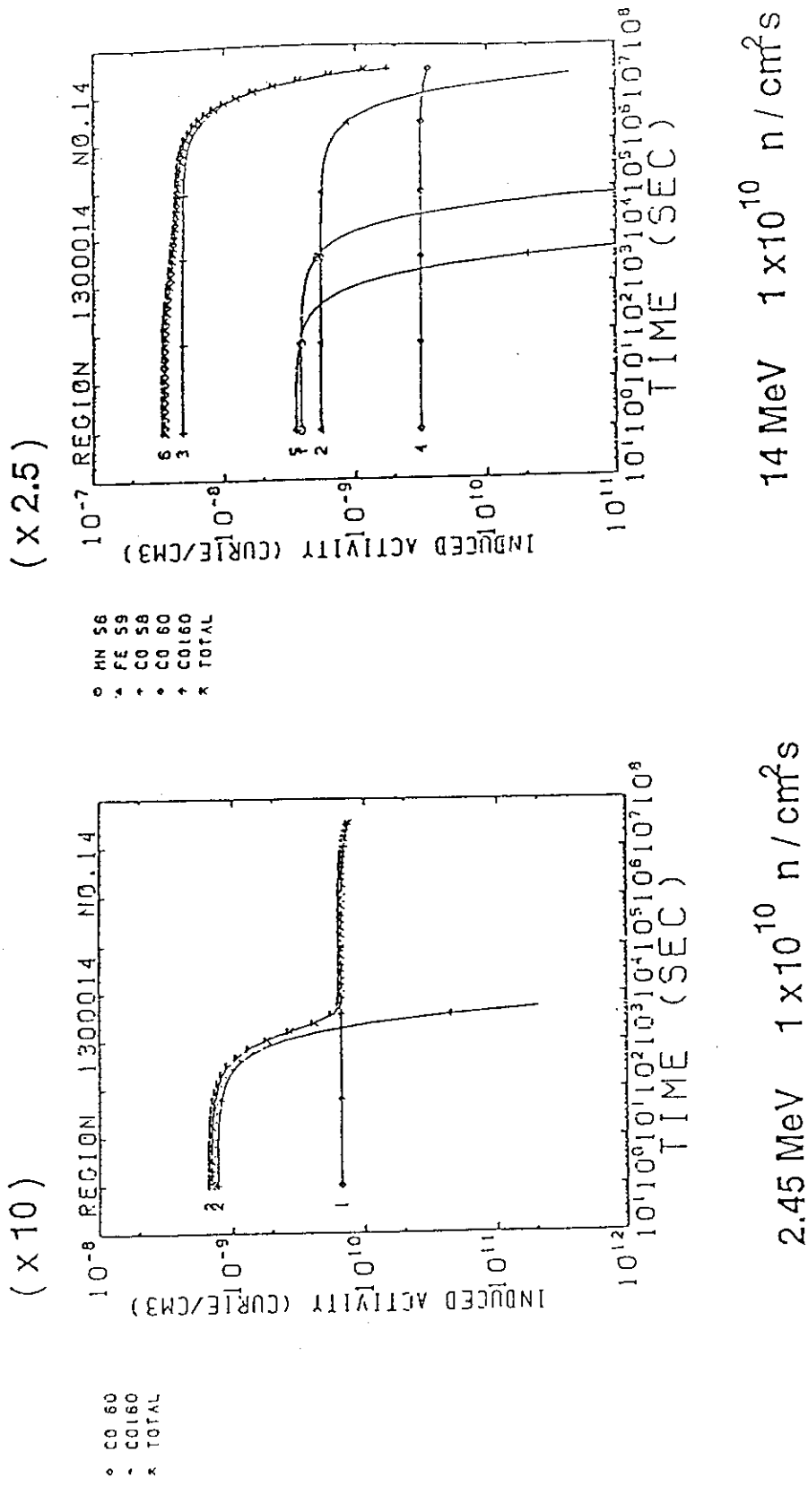

Fig. 5.4-12 The history of induced radioactivities transmuted from cobalt.

5.4.4 Neutronics in the NBI Room

In FY90, the considerations on the neutronics are being developed with the basis obtained in FY89. The main purpose of the calculation is to confirm that the activation of the concrete wall is suppressed below a permissible level. This is the minimum demand as introduced in section 5.1. In the present calculations, we are trying to use the neutron informations computed for the ITER torus configuration as an input data of the neutron flux entering the NB room.

(1) Model of the NB room

The first model being used in the present study is shown in Fig. 5.4-13. Also the composition of the model is summarized in Table 5.4-1. In order to watch the activation of the wall, the whole NB room was modeled to a cylindrical configuration. This model is based on a ITER NB common design proposed by JAERI.

From the results obtained in FY89, some of the points are specially modeled as shown below.

i) It was found that the beamline is penetrated by the high energy neutron flying directly from the torus. For further attenuation of the neutron, and to spread a room for maintenance, material of the neutron dump, located behind the ion source, was changed to SUS (100 cm thick), which is effective for the high energy neutrons.

ii) To prevent the fluence expansion of the reflected neutrons, the thickness of the source mounting flange and the partition in the beamline were taken to be thick enough (50 cm).

iii) The vacuum chamber, made of SUS, was used for a primary shield of the high energy neutrons. The thickness of the wall was chosen to be 10 cm for this function as a neutron container.

iv) The Beam drift duct was made of 90 cm thickness SUS to adjust Maki's ITER calculations.

v) Following the ITER reactor room safety concept, the NB room was filled with 1 atm helium gas.

vi) In the present model, one module of the beamline is placed in the center of the NB room. Therefore, it is necessary to multiply the neutron flux by nine (modules) to evaluate the actual value in the room.

vii) From Maki's evaluation described in section 5.3.1, the neutron flux at the module entrance is taken to be 2 x 10^{11} /cm^2. Although this is a value for total neutron, it is set to be monoenergetic (14 MeV). This will be an overestimation by about factor 0.5.

(2) A Preliminary Results

Some of the preliminary results are summarized as follows;

Neutron flux distribution

A flux distribution of 14 MeV neutron in the NB room is shown in Fig. 5.4-14, and the cross section along the Z axis is shown in Fig. 5.4-15. Those for high energy neutron (> 1MeV) are shown in Fig. 5.4-16, and 17, respectively. The high energy neutron flux on the wall is an order of 10^5 n/cm^2s. The neutron dump and the pertitions seem effective, while the thickness of the vacuum chamber is too thin to suppress the neutron leakage.

The Concrete Activation

The activations of the concrete used in the NB room wall are shown in Fig. 5.4-18 and 19. They show the time evolution after 2 weeks operation (a longest shot) and 1 year operation (corresponds to ITER life), respectively.

Considering a situation of 1 year after shut down following 1 year continuous operation, the concrete activation after the ITER life is estimated. The avarage induced radioactives in the concrete is evaluated to be an order of 10^{11} Ci/cm^3.

By adjusting Maki's torus calculation (x 0.5), and multiplying 9 for all the modules,

The flux at the wall : $\sim 10^6$ n/cm^2s

The induced activities : $\sim 10^{-10}$ Ci/cm^3

The flux have to be suppressed by two order of magnitude.

In order to reduce the flux by two orders at the wall, following options are suggested.

i)Increse the SS vacuum chamber thickness up to 40 cm, though the total weight will be more than 600 ton/module!

ii)Install igloo made of 60 cm thick concrete around the module.

iii)Use polyethylene/B_4C/water around the module.

Through this study, the NB room design including the beamline is reasonably optimized not only from the neutronics point of view but also requirement from the maintenance.

Table 5.4-1 Composition of the neutronics calculation for the NB room.

No.	Component	Material
1	Building wall	Concrete
2	Helium gas	He
3	Vacuum chamber	SUS
4	Cryopump	Al(0.995) + LHe(0.005)
5	Beam dump	Cu(0.91) + H_2O(0.09)
6	Neutralizer	Cu(0.83) + H_2O(0.17)
7	Accelerator insulator	Al_2O_3
8	Grid supports	Al
9	Grids	Cu(0.1) + Void(0.9)
10	Arc chamber	Cu(0.83) + H_2O(0.17)
11	Vacuum	Void
12	SF_6 gas	SF_6(5 atm)
13	Neutron dump	SUS
14	Air	N_2(0.8) + O_2(0.2)

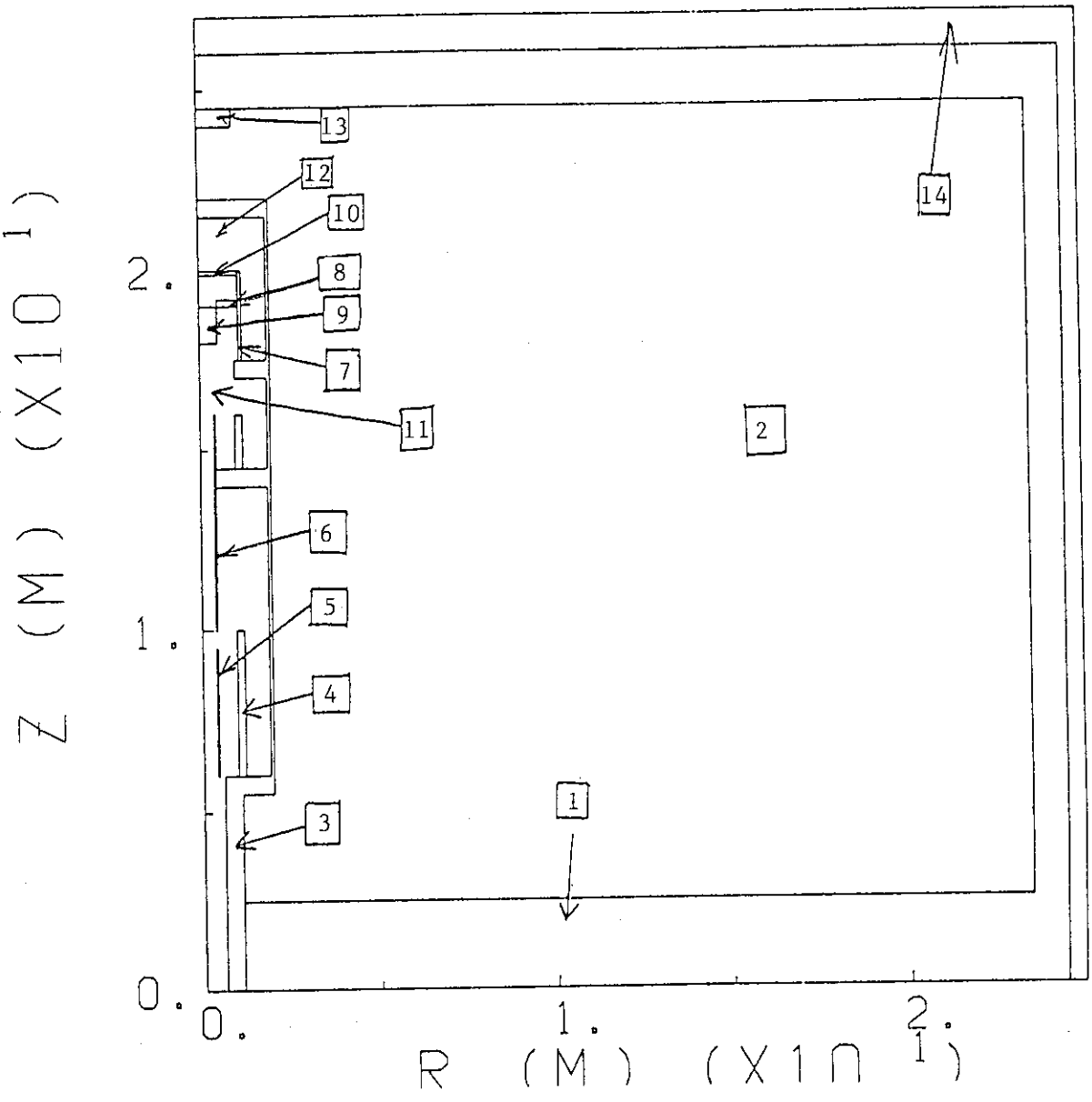

Fig. 5.4-13 The first model being used in the present study for the neutronics computation of the NB room.

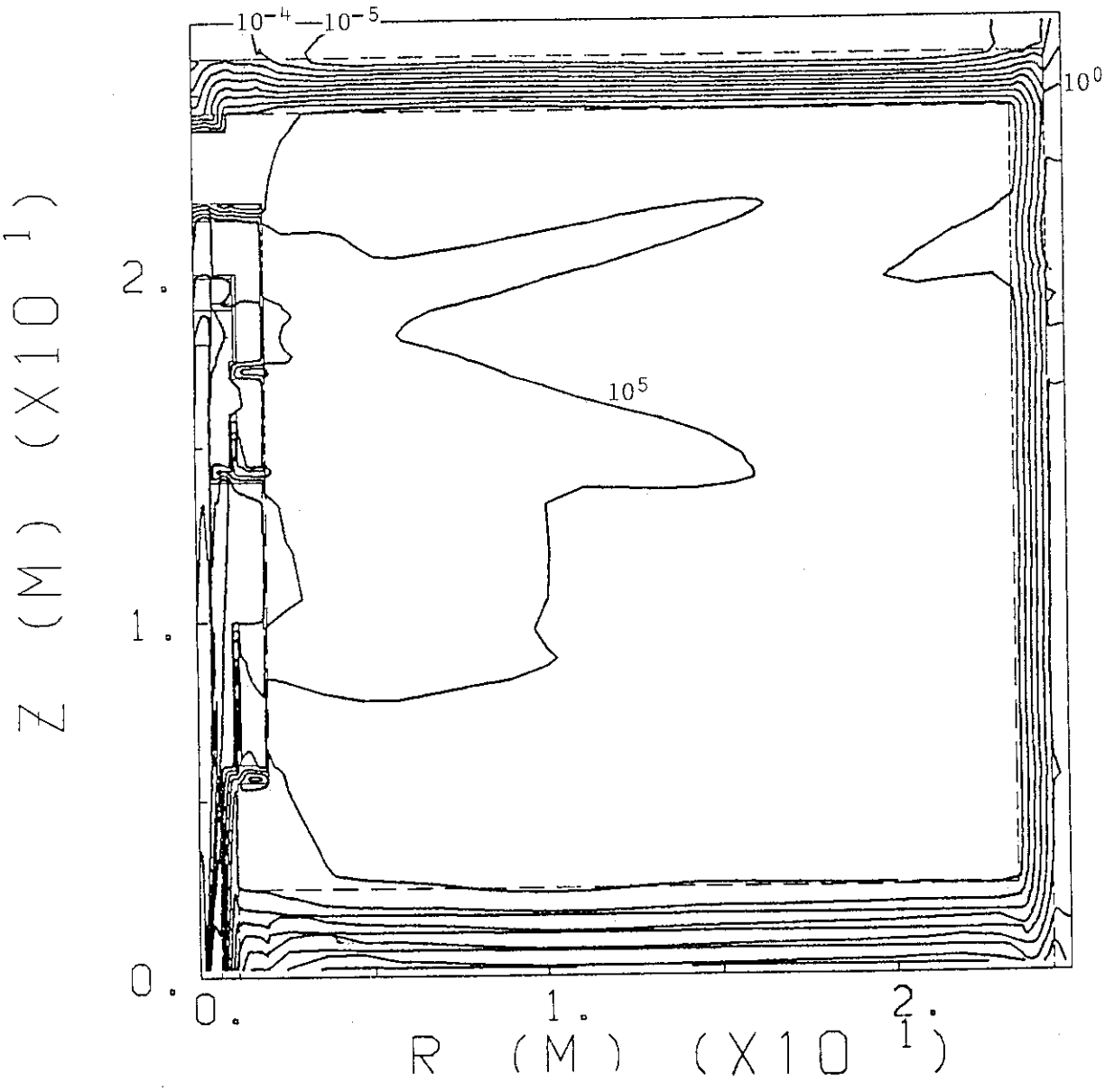

Fig. 5.4-14 Distribution of 14 MeV neutron flux.

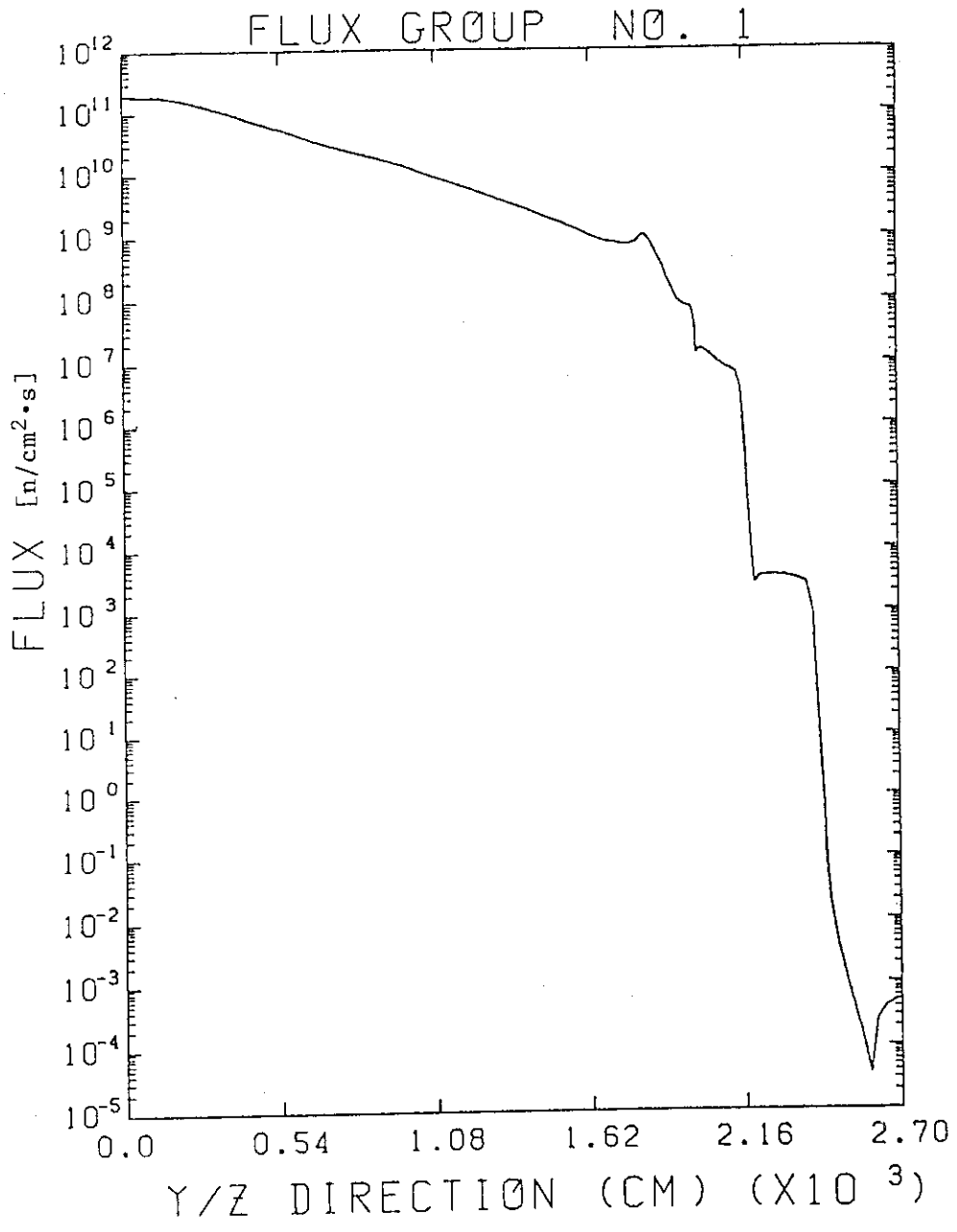

Fig. 5.4-15 Distribution of 14 MeV neutron flux along the Z-axis.

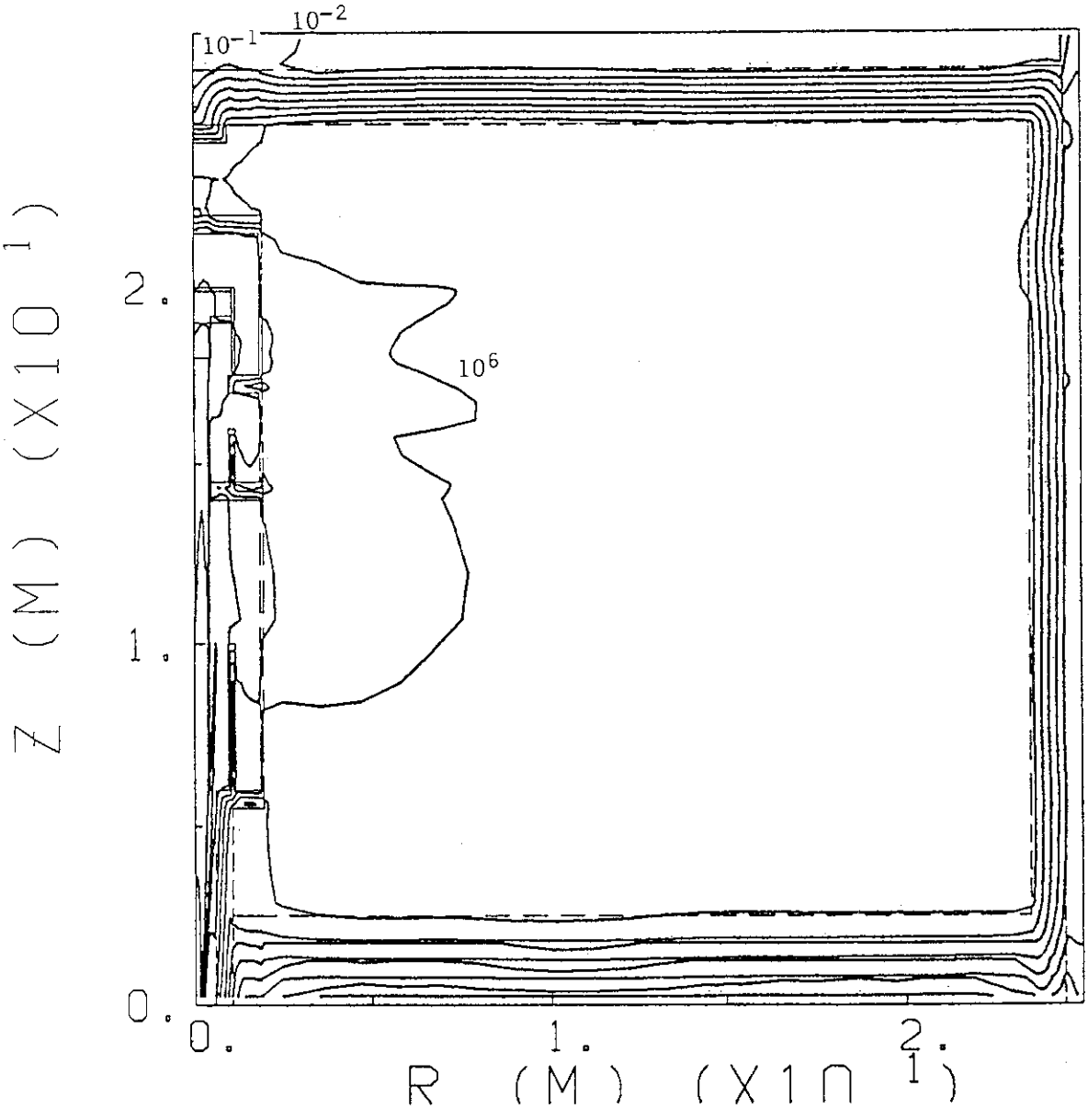

Fig. 5.4-16 Distribution of high energy neutron flux (> 1 MeV).

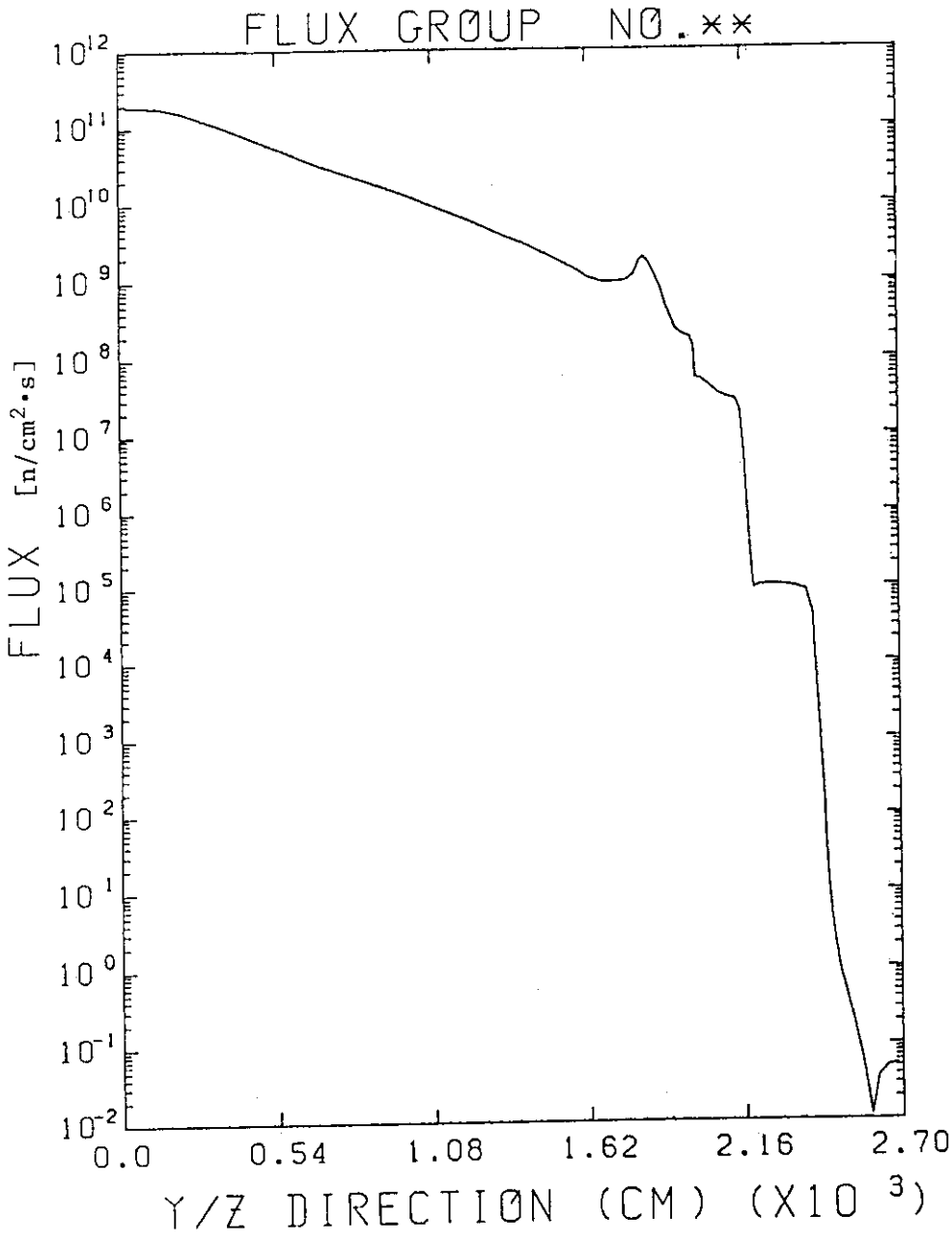

Fig. 5.4-17 Distribution of high energy neutron flux (> 1 MeV) along the Z-axis.

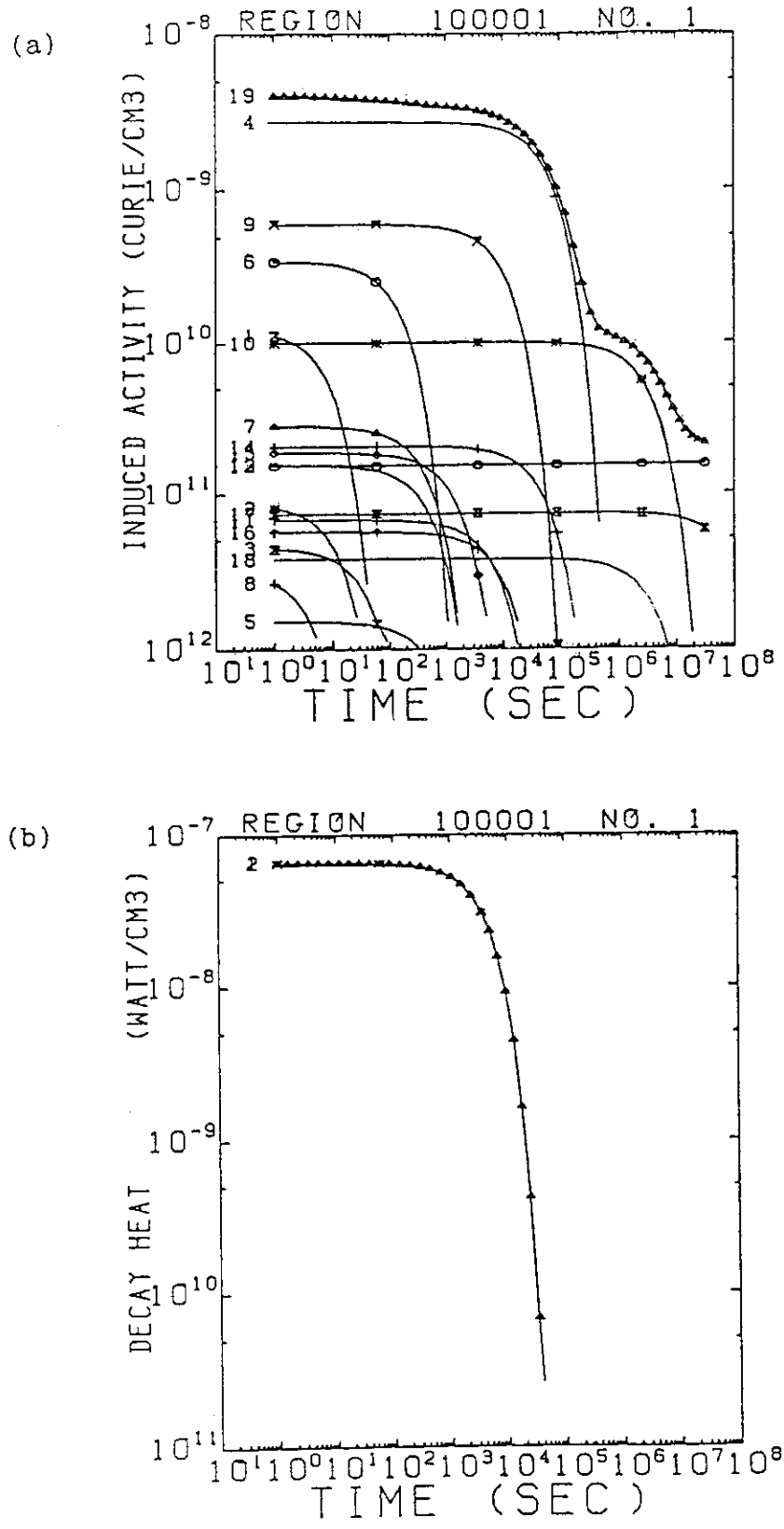

Fig. 5.4-18 Time evolution of induced activities of the wall concrete (a) and decay heat (b) after 2 weeks operation.

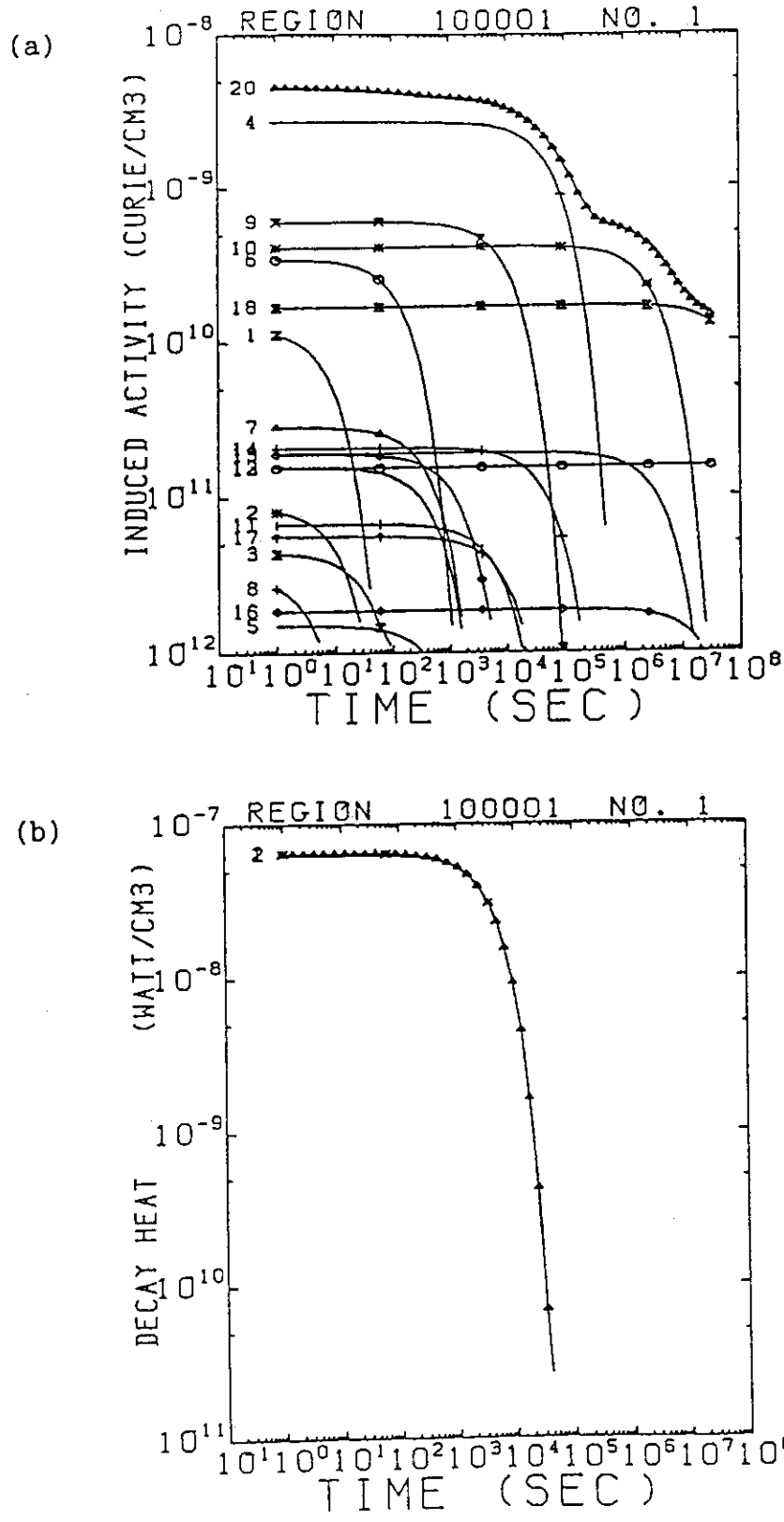

Fig. 5.4-19 Time evolution of induced activities of the wall concrete (a) and decay heat (b) after 1 year steady state operation.

6. MAINTENANCE OF BEAMLINE MODULE

6.1 NBI System Maintenance Data

Before proceeding to describing the maintenance procedure of the neutral beam injector, we assume the following conditions for the maintenance:

a) Components to be replaced

- Ion source unit (filaments, accelerator grids,insulators, O-rings,electric cables, water tubes, etc.)
- Beamline unit (ion dumps, calorimeter,neutralizer, coils, etc.)
- Large valves (source maintenance valve, double vacuum gate valve, etc.)

b) Maintenance status and frequency

- Ion source unit
  filaments : scheduled, more than 1/year
  other parts : unscheduled, 1/ 5 to 10 years
- Beamline unit
  unscheduled, 1/ 5 to 10 years
- Large valves
  scheduled, 1/100 cycles

c) Component size and weight

- Ion source unit
  4.0 m dia. x 5 m,70 tons (for 10 cm thick mild steel)
- Beamline unit
  4.0 m dia. x 12 m,150 tons (for 10 cm thick mild steel)
- Large valves
  source maintenance valve : about 4 m h x 7 m w x 0.5 m t, 40 tons
  double vacuum gate valve : about 2.5 m h x 3 m w x 0.8 m t. 10 tons

d) Environmental conditions during maintenance

- Atmosphere　　inert gas (He)/air
- Pressure　　1 atm
- Temperature　　room temperature around 20°C
- Radiation
  NBI room　　: personnel access is always prohibited.
  NBI power supply room : personnel access is permitted during shut down.

6.2 General Requirements

As for the maintenance of the neutral beam injectors, the following requirements are specified by the ITER Assembly and Maintenance Group:

- Remote removal/installation of both the ion source unit and the beamline unit.
- Remote transfer of the components , without spread of contamination, into the hot cell through the transfer hatch.
- Remote repair of the components in the hot cell if possible.
- Remote inspection, leak detection, welding/cutting and frange connection/disconnection.
- Ion source unit should be removable independently of the beamline unit.
- For transfer of the ion source unit and the beamline unit, dust/tritium containment should be considered.
- Double door system is necessary when local containment is required for transfer of such components as the ion source unit.
- During the maintenance where the ion source unit is removed, consideration should be given to the use of an inert gas(e.g. He).
- If components other than the ion source unit fail, the beamline unit will be removed independently of the ion source unit by separation of the double door system and the double large vacuum gate valves, and brought to a hot cell. The same beamline unit will then be replaced with a spare.

6.3 Basic Concept of the Maintenance

On the basis of the maintenance data and the general requirements, we propose basic concepts for the ITER NBI maintenance as follows:

- The ion source unit and the beamline unit can be separated by disconnecting the source maintenance valve(double door system) installed in between the units.
- The beamline unit and the drift tube can be separated by disconnecting the double vacuum gate valve.
- If any failure occurrs in an ion source unit, only the ion source unit of the module will be removed, leaving the beamline unit as it was.
- If any failure occurrs in a beamline unit, only the beamline unit will be removed, leaving the ion source unit of the module as it was.
- Initial troubles and failures in the NBI modules should be repaired by hands-on maintenance, during hydrogen operation of the tokamak.
- Once the DT operation of the reactor starts, any maintenance of the module should be done by remote handling.
- Walls,floor, and ceiling surrounding the NBI room are radiation shields against neutrons and gamma rays. Of these, only the ceiling can be opened.
- An overhead crane (200 ton) is installed above the ceiling of the NBI room to transport the components from the NBI room to the hot cell, through the hatch.
- From a view point of vertical location, there are three ion source units,i.e. upper, middle, and lower ion source units. Each ion source can be independently removed of the other ion source units. The upper ion source unit will be directly removed from the module and transported to the hatch by the overhead crane. The middle and lower ion source units will be removed backwards and sidewards using the rail system, and then vertically removed and transported to the hatch by the overhead crane.
- Similar to the ion source units, there are three beamline units,i.e. upper, middle ,and lower beamline units. The beamline units are not independently, but sequentially removed. That is, in order to remove the lower beamline unit, we should remove the

upper and the middle beamline units in advance, and lay them at a temporary laydown area, using the overhead crane. The beamline unit to be repaired is transported to the hot cell through the hatch.

Figures 6.3-1 and 6.3-2 show the elevation and plan views of ITER NBI system for explaining the concepts of maintenance descibed above.

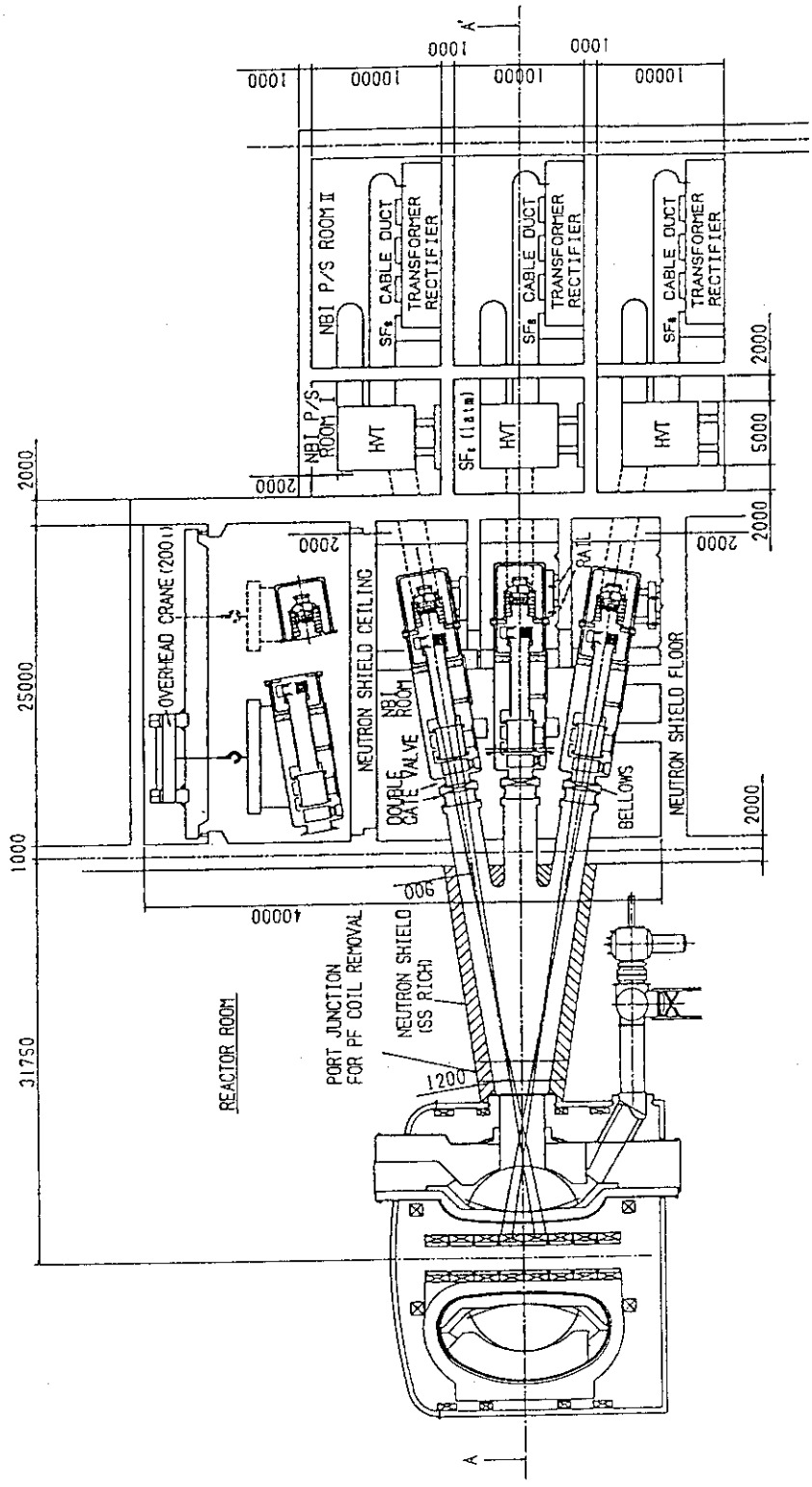

VIEW OF SECTION B-B'

LAYOUT OF THE BEAMLINE AND POWER SUPPLY SYSTEM FOR ITER-NBI (Elevation View)

Fig. 6.3-1 Elevation view of ITER NBI system for explaining the concept of maintenance.

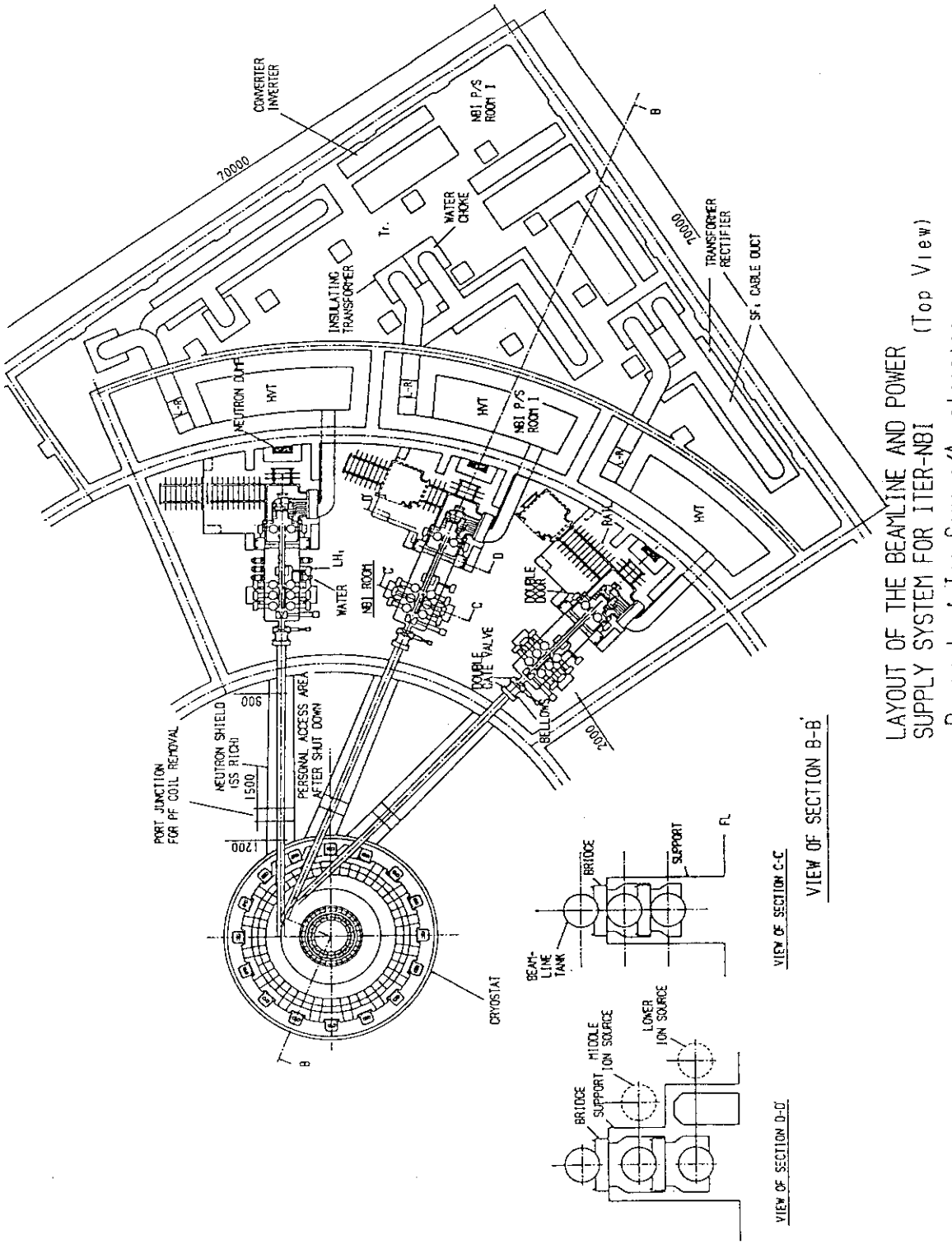

Fig. 6.3-2 Plan view of ITER NBI system for explaining the concept of maintenance.

6.4 Maintenance Procedure

(a) Ion source unit replacement

Disassembly

(C0.- C4.: common to upper, middle, and lower ion source units)

C0. Tokamak and neutral beam injector shut down.
C1. Stop the operation of cryopumps and warm them up.
Evacuate deuterium and tritium gases desorped from the cryopanels, by roughing pumps (turbo-molecular pumps, mechanical booster pumps, and rotary pumps).
Transfer the gases to the isotope separation section of the fuel cycling system.
Then,close the valves of the roughing pumps.
C2. Introduce inert gas(ex. He gas) into the ion source unit and the beamline unit up to 1 atm.
C3. Close the source maintenance valves installed in between the ion source unit and the beamline unit.
C4. Disconnect electric service lines, water cooling lines, and gas service lines connected to the ion source unit (see Figs.6.4-1 (a) and (b)), making use of remote handling devices, end effecters, and special tools,etc.

(In case of upper ion source unit)

5. Lift up one block of the radiation shield ceiling above the ion source unit by the overhead crane.
Store the one block of the ceiling, temporarily at other space.
6. Hold the weight of the upper ion source unit by the crane with a weight balancing tool.
7. Separate the ion source unit from the beamline unit, by disconnecting the source maintenance valves(double door system, see Fig.6.4.2)).
8. Slightly move the ion source unit backwards in horizontal direction and lift it up by the crane.

(In case of middle or lower ion source unit)

5. Separate the ion source unit from the beamline unit, by disconnecting the source maintenance valves (see Fig.6.4.2).
6. Move the ion source unit backwards in the beam axis direction on the rail, using an auto-mobile type truck installed below the ion source unit.
   Stop the truck when it reaches the stopper position.
7. Push down four wheels for side motion from the truck by motors, until the wheels hold the whole weight of the ion source unit and the truck.(Change of the wheels for beam axial motion to those for side motion).
8. Move the ion source unit sidewards on the side-ways rail, using the same truck.
   Stop the truck when it reaches the stopper position.
9. Lift up one block of the radiation shield ceiling above the ion source unit, and lay it down at other space by the overhead crane.
10. Lift up the ion source unit by the crane.

(C5.- C7.: common to upper,middle, and lower ion source units)

C5. Transfer the ion source unit in horizontal direction and lay it down in a cask prepared on the ceiling in advance, by the crane.
C6. Lift up the cask and transport it to the hot cell through the hatch,by the crane.
C7. Open the cask and repair the ion source unit in the hot cell.

Assembly

(C1.-C4.:common to upper,middle,and lower ion source units)

C1. Close the source maintenance valve of the repaired ion source unit, in the hot cell.
C2. Introduce inert gas into the repaired ion source unit, in the hot cell.
C3. Lay down the ion source unit in the cask, in the hot cell.
C4. Transport the cask from the hot cell to on the ceiling of the NBI room, through the hatch.

(In case of upper ion source unit)

5. Lift up one block of radiation shield ceiling above the position where the repaired ion source unit is to be attached, by the crane.
6. Open the cask and lift up the repaired ion source unit on the ceiling, by the crane.
7. Transfer the ion source unit horizontally to the opened position of the ceiling, and get it down to the appropriate position.
8. Connect the repaired ion source unit to the beamline unit by connecting the source maintenance valves (see Fig.6.4.2), holding the weight of the ion source unit by the crane.
9. Release the crane from the ion source unit.

(In case of middle or lower ion source unit)

5. Lift up one block of the radiation shield ceiling above the position where the auto-mobile type truck is waiting for, by the crane.
   Lay down the block at other place.
6. Open the cask and lift up the repaired ion source unit on the ceiling, by the crane.
7. Transfer the ion source unit horizontally to the opened position of the ceiling, get it down and lay it down on the truck.
8. Fix the ion source unit to the truck, and release the crane from the ion source unit.
9. Lift up the one block of the ceiling and return it to the original position.
10. Move the repaired ion source unit sidcewards on the side-ways rail, using the truck.
    Stop the truck when it reaches the stopper position.
11. Withdraw the four wheels for side motion into the truck by moters, until the whole weight is held by the four wheels for beam axial motion.
12. Move the truck forwards in the direction of the beam axis on the rail.
    Stop the truck at the appropriate position close to the beamline unit.
13. Connect the repaired ion source unit to the beamline unit by connecting the source maintenance valves (see Fig.6.4.2).

(C5.- C.7.:common to upper,middle, and lower ion source units)

C5. Connect electric service lines, water cooling lines, and gas service lines to the ion source unit (see Figs.6.4-1(a) and (b)).
C6. Open the source maintenance valves.
C7. Open the valves of roughing pumps and start to evacuate the inert gas by the roughing pumps.

(b) Beamline unit replacement

We descibe the replacement procedure of lower beamline unit, which is the most time consuming and troublesome, as the typical case.

Disassembly

0. Tokamak and neutral beam injector shut down.
1. Close the double vacuum gate valves installed in between the beamline units and the drift tubes of the vertically stacked three modules.
2. Stop the operation of all cryopumps in the three modules, and warm them up.
   Evacuate deuterium and tritium gases desorped from the cryopanels, by roughing pumps.
   Transfer the gases to the isotope separation section of the fuel cycling system.
   Then, close the valves of the roughing pumps.
3. Introduce inert gas into all the three modules up to 1 atm.
4. Close the source maintenance valves of all the three modules.
5. Disconnect electric service lines, water cooling lines,liquid helium sevice lines, and gas service lines connected to all the three beamline units.
6. Lift up a few blocks of the radiation shield ceiling above the modules by the overhead crane.
   Store the blocks, temporarily at other space.
7. Hold the weight of the upper beamline unit by the crane with a weight balancing tool.

8. Separate the upper beamline unit from the upper ion source unit, by disconnecting the source maintenance valves (see Fig.6.4.2).
9. Separate the upper beamline unit from the upper drift tube, by disconnecting the double vacuum gate valves (see Fig.6.4.2).
   After this, the bellows attached in the middle of the double vacuum gate valves should be shrunk to keep sufficient clearance between the drift tube and the beamline unit.
10. Lift up the upper beamline unit and then transport it to other space. Store it there temporarily.
11. Disconnect and remove two concrete bridges which have supported the weight of the upper beamline unit, with remote handling devices and the crane.
    Store the two concrete bridges, temporarily at other space.
12.-16. Similar to procedures 7.- 11. except that the term " upper " should be changed to " middle ".
17.-19. Similar to procedures 7.-9. except that the term "upper" should be changed to "lower".
20. Lift up the lower beamline unit by the crane.
21. Lay down the lower beamline unit in the cask prepared in advance on the floor of the NBI room.
22. Lift up the cask and transport it to the hot cell through the hatch by the crane.
23. Open the cask and repair the lower beamline unit in the hot cell.

During the repairment of the lower beamline unit in the hot cell, the following procedures are necessary to return the middle and the upper modules as they were.

24. Lift up the two concrete bridges for supporting the weight of the middle beamline unit, which was temporarily stored, and transport them to the original positions by the crane.
    Fix the two bridges to the support columns.
25. Lift up the middle beamline unit temporarily stored and transport it to the original position by the crane.
    Hold the weight of the middle beamline unit by the crane.
26. Connect the middle beamline unit with the middle drift tube, by connecting the double vacuum gate valves (see Fig.6.4.2).
27. Connect the middle beamline unit with the middle ion source unit, by connecting the source maintenance valves (see Fig.6.4.2).
28. Release the crane from the middle beamline unit.

29.-33. Similar to procedures 24.-28. except that the term "middle" should be changed to "upper".
34. Lift up the few blocks of the radiation shield ceiling temporarily stored, and return them to the original positions.
35. Connect electric service lines, water cooling lines,liquid helium service lines, and gas service lines to the middle and the upper beamline units.
36. Open the source maintenance valves of the middle and the upper modules.
37. Evacuate inert gas by roughing pumps.

Assembly

0.-16. Similar to procedures 0.- 16. in Disassembly case except that the term "three modules" should be changed to " upper and middle modules".
17. Close the source maintenance valve and the double vacuum gate valve of the repaired lower beamline unit, in the hot cell.
18. Introduce inert gas into the lower beamline unit, in the hot cell.
19. Lay down the lower beamline unit in the cask, in the hot cell.
20. Transport the cask from the hot cell to the floor of the NBI room, through the hatch, by the crane.
21. Open the cask and lift up the lower beamline unit over the radiation shield ceiling, by the crane.
22. Transfer the lower beamline unit horizontally to another opened position of the ceiling, and get it down to the original position, by the crane.
Hold the weight of the lower beamline unit by the crane.
23. Connect the repaired lower beamline unit with the lower drift tube, by connecting the double vacuum gate valves (see Fig.6.4.2).
24. Connect the lower beamline unit with the lower ion source unit, by connecting the source maintenance valves (see Fig.6.4.2).
25. Release the crane from the lower beamline unit.
26.-36. Similar to procedures 24.-34. of Disassembly case.
37. Connect electric service lines, water cooling lines, liquid helium service lines, and gas service lines to all the three beamline units.
38. Open the source maintenance valves of all the three modules.
39. Evacuate inert gas by roughing pumps.

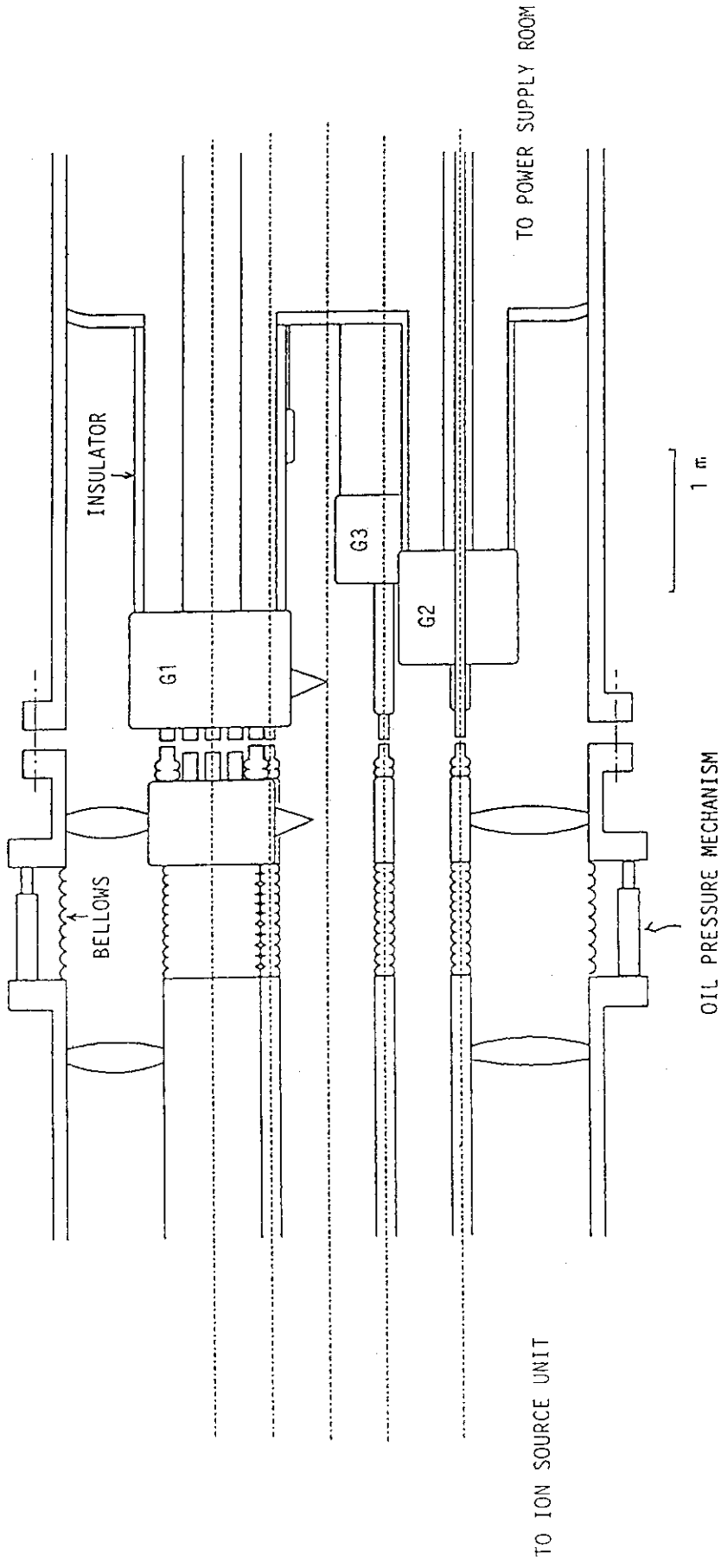

Fig. 6.4-1(a) Concept of connection/disconnection of electric power cables and water pipes in large diameter FS6 gas duct connected to the ion source unit (Plane view).

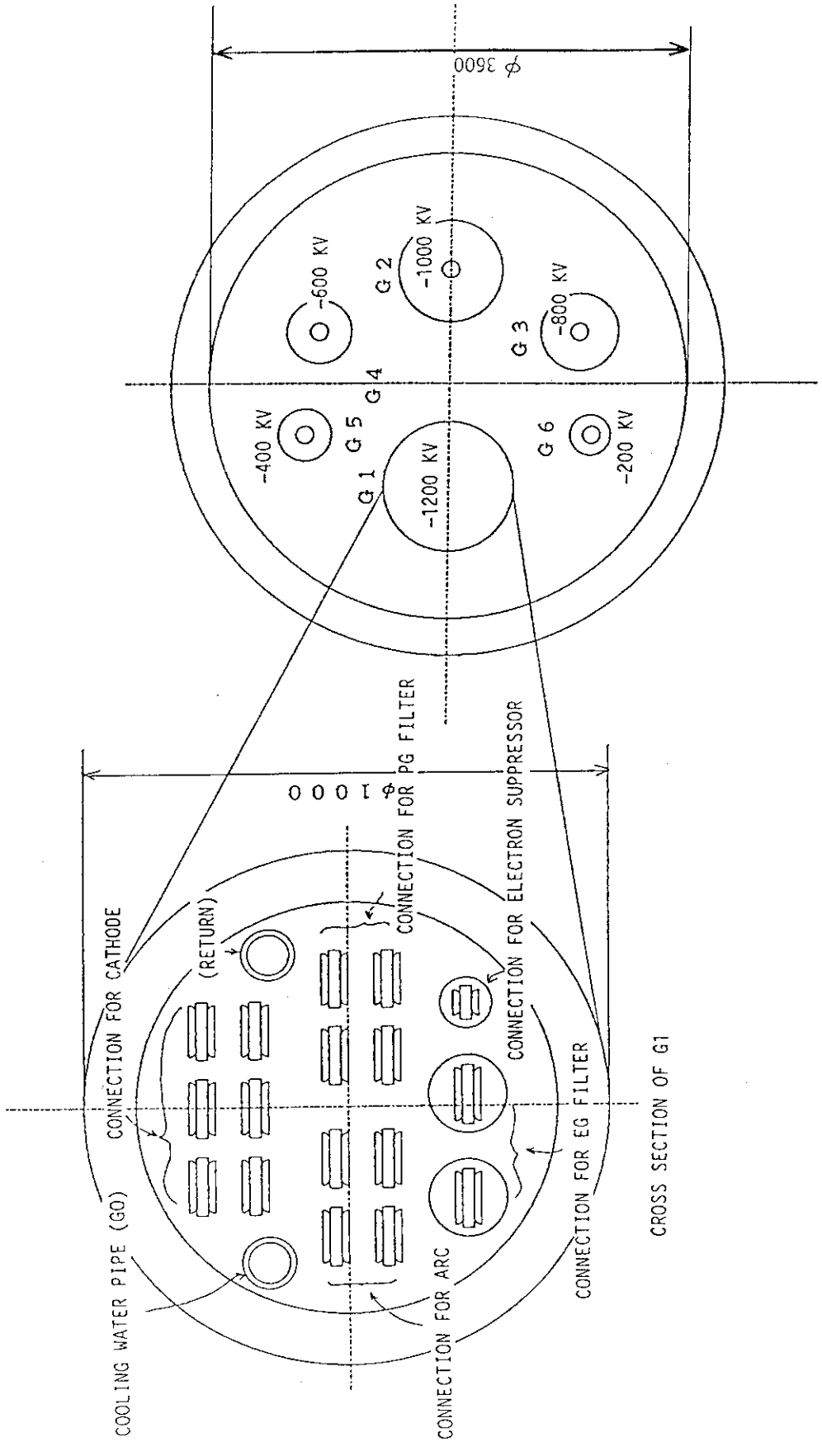

Fig. 6.4-1(b) Cross-sectional view of connection terminals

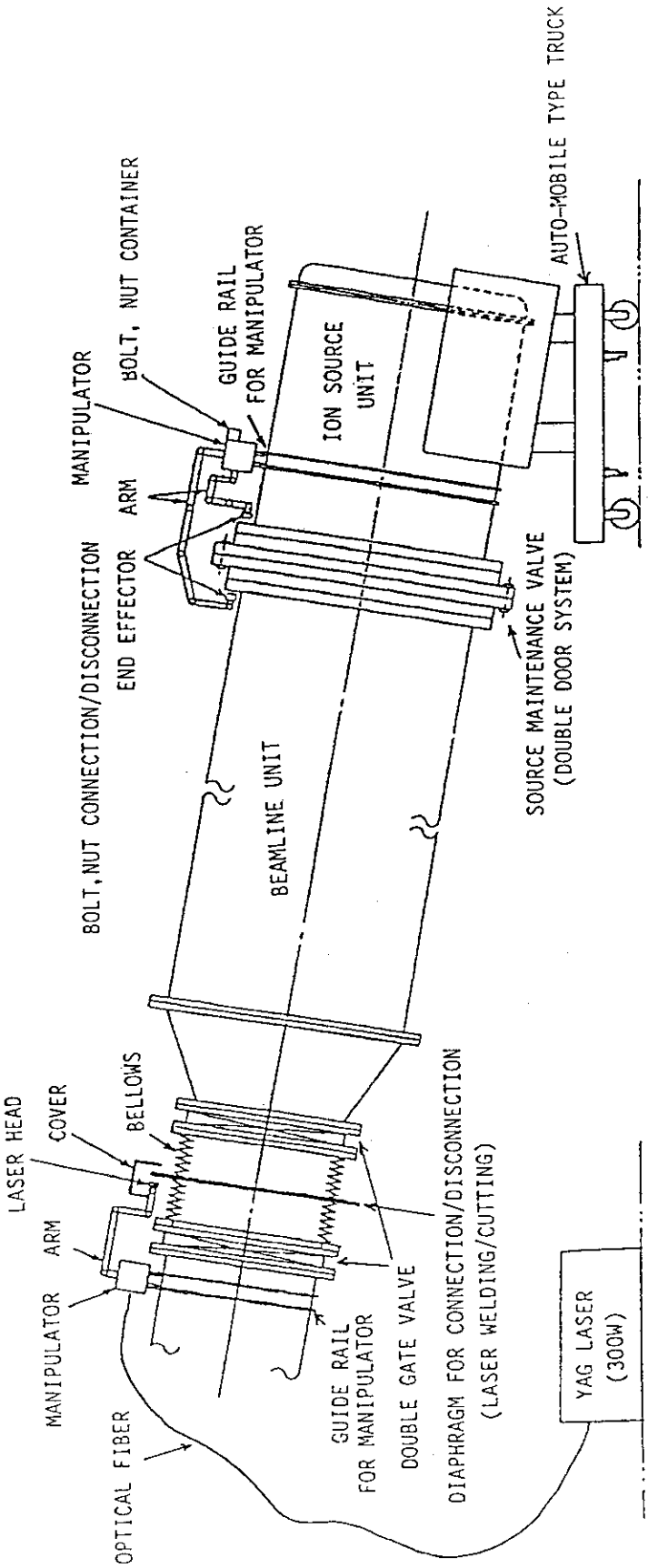

Fig. 6.4-2 Concept of connection/disconnection of the source maintenance valve and the double gate valve

6.5 Concept of Connection/Disconnection

(a) Electricity

For low current feed, SMA (Shape Memory Alloy) can be used for connection/disconnection of electric cables.

- Sleeve type SMA (Ni-Ti alloy)

Figure 6.5-1 shows Sleeve type SMA for cable connection and disconnection. The SMA sleeve shrinks (Austenite phase)at temperature above 45 ^{o}C (connection), and enlarge (Martensite phase) at temperature below 25 ^{o}C (disconnection). Thus, connection/ disconnection of the electric cables can be done by only cooling/heating SMA sleeve.

R & D activities on the sleeve type SMA of up to 20 to 30 mm in diameter is in progress in Toshiba Co. Limited.

- SMA bolt

Figure 6.5-2 shows concept of the SMA bolt. One metal plate is sandwiched between other two metal plates which are connected with each other by SMA bolts. When the SMA bolts are heated up, the length of the SMA bolts decreases at a certain temperature and the sandwiched metal plate is fastened by other two plates (connection). On the contrtary, if the SMA bolts are cooled down below a certain temperature, the length of the SMA bolts increases. Then, the sandwiched metal plate is released from other two plates (disconnection).

- Quick couplers

Quick couplers such as Solton couplers are commercially available for relatively low current and low voltage. Resistance against neutrons and gamma rays should be checked.

(b) Water

- Flange connection/disconnection

Figure 6.5-3 show the concept of flange connection/disconnection for water service line. Double valve system is necessary to minimize leak of contaminated water during disconnection of the line.

- Quick couplers

Various quick couplers are commercially available for relatively small water flow rate. Resistance against neutrons and gamma rays should be checked.

- Laser welding/cutting

Figure 6.5-4 shows the concept of laser welding/cutting of water pipe . This technique can be applicable to relatively large diameter pipe (about 200 mm in diameter).

(c) Gas

- Flange connection/disconnection

Similar to water service lines.

- Wilson seal

Usually, Wilson seal uses viton O-ring . Thus, Wilson seal can be used only at the place where radiation dose rate is very low.

- Swedgelock

Swedgelock is commercially available gas connectors. This connector is metal seal type and seems to be resistive against radiations. Improvement to fit remote handling is necessary.

(d) Vacuum

- Flange connection/disconnection

Similar to water service lines.

(e) Liquid helium

To keep thermal insulation, coaxial pipe structure is necessary for liquid helium service line. The concept of connection and disconnection of the coaxial structure suitable for remote handling should be devised out.

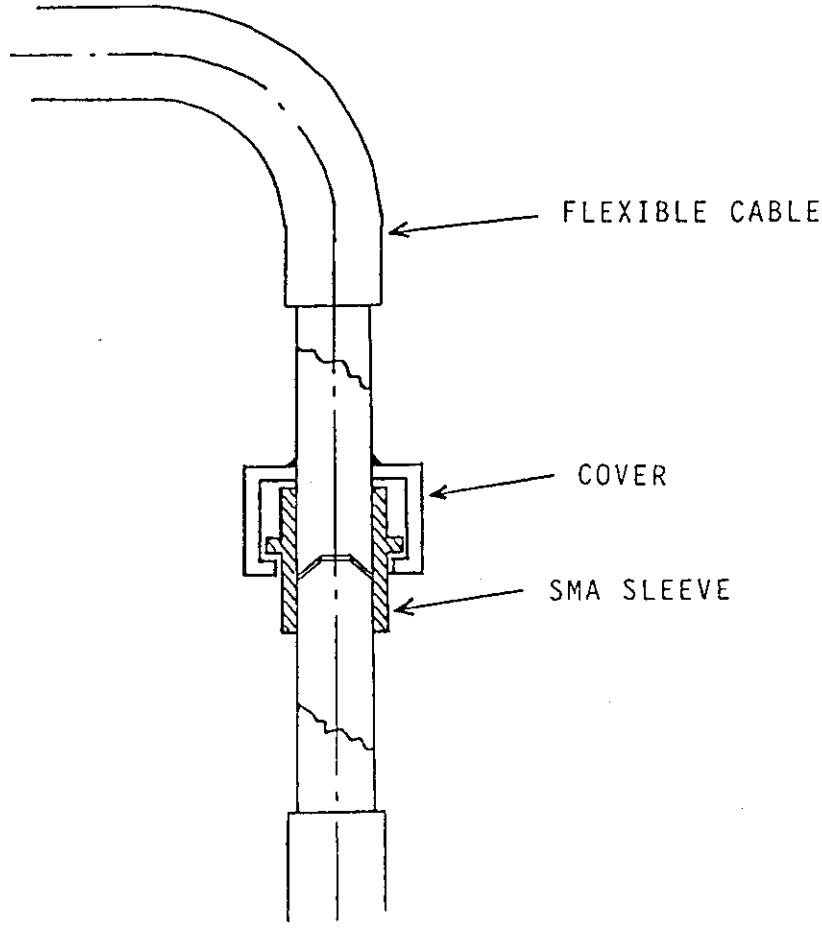

Fig. 6.5-1 Concept of sleeve type SMA (Shape Memory Alloy) for cable connection and disconnection.

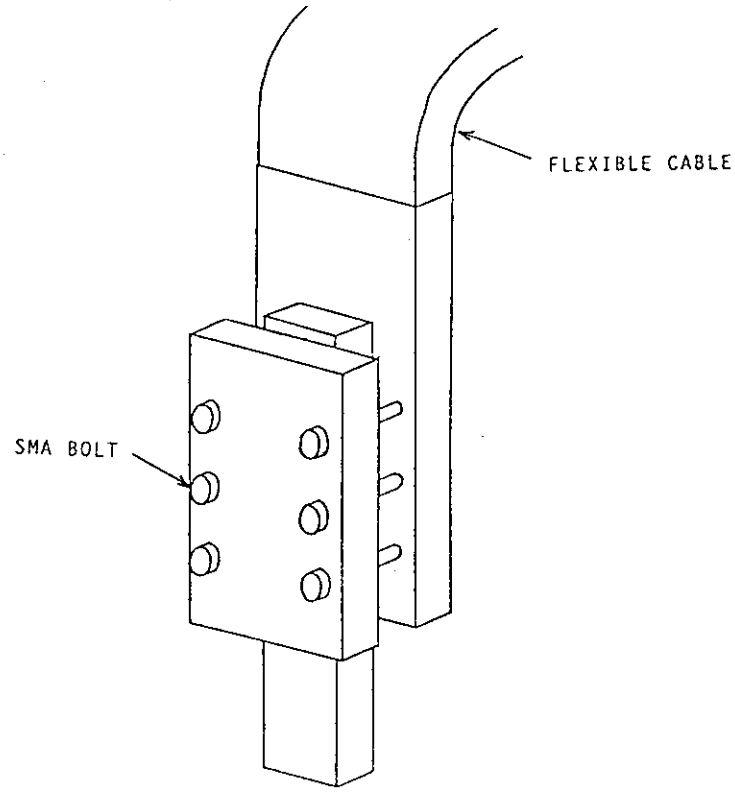

Fig.6.5-2 Concept of SMA bolt for cable connection and disconnection.

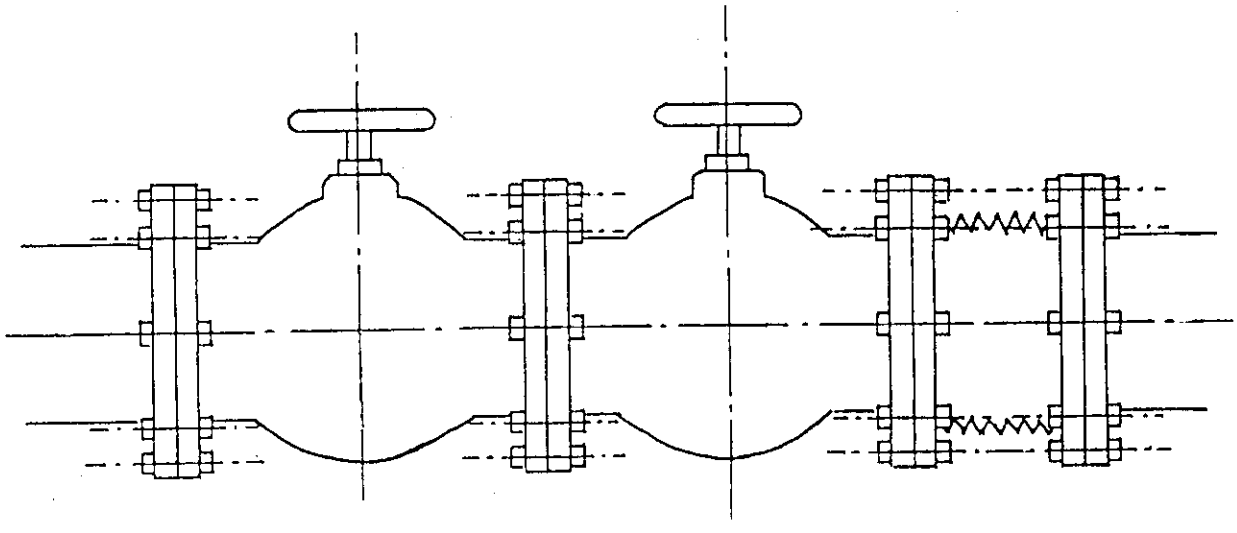

Fig.6.5-3 Concept of flange connection/disconnection of water service line.

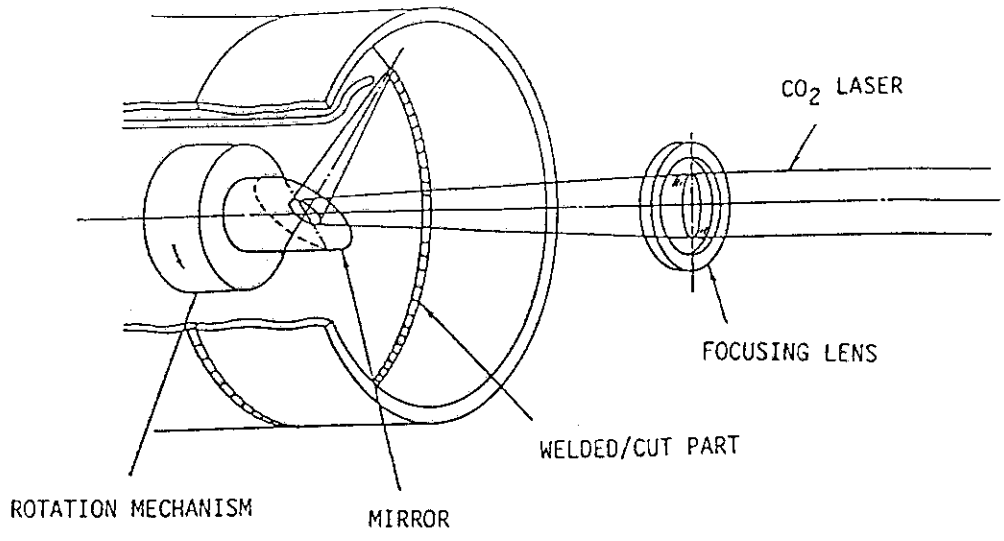

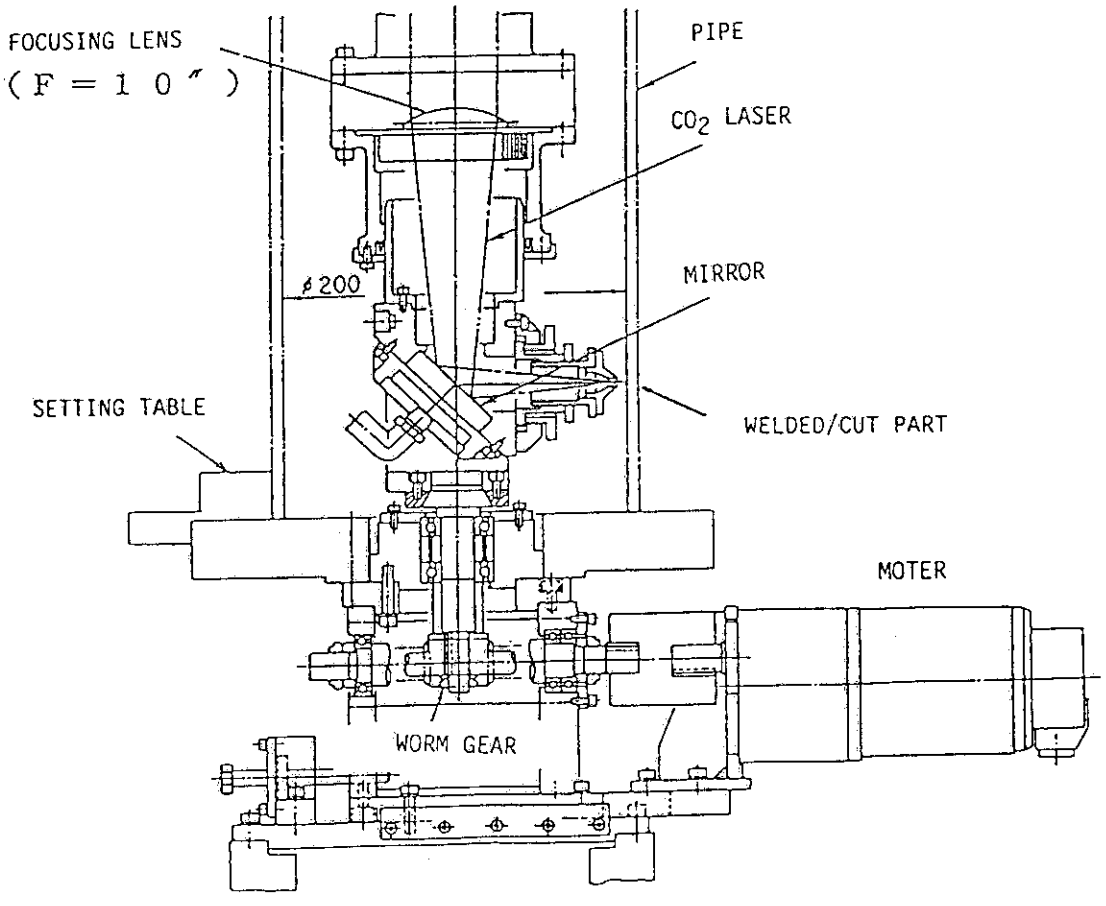

Fig.6.5-4 Concept of LASER welding/cutting of water pipe.

6.6 Description of Maintenance Equipment

(a) General requirement to remote handling equipments

- The location and storage of remote handling equipment should be such that the activation due to neutron scattering is prevented during normal operation of NBI system.
- The area where the maintenance of remote handling equipment will be carried out should allow personnel access.
- Some form of gaitering or flexible diaphragm should be incorporated when feasible over the remote handling equipment to prevent the ingress of contamination and facilitate cleaning.

(b) Equipment function and description

- Overhead crane (200 ton):
  which transports the ion source unit, the beamline unit, the weight supporting bridge, the blocks of radiation shield ceiling, the cask,etc.
- Auto-mobile type truck:
  which supports the weight of the middle or the lower ion source unit, during operation of NBI system. If any failure occurrs in the ion source unit, the truck moves on the rail, in the direction of the beam axis as well as in the direction perpendicular to the beam axis, to the position where the overhead crane is accessible. This truck has two sets of wheels; one for movement in beam axis direction, another for side-ways motion. The latter can be pushed down and retracted by a moter drive jack system (see Fig.6.6.1).
- Bridge mounted overhead telescopic mast:
  which has a master-slave manipulator or power manipulator at the end of an arm for inspection, leak detection, welding/cutting machine setting, and flange connection/disconnection.
- End effector/tool:
  - transport rig of ion source unit
  - transport rig of beamline unit
  - end effector/tool for electrical connection, pipe connection etc.

6.7 Hot Cell

- An inner space about 5 m wide, 5 m high, and 20 m long is necessary to contain and repair a beamline unit (4 m in outer diameter, 12 m long) or an ion source unit (4 m in outer diameter, 5 m long).
- A trolley and trolley tracks are necessary to move a beamline unit (about 150 ton) or an ion source unit (about 70 ton) in one direction.
- Inner cranes (about 10 ton) are necessary to extract and transport various components (ion source body, neutralizer, beam dump, caloriemeter,etc.).
- Surrounding walls and windows with sufficient thickness to shield gamma rays from beamline unit or ion source unit are necessary.
- The hot cell is tightly closed and pumped to keep inner pressure slightly lower than atmosphere.
- Master-slave type manipulaters, power manipulaters, and various end effectors/tools are necesasary to repair the components in the beamline unit, and the ion source unit.
- Welders, cutters, inspecting devices,etc. are also necessarey in the hot cell.

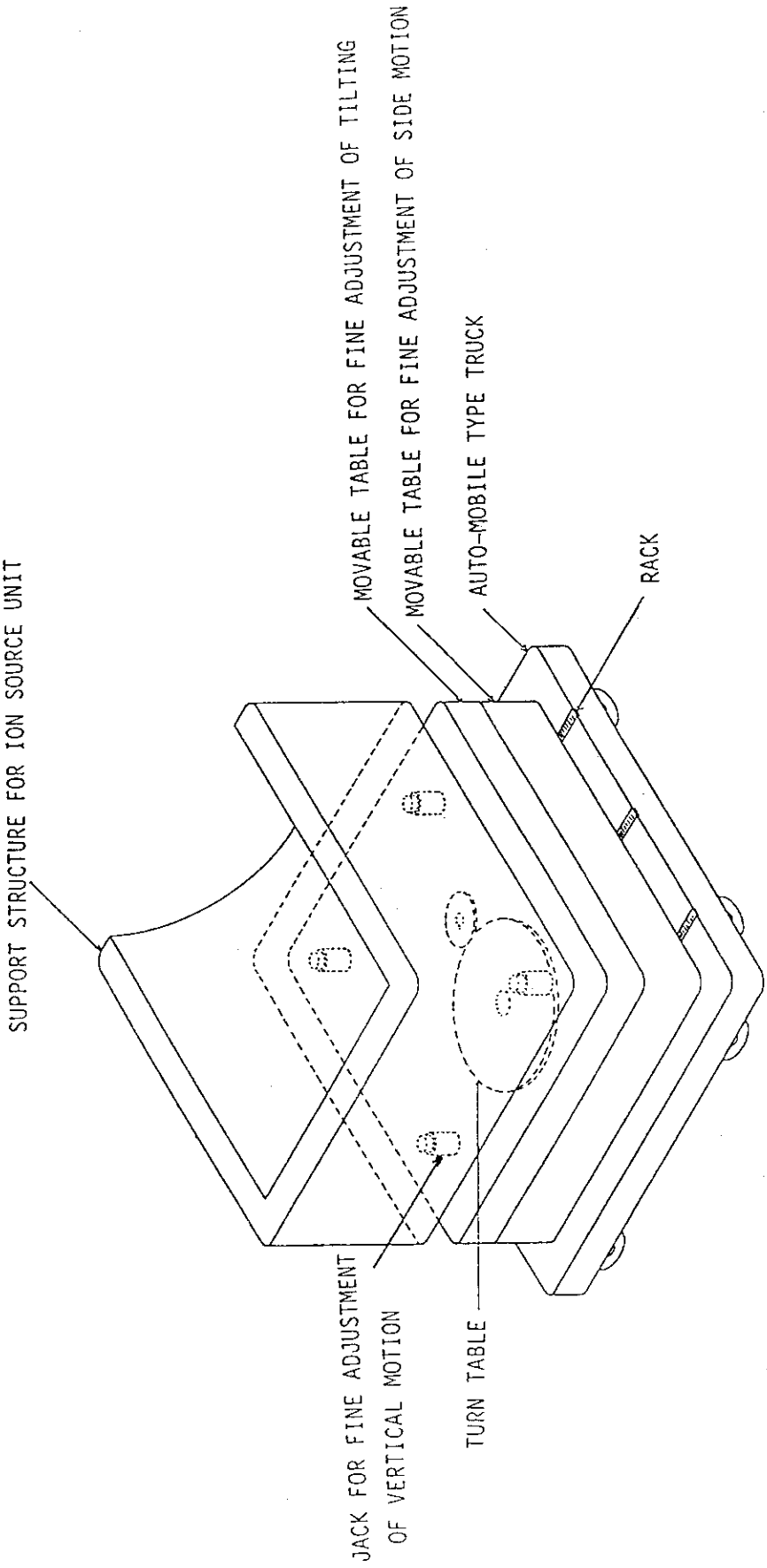

Fig. 6.6-1 Concept of auto-mobile type truck for maintenance of the ion source unit.

7. CONCLUDING REMARKS

A neutral beam injection system that satisfies the ITER/NBI common design requirements has been proposed. The most important point in the design is that the NBI system is based on the utilization of a cesium-seeded volume negative ion source which can produce an intense negative ion beam with high current density at a low source operating pressure. The design values of the source are equivalent to the experimental values achieved at JAERI. The utilization of the Cesium-seeded volume source is essential to the design of an efficient and compact neutral beam injection system which satisfies the ITER common design requirements.

The present design proposal has been made so as to be realized technologically within 5 or 6 years, assuming that properly supported R&D efforts will be made. The most critical breakthrough in the R&Ds is to develop a reliable ion source/accelerator which can produce a 1.3MeV, 17A deuterium negative ion beam. Acceleration of a mili-ampere ion beam up to several MeV is within a conventional technology. However, a multi-ampere ion beam has never been accelerated above 1MeV. The ion beam current must be increased by three orders of magnitude without degrading the reliability,i.e., the voltage holding characteristics. It must be noted that the design will be modified depending on the results of the accelerator R&Ds.

Major items to be studied further in the design are shown below.

(1) Beamline Configuration

The integrated beamlines in the NBI room are still too big compared with the reactor itself. This is mainly due to that three beamlines are mounted on each injection port vertically. Generally speaking, many smaller beamlines make the system complicated and the construction cost will be increased. On the contrary, few bigger beamlines imposes on the system a very high reliability, though the system becomes simple and less expensive. A version of two beamlines per port should also be studied to make the system simpler and reduce the construction cost. This version will be possible at least when an efficient plasma neutralizer would be developed.

(2) Ion Source

In the present design of the ion source, Cesium is utilized in the negative ion source. However, influences of Cs on the accelerator reliability are not investigated in detail so far. Preliminary results on the influence of Cs indicate that the degradation of the voltage holding characteristics is allowable so long as its consumption rate is small. However, it is not yet clear that Cesium can be utilized in steady-state operation.

(3) Accelerator

Though an electrostatic accelerator is applied in the design, it is not a conventional one which is similar to that used for high energy accelerator area. In order to improve the voltage holding in the accelerator at high acceleration current, electrons produced in each acceleration gap are reflected magnetically and dumped in each gap concerned, so as to suppress the production of high energy electrons and subsequent X-rays. However, the influences of strong neutrons and r-rays from the reactor plasma is not considered. If the accelerator reliability depends sensitively on the flux of r-rays and neutrons inspite of the magnetical electron suppression, the negative ion beam must be deflected before entering the neutralizer, so that the accelerator should not be exposed directly to the radiation. In this case, the beamline design must be modified appreciably.

(4) Neutron Shield

Neutron shielding in the present design is made in the two steps, namely, high energy neutron shielding by the beamline chamber wall and thermal neutron shielding by the neutron absorber on the room wall. By this concept, the weight of the beamline can be reduced but still too heavy to be maintained easily. Neutron shielding concept which is more compatible with the remote maintenance scenario should be studied.

(5) System Interface

System interface between the NBI system and the ITER common utilities is not determined yet. Specifications of the hot cell should be determined from the NBI maintenance point of view.

Finally, we have to make further efforts to make the NBI system more compact, more simple and more efficient so that the system design

should be accepted by the fusion experimental reactor. This depends entirely on the development of high performance ion source/accelerator and the plasma neutralizer.

Acknowledgement

The authors would like to thank S. Matsuda for his continuous advice and encouragement, and Y. Hasegawa for preparing many figures. The present design proposal has been completed through the discussions in the ITER Specialist Meetings held during 1989 ~ 1990 at Garching. Hence, they would like to express their special gratitude to W. Lindquist, A.J.T. Holmes, R.S. Hemsworth, H. Hopman, C. Jacquot, V.M. Kulygin, A.A. Panasenkov, P. Purgalis, and W.S. Cooper. They are also grateful to other members of the JAERI NBI group, M. Matsuoka, M. Kuriyama, S. Kunieda, Y. Tanaka, S. Shimamoto, S. Tamura and T. Iijima for their continuous support and encouragement.

should be accepted by the fusion experimental reactor. This depends entirely on the development of high performance ion source/accelerator and the plasma neutralizer.

Acknowledgement

The authors would like to thank S. Matsuda for his continuous advice and encouragement, and Y. Hasegawa for preparing many figures. The present design proposal has been completed through the discussions in the ITER Specialist Meetings held during 1989 ~ 1990 at Garching. Hence, they would like to express their special gratitude to W. Lindquist, A.J.T. Holmes, R.S. Hemsworth, H. Hopman, C. Jacquot, V.M. Kulygin, A.A. Panasenkov, P. Purgalis, and W.S. Cooper. They are also grateful to other members of the JAERI NBI group, M. Matsuoka, M. Kuriyama, S. Kunieda, Y. Tanaka, S. Shimamoto, S. Tamura and T. Iijima for their continuous support and encouragement.

Appendix Sputtering Yield of Copper by Deuterium Beam

Though the ions impinge on the beam dump at some incident angle, we assume that the incident angle is normal to the surface. The sputtering yield at normal incidence is expressed by the following equation indicated in reference [1],

$$Y(E_0,0) = Q\{[\ 3.441\sqrt{\frac{E_0}{E_{TF}}}\ln(\frac{E_0}{E_{TF}} + 2.718\ )]\ /\ [\ 1 + 6.355\sqrt{\frac{E_0}{E_{TF}}} + \frac{E_0}{E_{TF}}(\ 6.882\sqrt{\frac{E_0}{E_{TF}}} - 1.708\ )]\}(\ 1 - \frac{E_0}{E_{TF}})^{2/3}(\ 1 - \frac{E_{th}}{E_0})^2$$

where Q is a yield factor, E_0 is an incident ion energy at normal incident, E_{TF} is an energy in the center-of-mass system for a head-on collision with the screening radius as the nearest approach, and E_{th} is a threshold energy for the target-ion combination considered. When the target is cooper and the ions are deuterium, E_{TF} is 2.97 keV, E_{th} is 38 eV, and Q is 0.24 atoms/ion which are also quoted from reference [1]. The sputtering yield at normal incidence is calculated as a function of the ion energy as shown in Fig. A-1. The sputtering yield is 3.88×10^{-3} atoms/ion at the ion energy of 1.3 MeV which is a required energy for ITER.

Reference

[1] R.A.Langley, J.Bohdansky, W.Eckstein, P.Mioduszewski, J.Roth, E.Taglauer, E.W.Thomas, H.Verbeek, and K.L.Wilson, Nuclear Fusion (Journalof Plasma Physics and Thermonuclear Fusion), Special issue,(1984), pp 55 (data compedium for plasma-surface interactions)

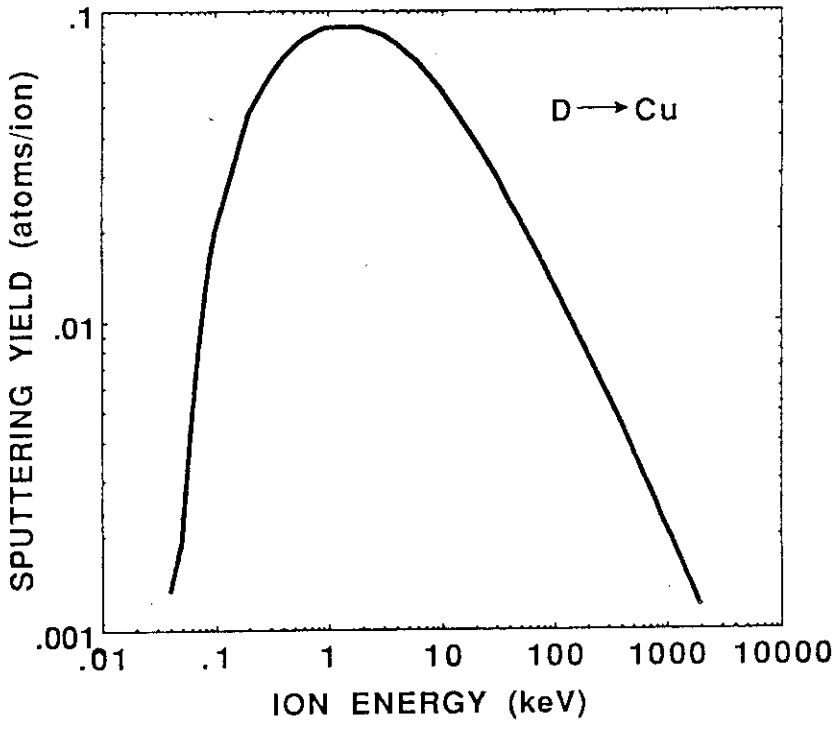

Fig. A-1 Dependence of the sputtering yield at normal incidence on the beam energy.